UNIVERSITÀ
DEGLI STUDI
DI PADOVA

Sede Amministrativa: Università degli Studi di Padova

Dipartimento di Biologia

SCUOLA DI DOTTORATO DI RICERCA IN : BIOSCIENZE E BIOTECNOLOGIE
INDIRIZZO: BIOTECNOLOGIE
CICLO XXVII

CARBON NANOTUBE-POLYMER SCAFFOLDS AND BIOMIMETIC PEPTIDES AS A SYSTEM TO PROMOTE HUMAN CELL DIFFERENTIATION TOWARD THE NEURONAL PHENOTYPE: ANALYSIS OF A MODEL CELL LINE AND CIRCULATING MULTIPOTENT CELLS

Direttore della Scuola: Ch.mo Prof. Giuseppe Zanotti
Coordinatore d'indirizzo: Ch.ma Prof.ssa Fiorella Lo Schiavo
Supervisore: Ch.mo Prof. Francesco Filippini

Dottoranda: Giorgia Scapin

ABSTRACT

Carbon nanotubes (CNTs) are attractive candidates for the development of scaffolds for neural regeneration thanks to their ability to conduct electrical stimuli, to interface with cells and to mimic the neural environment. This thesis work concerns the development of a freestanding nanocomposite scaffold composed of multi-walled CNTs in a poly-L-lactic (PLLA) matrix that combines the conductive, mechanical and topographical features of CNTs with the biocompatibility of PLLA. Such CNT-PLLA scaffold resulted to support growth and differentiation of neuronal SH-SY5Y cells better than PLLA alone. In order to mimic guidance cues from the neural environment, biomimetic peptides were designed to reproduce regulatory motifs from L1CAM and LINGO1 proteins, that are involved in neurite outgrowth control. Both peptides - which neither alter cell proliferation nor induce cell death - could specifically and positively modulate neuronal differentiation when either used to coat well bottoms or added to the culture medium (with highest efficiency at 1 μM concentration). Furthermore, cell differentiation resulted to be synergistically improved by the combination of the nanocomposite scaffold and the peptides, thus suggesting a prototype for the development of implants for long-term neuronal growth and differentiation.

Then, the CNT-PLLA matrix was electrospun into fibres of submicrometric size in order to better mimic the neural environment, i.e. neuronal processes and collagenous components of the extracellular matrix. These scaffolds were shown to be biocompatible and to promote the formation of new neurites that extend along the scaffold fibres. Since cells are influenced by the scaffold topography, the orientation of the scaffold fibres opens up the perspective to promote a polarized neurite outgrowth. Moreover, the neuritogenic properties of the scaffolds are further enhanced when LINGO1 derivative peptide is added to culture medium; this represents a good starting point for developing next

generation scaffolds upon peptide functionalization. Moreover, human circulating multipotent cells (hCMCs) were grown onto the scaffolds and treated with peptides in order to asses if this autologous and accessible source of stem cells is capable of neuronal differentiation thanks to the scaffold and peptide characteristics. The CNT-PLLA scaffolds and its respective electrospun version resulted to be suitable for hCMCs adhesion and growth, showing a very good level of biocompatibility, and the hCMCs growing onto the scaffolds showed typical features of cells from the neuronal lineage, such as long neuritic protrusions that are tipped with fan-shaped structures resembling growth cones. Moreover, soon after cell seeding, the scaffolds were shown to promote the upregulation of markers typical of the neuronal lineage.The biomimetic peptides were also shown to influence cell morphology and to upregulate neuronal markers. These results suggest that hCMCs can acquire neuronal commitment thanks to scaffold/peptide properties *per se*, i.e. even in the absence of those typical growth factors that are normally used to promote the neuronal differentiation of stem cells. Further improvements in the scaffold geometry and composition, functionalization with peptides and culture conditions are necessary to achieve the complete neuronal differentiation of cells and to control the neuron subtype obtained, but our system resulted to be a good starting point for setting up implantable scaffolds for autologous neuronal differentiation. Future functional assessment of synaptic transmission and electrophysiological properties of cells onto the scaffolds will be of great interest. Moreover, coupling such scaffolds with electrical stimulation (which is readily achievable using CNT based materials) can boost further analyses aimed at studying neuronal differentiation and has great potential in nerve injury repair as well as neuron prosthesis.

RIASSUNTO

I nanotubi di carbonio (CNTs) sono i candidati ideali per lo sviluppo di supporti volti a promuovere la rigenerazione neurale grazie alla loro abilità di condurre gli stimoli elettrici e alla loro nanotopografia in grado di mimare l'ambiente neurale. Questo lavoro riguarda lo sviluppo di supporti nanocompositi costituiti da CNTs dispersi in una matrice di acido polilattico (PLLA) e quindi in grado di combinare le caratteristiche nanotopografiche e di conduttività dei CNTs con la biocompatibilità del PLLA. Tali supporti, sono risultati essere in grado di supportare la crescita e il differenziamento delle cellule neuronali SH-SY5Y in modo migliore rispetto al solo PLLA. Al fine di mimare gli stimoli guida dell'ambiente neurale, sono stati sintetizzati anche dei peptidi biomimetici ricavati da specifici motivi regolativi delle proteine L1CAM e LINGO1, le quali sono coinvolte nel controllo dell'accrescimento neuritico. Entrambi i peptidi non hanno dimostrato effetti negativi sulla vitalità e la proliferazione cellulare, promuovendo invece il differenziamento neuronale in modo sequenza specifico e con i maggiori effetti quando utilizzati a concentrazione 1 μM. Inoltre, quando usati in combinazione, supporti e peptidi sono in grado di agire in modo sinergico e di aumentare ulteriormente il differenziamento cellulare.

Successivamente, al fine mimare al meglio l'ambiente neurale, la matrice CNT-PLLA è stata elettrospinnata in fibre di dimensione submicrometrica con lo scopo di rappresentare i processi neuronali e la componente collagenosa della matrice extracellulare. Tali supporti si sono rivelati essere biocompatibili e in grado di promuovere la formazione di nuovi neuriti che si allungano seguendo l'orientamento delle fibre del supporto. Dal momento che le cellule sono influenzate dalla topografia del supporto, l'allineamento delle fibre suggerisce la possibilità di poter ottenere una crescita neuritica polarizzata. Inoltre, le proprietà neuritogeniche del supporto aumentano quando il peptide derivato da LINGO1 viene aggiunto al terreno di coltura; questi risultati rappresentano un

buon punto di partenza per sviluppare supporti più avanzati a seguito della funzionalizzazione con tale peptide. In aggiunta, cellule circolanti multipotenti umane (hCMCs) sono state coltivate sui supporti e trattate con i peptidi al fine di determinare se tale fonte di cellule staminali autologa ed accessibile sia capace di differenziazione neuronale grazie soltanto alle caratteristiche dei supporti e dei peptidi. I supporti CNT-PLLA e la rispettiva versione elettrospinnata sono risultati essere adatti all'adesione e alla crescita delle hCMCs, mostrando buoni livelli di biocompatibilità; inoltre, le hCMCs coltivate sui supporti hanno mostrato caratteristiche tipiche delle cellule neuronali come lunghe protrusioni neuritiche terminanti con strutture a forma di ventaglio simili ai coni di crescita. I supporti inoltre promuovono l'espressione di marcatori tipici del lignaggio neuronale. Anche i peptidi si sono rivelati essere in grado di influenzare la morfologia cellulare e di upregolare marcatori neuronali. Questi risultati suggeriscono che le hCMCs sono capaci di acquisire un *commitment* neuronale solo grazie alle caratteristiche dei supporti e dei peptidi e senza l'ausilio dei fattori di crescita che sono tradizionalmente usati per promuovere il differenziamento neuronale di cellule staminali. Sono necessari ulteriori studi riguardanti la composizione e geometria dei supporti, funzionalizzazione con i peptidi e condizioni di coltura per acquisire una completa differenziazione neuronale e controllare il tipo neuronale ottenuto; ma tale sistema sembra essere un buon punto di partenza per progettare supporti trapiantabili per promuovere la rigenerazione neurale. Sarebbe interessante poter valutare la trasmissione sinaptica e le proprietà fisiologiche delle cellule cresciute sui supporti così come utilizzare tali supporti per stimolare elettricamente le cellule e valutare un eventuale miglioramento nel differenziamento.

INDEX

ABBREVIATIONS 1

1. INTRODUCTION 3

1.1 REGENERATIVE MEDICINE 3

1.1.1 MULTIPLE CUES TO IMPROVE REGENERATION 4

1.1.1.1 Biochemical cues 5

1.1.1.1.1 Synthetic peptides for mimicking protein regulatory motifs 5

1.1.1.2 Physical cues 7

1.1.1.2.1 Electrospun fibres for mimicking ECM topography 8

1.1.1.2.2 Electrospinning technique 9

1.1.1.3 Electrical cues 10

1.1.1.3.1 Conductive materials for mimicking electrically conductive tissues 10

1.1.2 CELLS HAVE MICRO- AND NANOMETER SENSITIVITY 11

1.2 NANONEUROSCIENCE 12

1.2.1 NANOPATTERNING OF MOLECULES FOR GUIDING CELL ORGANIZATION 13

1.2.2 NANOTOPOGRAPHY FOR CONTROLLING CELL BEHAVIOURS 13

1.2.3 NANOELECTRODS FOR SELECTIVE STIMULATION OF TARGETED NEURONAL POPULATIONS 15

1.2.4 NANOCARRIERS FOR DRUG DELIVERY 15

1.3 THE NERVOUS SYSTEM: INJURY AND REGENERATION 16

1.3.1 NEURONS AND NEURITE OUTGROWTH 16

1.3.2 PNS INJURY 19

1.3.3 CNS INJURY 21

1.3.4 CURRENT CLINICAL APPROACHES FOR TREATING NERVE INJURIES 23

1.3.4.1 Nerve guidance scaffolds 24

1.3.4.2 Biomaterials for brain repair 26

1.3.4.3 Nanostructured scaffolds for neural tissue engineering 27

1.4 CARBON NANOTUBES (CNTS) 28

1.4.1 CNT-BASED SCAFFOLDS FOR NEUROLOGICAL APPLICATIONS 29

1.4.1.1 CNTs nanotopography favours cell adhesion and neuronal differentiation 29

1.4.1.2 CNT functionalization improves the scaffold properties 30

1.4.1.3 CNTs incorporation in polymer scaffolds supports cell growth and maturation 32

1.4.1.4 CNT conductivity boosts neuronal electrical signaling and differentiation 34

1.4.1.5 CNT substrates can be used to electrically stimulate neurons 36
1.4.1.6 CNTs can act as guidance cues for neurite outgrowth 37
1.4.2 CNT CYTOTOXICITY 38
1.5 PROTEINS INVOLVED IN NEURITE OUTGROWTH 40
1.5.1 L1CAM 40
1.5.2 LINGO1 42
1.6 STEM CELLS AND NEURONAL DIFFERENTIATION 45
1.6.1 STEM CELLS IN REGENERATIVE MEDICINE 45
1.6.2 STEM CELLS FOR NEURAL REPAIR 45
1.6.2.1 Human circulating multipotent cells (hCMCs) 46
1.6.3 NEURONAL MARKERS 47
1.6.4 STEM CELLS CULTIVATED ONTO CNT-BASED SCAFFOLDS 49
1.7 SH-SY5Y CELL LINE 51
2. AIM OF THE PROJECT 53
3. METHODS 55
3.1 SCAFFOLD PREPARATION AND CHARACTERIZATION 55
3.1.1 CNT-PLLA SCAFFOLD 55
3.1.2 ELECTROSPUN CNT-PLLA SCAFFOLD 55
3.2 PEPTIDE SYNTHESIS AND CHARACTERIZATION 56
3.3 CELL CULTURE, DIFFERENTIATION AND EXPERIMENTAL DESIGN 57
3.3.1 SH-SY5Y 57
3.3.2 HUMAN CIRCULATING MULTIPOTENT CELLS (ĥCMCS) 59
3.4 ANALYSIS OF CELL VIABILITY/PROLIFERATION AND NEURONAL DIFFERENTIATION 60
3.4.1 CELL PROLIFERATION 60
3.4.2 CELL VIABILITY 61
3.4.3 NEURITE LENGTH ANALYSIS (SH-SY5Y CELLS) 61
3.4.4ĥCMC MORPHOLOGICAL ANALYSES 62
3.4.5 SCANNING ELECTRON MICROSCOPY ANALYSIS 63
3.4.6 RNA EXTRACTION AND RETROTRANSCRIPTION 63
3.4.7 REAL TIME RT-PCR (qPCR) 64
3.4.8 IMMUNOFLUORESCENCE 65
3.5 BIOINFORMATIC ANALYSES 66
3.5.1 HOMOLOGY SEARCHES AND STRUCTURAL MODELING 66
3.5.2 PRIMER DESIGN 66
3.6 STATISTICAL ANALYSES 67
4. RESULTS 69
4.1 SET UP AND VALIDATION OF A POLYMER-CNT SCAFFOLD 69

4.2 THE NEURITOGENIC PEPTIDES 74
4.2.1 IDENTIFICATION OF PEPTIDES DERIVED FROM L1 AND LINGO1 74
4.2.2 L1-A AND LINGO1-A EFFECTS ON NEURONAL GROWTH AND DIFFERENTIATION 77
4.2.2.1 Peptides in solution 77
4.2.2.2 Peptides adsorbed onto the substrate 81
4.3 COMBINED EFFECTS OF THE CNT-PLLA SCAFFOLD AND NEURITOGENIC PEPTIDES ON NEURONAL GROWTH AND DIFFERENTIATION. 84
4.4 EFFECTS OF L1-A AND LINGO1-A PEPTIDES ON SH-SY5Y GENE EXPRESSION 86
4.5 PROTEOME-WIDE AND PRELIMINARY MUTATIONAL ANALYSIS OF THE PEPTIDES 88
4.6 eCNT-PLLA SCAFFOLD EFFECTS ON SH-SY5Y CELL ADHESION, GROWTH AND DIFFERENTIATION 90
4.7 COMBINED EFFECTS OF THE eCNT-PLLA SCAFFOLD AND NEURTIOGENIC PEPTIDES ON NEURONAL GROWTH AND DIFFERENTIATION 95
4.8 TESTING SCAFFOLDS AND PEPTIDES WITH A STEM CELL POPULATION 97
4.8.1 CNT-PLLA SCAFFOLD EFFECTS ON ɦCMC ADHESION, GROWTH AND DIFFERENTIATION 97
4.8.2 L1-A AND LINGO1-A EFFECTS ON ɦCMC GROWTH AND DIFFERENTIATION 102
4.8.3 eCNT-PLLA SCAFFOLD EFFECTS ON ɦCMC ADHESION AND DIFFERENTIATION 105
5. DISCUSSION 109
6. CONCLUDING REMARKS 119
7. REFERENCES 123
8. PUBLICATIONS 135

ABBREVIATIONS

a.m.u.: Actual peptide mass
APP: amyloid precursor protein
BDNF: Brain-derived neurotrophic factor
bFGF: basic fibroblast growth factor
Calcein-AM: Calcein acetoxymethyl ester
CAMs: Cell adhesion molecules
CD: Circular dichroism
CMCs: Circulating multipotent cells
CNS: Central nervous system
CNT-PLLA scaffold: CNT dispersed in the PLLA matrix
CNTs: Carbon nanotubes
CRASH:Corpus callosum hypoplasia, Retardation, Adducted thumbs, Spasticity and Hydrocephalus
CREB: cAMP response element-binding protein
CT: Threshold cycle
DAT: Dopamine transporter
dBcAMP: dibutyryl cyclic AMP
DMEM/F-12: Dulbecco's Modified Eagle Medium/Nutrient Mixture F-12
DMSO: Dimethyl sulfoxide
DRG: Dorsal root ganglion
DSC: Differential scanning calorimetry
ECM: Etracellular matrix
eCNT-PLLA: electrospun CNT-PLLA scaffold
EGFR: Epidermal growth factor receptor
EN: Ethylenediamine
ePLLA: electrospun PLLA
ESCs: Embryonic stem cells
FBS: Foetal bovine serum
FDA: Food and Drug Administration
FGFR:Fibroblast growth factor receptor
FITC: Fluorescein isothiocyanate
Fmoc: Flurenylmethyloxycabonyl
Fn: Fibronectin
GDNF:Glial-derived neurotrophic factor
GFAP: Glial fibrillar acidic protein
GFP: Green fluorescent protein
HBSS: Hank's Balanced Salt Solution
Ig: Immunoglobulin
iPSCs: induced pluripotent stem cells
LDH: Lactate dehydrogenase
LINGO1: LRR and Ig-like domain containing Nogo receptor interacting protein
LRR: Leucine rich repeat
MAP2: Microtubule associated protein 2
MEAs: Multi-electrode arrays
MTs: Microtubules
MWCNTs: Multi-walled carbon nanotubes
NCAM: Neural cell adhesion molecule
NeuN: Neuronal nuclear antigen

NFM: neurofilaments
NGF: Nerve growth factor
NSCs: Neural stem cells
NT-3: Neurotrophin 3
PABS: Poly-m-aminobenzene sulfonic acid
PBS: Phosphate buffered saline
PCL: Poly(ε-caprolactone)
PCR: Polymerase Chain Reaction
PD: Parkinson' s disease
PGA: Poly(glycolic acid)
PGFs: Phosphate glass microfibers
PhOMe: Methoxyphenyl group
PI: polyimide
PLDLA: poly(l/d-lactic acid)
PLGA: Poly(lactic acid-co-glycolic acid)
PLLA: Poly(L-lactic acid)
PPy: Polypyrrole
qPCR: Quantitative Real time RT-PCR
RA: all-*trans*-retinoic acid
RARE: Retinoic acid response element
RARs: Retinoic acid receptors
REST: Repressor Element-1 Silencing Transcription factor
RMSD: Root mean square deviation
RH: Relative humidity
ROS: Oxygen reactive species
RP-HPLC: Reversed-phase high-performance liquid chromatography
RTKs: Receptor tyrosine kinases
RXRs: Retinoid X receptors
SAMs: Self-assembly monolayers
SCI: Spinal cord injury
SEM: Scanning electron microscopy
SYP: Synaptophysin
SWCNTs: Single-walled carbon nanotubes
TBI: Traumatic brain injury
TGA: Thermogravimetric analyses
TPA: Phorbol ester 12-O-tetradecanoylphorbol-13-acetate
TRKB: Tyrosine receptor kinase B
TUBβ3: Tubulin β Ⅲ
VAMP7: Vesicle associated membrane protein 7

1. INTRODUCTION

1.1 REGENERATIVE MEDICINE

Regenerative medicine and tissue engineering evolved as interdisciplinary technologies combining principles from the life, material and engineering sciences with the goal of restoring the function of damaged tissues by delivering a combination of cells, biological factors and biomaterial scaffolds on which cells can adhere, proliferate, differentiate and organize similarly to native tissue.

Multiple approaches have been developed, depending on variety of injured tissue type and injury entity:

1) Scaffolds functionalized with factors are implanted to recruit progenitor cells at the defective site to stimulate their differentiation;
2) Stem cells are loaded onto the scaffold *in vitro*, and after their differentiation the cell-scaffold composite is implanted into the defective site.

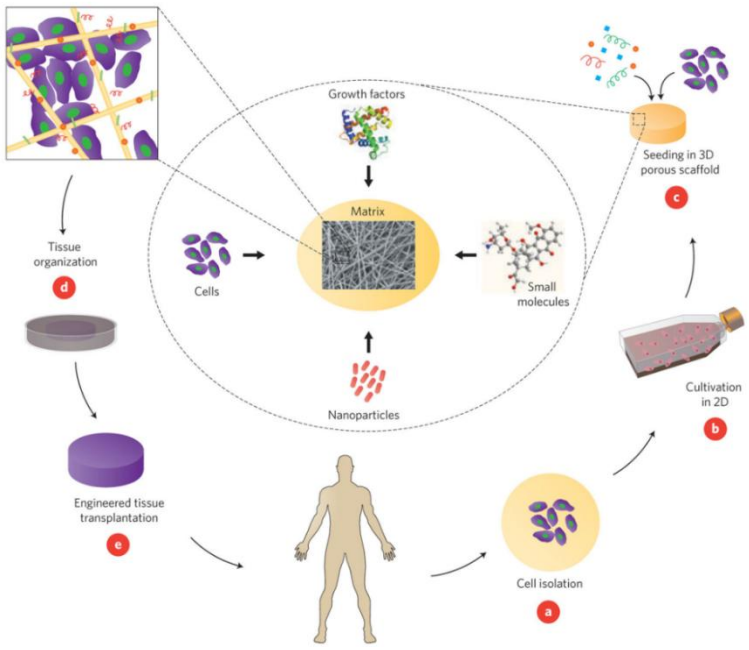

Figure 1. An example of a tissue engineering strategy. Cells are isolated from the patient **(A)** and may be cultivated *in vitro* on two-dimensional surfaces **(B)** for efficient

expansion. Next, the cells are seeded onto scaffolds **(C)** together with growth factors, small molecules, and micro- and/or nanoparticles. The cell constructs are further cultivated in bioreactors to allow cell differentiation **(D)** and then transplanted **(E)** into the damaged site to restore its function. (Adapted from Dvir et al., 2011).

1.1.1 MULTIPLE CUES TO IMPROVE REGENERATION

The cells reorganize via multiple interactions with the extracellular environment that provides topographical and mechanical stimuli, concentration gradients of growth factors or extracellular matrix (ECM) molecules and electrical signals. Therefore, scaffolds for regenerative medicine should recapitulate/mimic as more such features of the native tissue environment as possible in order to properly provide cells with information important for differentiation and tissue development (Dvir et al., 2011).

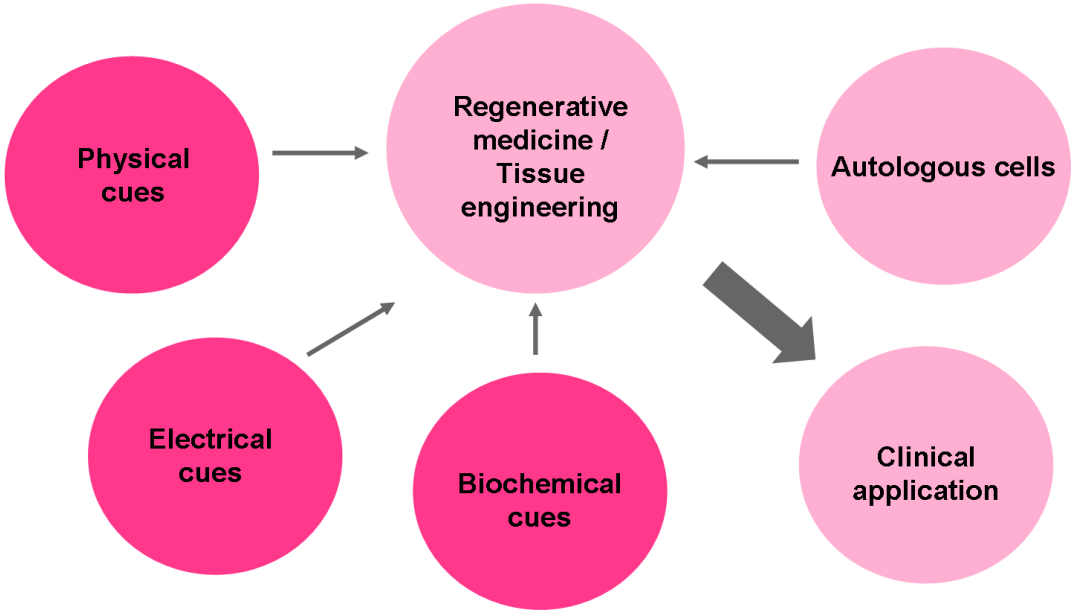

Figure 2. Multiple cues to improve regeneration. Regenerative medicine strategies try to incorporate different biosignals to recreate a controlled environment to direct stem cell tissue-specific differentiation.

1.1.1.1 Biochemical cues

Biochemical cues are provided by reciprocal interactions between the cell, soluble bioactive agents, and the ECM. Such biochemical cues are able to interacts with cell receptors activating signalling cascade and determining cell differentiation. Most of them fall within three categories:

- insoluble ECM macromolcules (e.g. collagens, elastin and laminin), glycoproteins (e.g. fibronectin and vitronectin), as well as polysaccharides such as heparan sulfate and hyaluronic acid. *In vivo*, these ECM proteins form a meshwork of fibres or fibrils with ECM glycoproteins incorporated into them. The resulting matrix functions as both a structural and signaling scaffold to cells;

- diffusible/soluble molecules such as growth factors, chemokines and cytokines. Growth factors are naturally occurring protein hormones which may act through autocrine or paracrine mechanisms and have potent effects on cell growth, proliferation, and differentiation. Growth factors are often stored and sequestered in the ECM and interact with cells through receptor tyrosine kinases (RTKs).

- Cell-cell receptors such as cadherins, cell adhesion molecules (CAMs), and ephrins. Cell-cell receptors are crucial to intercellular communication and regulate cell behaviours like proliferation and differentiation.

1.1.1.1.1 Synthetic peptides for mimicking protein regulatory motifs

Many works showed that some of the aforementioned molecules - if administrated both *in vitro* and *in vivo* - are able to elicit specific cell responses (Alberts et al., 2003); moreover, different strategies have been developed to link such proteins to biomaterial scaffolds in order to help delivery at the injured

sites (Matsumoto et al., 2007). However, coating surfaces with recombinant proteins or native matrix macromolecules extracted from animal tissues encounters the problem of eliciting immunoresponses, in particular when using proteins from different species. Furthermore, their isolation and purification from native tissues or their production as recombinant proteins at larger scale for tissue engineering purposes is expensive and subjected to batch to batch variability (Von der Mark et al., 2010). Moreover, protein conformation may be changed by immobilization onto the scaffold surface and the polypeptide chain orientation is difficult to control or even to predict. For these reasons, the production of specific motifs known to mediate regulatory signals as synthetic peptides presents significant advantages compared to using entire recombinant/native tissue proteins: (i) low immunogenic activity, (ii) increased stability, (iii) low production costs and (iv) simplified preparation and immobilization onto substrates. Moreover, peptides can be: (v) presented to cells at surface densities significantly higher than those possibly achieved with entire proteins or domains and (vi) tailored in composition for each tissue - specific application (Chen et al., 2008). The biomimetic peptides most used for scaffold functionalization are the ones representing the ECM protein epitopes for integrin binding and therefore promoting cell adhesion (Shekaran et al., 2010); however, the laminin IKVAV epitope for integrin binding has been shown to promote and enhance neurite elongation and neuronal differentiation of neural progenitor cells (Silva et al., 2004). Furthermore, some peptides mimetic of growth factors have been developed to promote cell survival and differentiation; for example, after the identification of specific loops important for nerve growth factor (NGF) function, peptides corresponding to these active regions were produced, showing good NGF agonist activity and cell differentiation trough the activation of tyrosine kinase receptor A (Colangelo et al., 2008). Once a protein structure is solved, several mimetic peptides can be designed; for example, a number of peptides reproducing homophilic binding sites of the neural cell adhesion molecule (NCAM) have been synthesized and they are able to interfere

with neuronal cell adhesion molecules and to promote differentiation and cell survival (Berezin et al., 2004).

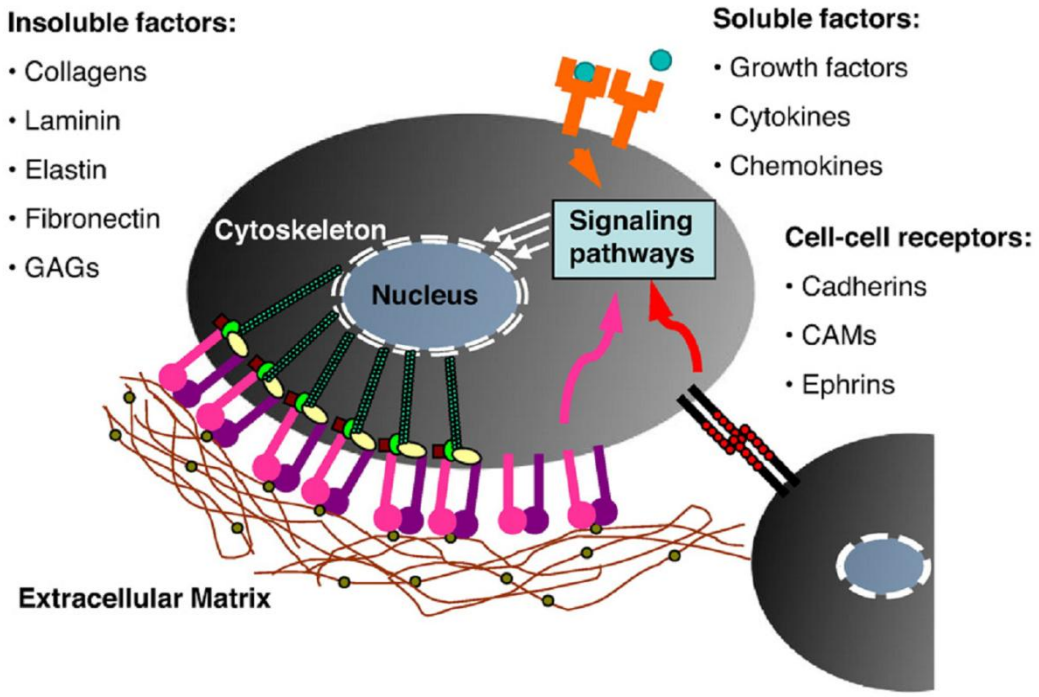

Figure 3. Biochemical signals from the extracellular environment. Insoluble ECM macromolecules; soluble diffusible factors and cell–cell receptors interact with cells controlling their proliferation and differentiation. (Adapted from Shekaran et al., 2010).

1.1.1.2 Physical cues

Cells are capable of sensing and responding to biophysical cues, over a wide range of length scales. Many of these cues are provided by the ECM, which acts as a cellular scaffold and is the primary extracellular component in tissues. *In vivo*, the ECM, through its structure and molecular composition, presents a variety of geometrically defined, three-dimensional (3D) physical cues in the submicron to micron scale, referred to as topographies. Cell response to topographies is mediated by a phenomenon called contact guidance, which is known to affect cell adhesion, morphology, migration, and differentiation (Nikkhah et al., 2012). Another physical cue displayed by the ECM is mechanical stiffness through which, similar to topography, a diverse set of cellular functions

can be modulated. Matrix sensing requires the ability of cells to pull against the matrix and cellular mechano-transducers to generate signals based on the force that the cell must generate to deform the matrix. Mechano-sensitive pathways subsequently convert these biophysical cues into biochemical signals that commit the cells to a specific lineage (Engler et al., 2006). Neurons are able to transduce topographical stimuli through interaction of the growth cone with the immediate environment and mechanical cues that can direct neurite extension. Guided neurite and axonal growth ensures appropriate and regulated connectivity within the overall neural circuitry, giving rise to specialized nuclei with specific functions within the brain (Pettikiriarachchi et al., 2010).

1.1.1.2.1 Electrospun fibres for mimicking ECM topography

The architecture of ECM is of special importance because it supports 3D cellular networks to form tissues and control many cellular behaviours. Electrospun polymer fibrous substrates with controlled fibre architectures and diameter provide topographical cues to cells by presenting geometries mimetic of the scale and 3D arrangement of the collagen and laminin fibrils of the ECM. Such polymer fibres present an high surface-to-volume ratio and porosity and are hence well suited for promoting cell adhesion, growth and differentiation and enable growth factor/drug loading; such properties are inherent to bioactive matrix microniches (Landers et al., 2014). In the case of neuronal precursor cells, it has been shown that fibre diameter is able to control their differentiation; specifically, small nanofibers, which mimic a glial-like morphology, result in a differentiation biased toward an oligodendrocyte fate. On the other hand, scaffolds composed of largerfibres, which restricted cell spreading along a single fibre,improve differentiation towards the neuronal lineage (Christopherson et al., 2009). Electrospun scaffolds also have the ability to control cell morphology and, in the case of neuronal cells, the direction of neurite elongation (Cirillo et al., 2014).

1.1.1.2.2 Electrospinning technique

Electrospun fibres are generally obtained through the electrospinning technique. This unique approach uses electrostatic forces to generate thin fibres from polymer solutions and the fibres thus produced have a thinner diameter (from nanometer to micrometer) and a larger surface area than those obtained with traditional spinning processes.

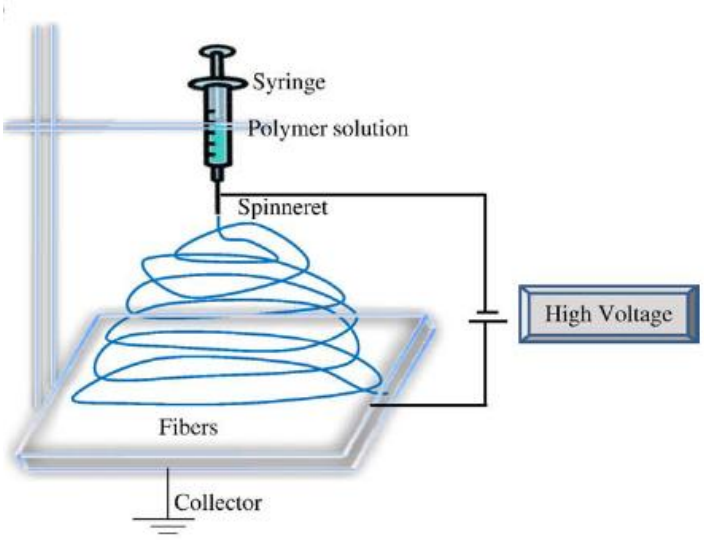

Figure 4. Schematic diagram of set up of electrospinning apparatus.(Adapted from Bhardwaj et al., 2010).

Furthermore, a direct current voltage in the range of several tens of kVs is required to generate theelectrospinning. This process is founded on the principle that strong mutual electrical repulsive forces overcome weaker forces of surface tension in the charged polymer liquid (Chew et al., 2006). Electrospinning is conducted at room temperature with atmosphere conditions and consists of three major components:a high voltage power supply, a spinneret (e.g., a pipette tip) and a grounded collecting plate (usually a metal screen, plate, rotating mandrel) and utilizes a high voltage source to inject charge of a certain polarity into a polymer solution, which is then accelerated towards a collector of opposite polarity. Most of the polymers are dissolved in some solvents before electrospinning, and when it completely dissolves, forms polymer solution. The polymer fluid is then introduced into the capillary tube for electrospinning. In the

electrospinning process, a polymer solution held by its surface tension at the end of a capillary tube is subjected to an electricfield and an electric charge is induced on the liquid surface due to this electric field. When the electric field applied reaches a critical value, the repulsive electrical forces overcome the surface tension forces. Subsequently, a charged jet of the solution is ejected from the tip of the spinneret and an unstable and a rapid whipping of the jet occurs toward the collector which leads to evaporation of the solvent, leaving a polymer behind. (Bhardwaj et al., 2010).

1.1.1.3 Electrical cues

Endogenous electrical signals are present in many developing systems and crucial cellular behaviours - such as cell division, cell migration, and cell differentiation - are all under the influence of such electrical cues (Yao et al., 2011). This is particularly true for neuronal cells in which electric signals activate membrane receptors and downstream intracellular signalling elements leading to asymmetrical activation/redistribution of the cytoskeleton and the consequent cell polarization. Indeed, some studies suggested the involvement of electrical activity in pathfinding of growing axons and the formation of initial connections in the developing nervous system (Yao et al., 2009). Moreover, it was discovered that an endogenous electric field arises at the onset of neural tissue repair (Huang et al., 2012).

1.1.1.3.1 Conductive materials for mimicking electrically conductive tissues

Neural circuits generate spontaneous electrical activity due to the electrophysiological properties of their constituent neurons and connections. Neuronal electrophysiological and synaptic properties can be affected by neuron-surface interactions, in particular for cells growing onto a substrate characterized by an inherent electrical conductivity. For these reasons, electroactive materials are the best choice to mimic the features of electrically

conductive tissues and to interface with neural cells providing electrical shortcuts between developing cells and a platform for supporting neuronal network activity and regeneration (Schmidt et al., 1997; Lovat et al., 2005). Moreover, electrically conductive scaffolds may improve cell survival and functional integration after transplantation *in vivo* by providing structural support for transplanted cells and facilitating synaptogenesis with host cells. Furthermore, electrically conductive materials can also allow application of electrical stimuli that can mimic the electrophysiological environment experienced by cells in a variety of biological processes, including muscle contraction, wound healing, and synaptic transmission (Landers et al., 2014)

1.1.2 CELLS HAVE MICRO- AND NANOMETER SENSITIVITY

Cells have micro and nanoscale sensitivity because the extracellular environment presents a variety of spatially defined cues in the the sub-micron to micron scale:

- At the nanometer level, extracellular environment affects sub-cellular behaviors such as the organization of cell adhesion molecule receptors;
- At the micron level, extracellular environment affects cellular and supracellular characteristics such as cell morphology and migration (Nikkhah et al., 2012).

Therefore, in order to mimic such submicron ECM organization, nanomaterials and nanotechnology tools can be used to develop special biomaterials able to recapitulate the architecture and spatial organization of structural proteins within ECM and the nanoscale features that model native ECM nanotopography (Shekaran et al., 2010). This approach - able to precisely regulate cell differentiation, morphology and polarization - is fundamental in order to proceed with clinical applications.

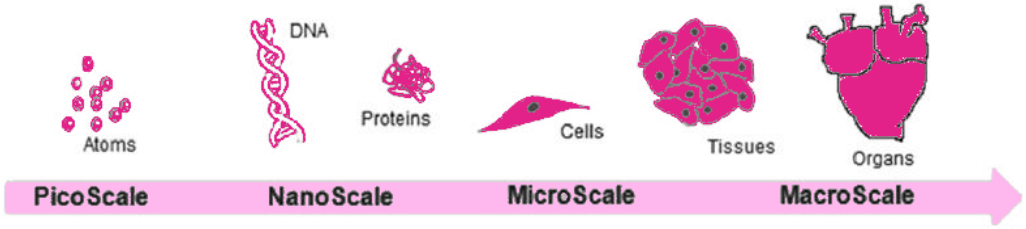

Figure 5. The relative scale of biological molecules and structures.

Combinations of stimulatory cues may be used to incorporate nanoscale topographical, chemical and electrical cues in the same scaffold to provide an environment for tissue regeneration that is superior to inert scaffolds.

1.2 NANONEUROSCIENCE

Nanomaterials can take advantage of their unique molecular features to induce, with high specificity, a number of desired physiological responses in target cells and tissues, while minimizing undesirable effects (Silva et al., 2006). Nanoneuroscience is an emerging field combining nanotechnology, chemistry, engineering and neurobiology. The application of nanotechnology to neural tissues is of particular interest because neural cells are electroactive and the electronic properties of nanostructures can be tailored to match the charge transport requirements of electrical cellular interfacing. The peculiar mechanical and chemical properties of nanomaterials can be exploited for integration with neural tissue in long term implants; moreover, their nanoscale features have the potential to interact with the biological system at the molecular scale, while offering elevated levels of control (Kotov et al., 2009). Indeed, recent studies regarding the interaction of nanomaterials with neural systems have provided a foundation for generating a new class of multifunctional devices and hybrid systems that could help in the repair of damaged nervous tissue, and that have paved the road to nanoneuroscience as a new discipline (Sucapane et al., 2009).

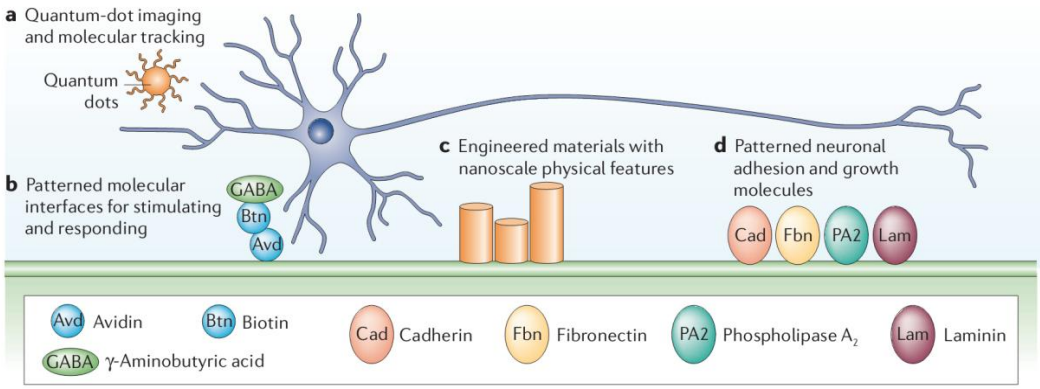

Figure 6. Applications of nanotechnologies in neuroscience. Nanomaterials and nanodevices that interact with neurons and glia at the molecular level can be used to influence and respond to cellular events. In all cases, these engineered technologies allow controlled interactions at cellular and subcellular scales. **(A)** Chemically functionalized fluorescent quantum dot nanocrystals used to visualize ligand–target interactions. **(B)** Surfaces modified with neurotransmitter ligands to induce controlled signalling. **(C)** Engineered materials with nanoscale physical features that produce ultrastructural morphological changes. **(D)** Surfaces and materials functionalized with different neuronal-specific effector molecules, such as cadherin and laminin, to induce controlled cellular adhesion and growth. (Adapted from Silva et al., 2006).

1.2.1 NANOPATTERNING OF MOLECULES FOR GUIDING CELL ORGANIZATION

Molecular deposition and lithographic techniques allow the patterning of neuronal-specific molecules with nanometre resolutions. The deposition of proteins/peptides and other molecules that promote and support neuronal adhesion, growth and differentiation on regenerating scaffolds enables the selective adhesion and growth of neural cells and a controlled neurite extension along the geometric pattern (Staii et al., 2011).

1.2.2 NANOTOPOGRAPHY FOR CONTROLLING CELL BEHAVIOURS

The nanoscale physical features of the scaffolds can affect neuronal behaviour. Natural tissues have indeed a hierarchical structure ranging from the macroscale (>1 mm), to microscale (1 μm – 1 mm), and nanoscale (< 1 μm). As a result, individual cells (typically in the size range 10-50 μm) respond in different ways to

structures at different length scales. It was shown that integrin receptors possess characteristic dimensions on the order of 10 nm (Comisar et al., 2006). The basement membrane of organs consists of nanoscale fibres (line topography) and pores (holes) that range in diameter from a few nanometers to several hundred nanometers (Abrams et al., 2000). The tubular fibers of collagen also have nanoscale dimensions (Curtis et al., 2001) and Laminin shows nanoscale texture as well (Rodríguez Hernández., et al., 2007). Given that cells' ECM is patterned down to the nanoscale, cell-biomaterial interactions in scaffolds can be optimized by incorporating features of nanoscale dimensions. Indeed, surfaces topographically structured at the submicron scale can affect a wide variety of growth parameters, such as cell adhesion, morphology, viability, genetic regulation, apoptosis, motility and differentiation (Gaharwar et al., 2013). Recent evidence from nanoscale topography analysis suggests that nanoscale features eliciting cell response are in the same size range (50-70 nm) that is associated with integrin cluster formation (Arnold et al., 2004). Further studies showed that scaffold nanotopography can control cell fate by altering cell and nucleus shapes, hence activating intracellular signal transduction and silent gene expression (Kim et al., 2012; Yang et al., 2013). This is particularly true for neurons that, thanks to their growth cones, sense and actively respond to the surface nanotopography with a surprising sensitivity to variations of few nanometers (Brunetti et al., 2010). In such a context, great potential is represented by Carbon Nanotubes (CNTs): thanks to their nanometer dimensions and high aspect ratio they could be used to develop nanotextured substrates influencing cell behaviours. Nanostructured surfaces have therefore the potential to define new types of interactions between scaffolds and cells: the scaffold surface area increases and can better resemble the native neural tissue.

1.2.3 NANOELECTRODS FOR SELECTIVE STIMULATION OF TARGETED NEURONAL POPULATIONS

Another emerging area of neuroscience nanotechnology regards the materials and devices designed to stimulate neurons. Neural prostheses, for example, are assistive devices to restore lost neuronal functions. These devices electrically stimulate nerves replacing injured neurons and fine control at molecular level is crucial to develop devices able to properly interact with the nervous system. Given that size should be small enough to enable selective stimulation of a targeted population of neurons (Schmidt et al., 2003; Silva et al., 2006), nanomaterial based neural electrodes are likely to improve signal transfer specificity and to reduce as well glial scarring at the injured site. Again, the conductive features and nanometric size of CNTs render them ultimate materials for developing/coating such electrodes.

1.2.4 NANOCARRIERS FOR DRUG DELIVERY

Another area in which nanotechnology may significantly impact in clinical neuroscience is the development of nanocarriers able to selectively deliver drugs, peptides, and oligonucleotide to specific regions or tumors to improve their pharmacological activity and simultaneously diminishing their undesirable systemic side effects. Thanks to their nanometric dimensions, such nanocarriers can be exploited to cross the blood brain barrier to target therapeutics to the Central Nervous System (CNS) (Silva et al., 2007). CNTs possess a number intriguing features that make them attractive drug delivery carriers:(i) they exhibit high accumulation in tumor tissues; (ii) their needle-like shape facilitates transmembrane penetration and intracellular accumulation of drugs via the "nanoneedle" mechanism that is independent of additional CNTfunctionalization and cell types; (iii) aside from direct translocation through cellular membranes,

CNTs are also able to enter cells via energy-dependent endocytic pathways; (iv) as a platformfor drug attachment, CNTs, owing to their high aspect ratios and surface areas, display extraordinary ability for drug loading onto the surface or within the interior core of CNTs via both covalent and non-covalent interactions (Wong et al., 2013).

1.3 THE NERVOUS SYSTEM: INJURY AND REGENERATION

The CNS consists of the brain and the spinal cord. The peripheral nervous system (PNS) is located outside the CNS and includes the cranial, spinal and peripheral nerves that conduct impulses from and to the CNS. Injury in peripheral nerves could lead to loss of neuronal communication along sensory and motor nerves between the CNS and the peripheral organ scausing reduction in motor and sensory functions. CNS injury, like traumatic brain injury (TBI) or stroke, can result in several symptoms including cognitive, motor and psychotic dysfunction. (Pettikiriarachchi et al., 2010; Arslantunali et al., 2014).

1.3.1 NEURONS AND NEURITE OUTGROWTH

Neurons are polarized cells involved in the synaptic transmission of much information necessary for regulating all biological functions. The formation of neural circuits in the brain requires that a correct connectivity is established between neurons during development. Every neural circuit is represented by the structure of axons and dendrites, with individual axons stimulating multiple targets, and single dendrites assimilating inputs from various sources. During nervous system development, neurons extend axons to find their final destination toward a complex and changing environment and establish a functional synaptic network. Each axon is tipped with the growth cone; such a

specialized structure shows highly dynamic behaviour and responsiveness to multiple sources of spatial information and is hence able to guide the axon itself toward right targets with an impressive level of accuracy. The growth cone travels on a road made up of adhesive molecules presented on a neighbouring cell surface, such as transmembrane CAMs or assembled into a dense ECM (including laminin and fibronectin). These molecules provide defined "roadway" surfaces to which growth cone receptors can adhere, but they also activate intracellular signalling pathways utilized by the growth cone guidance machinery. Additionally, anti-adhesive surface-bound molecules (such as e.g. Slits and Ephrins) can prohibit growth cone advance and thus provide "guardrails" that determine roadway boundaries. Finally, diffusible chemotropic cues represent the "road signs" that present further steering instructions to the travelling growth cone. It is clear now that the response of attraction versus repulsion is not due to the intrinsic property of the cue, but rather to the specific receptors engaged and the internal signalling milieu of the growth cone (Lowery et al., 2009).

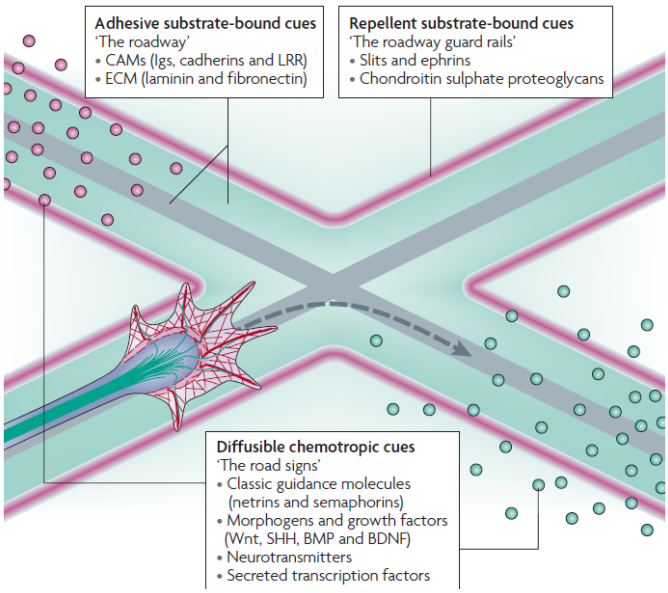

Figure 7. Directions for the trip. The growth cone encounters many different types of cues in its environmental terrain. It travels on a 'road' that is made up of adhesive molecules that are either presented directly on a neighbouring cell or assembled into a dense and complex extracellular matrix. Additionally, anti-adhesive surface-bound molecules can prohibit growth cone advance and thus provide the 'guard rails' that determine the road boundaries. (Adapted from Lowery et al., 2009).

Structural organization is central to growth cone function. The leading edge consists of dynamic, finger-like filopodia that explore the road ahead. Filopodia are separated by membrane sheets called lamellipodia-like veils. The cytoskeletal elements in the growth cone underlie its shape, and three growth cone regions can be distinguished based on cytoskeletal distribution. The peripheral (P) domain contains long F-actin bundles, which form the filopodia, as well as mesh-like branched F-actin networks, which give structure to lamellipodia-like veils. Additionally, individual dynamic "pioneer" microtubules (MTs) explore this region, usually along F-actin bundles. The central (C) domain encloses stable, bundled MTs that enter the growth cone from the axon shaft, in addition to numerous organelles, vesicles and central actin bundles. Finally, the transition (T) zone sits at the interface between the P and C domains, where actomyosin contractile structures lie perpendicular to F-actin bundles and form a hemicircumferential ring. The dynamics of these cytoskeletal components determine growth cone shape and movement on its journey during development (Lowery et al., 2009).

The growth cone engages its cytoskeleton to drive forward and turn, continuously influenced by environmental factors. The binding of the growth cone receptor to an adhesive substrate induces the generation of a complex that acts like a molecular "clutch", mechanically coupling the receptors and F-actin flow, thus anchoring F-actin to prevent retrograde flow and driving actin-based forward growth cone protrusion on the adhesive substrate. Traction also requires myosin II. Filopodia are guidance sensors located at the "front line" of the growth cone and they might have a major role in establishing growth cone-substrate adhesive contacts during environmental exploration. Several studies show that filopodia function as substrate attachment points and produce tension needed for growth cone progression. In order for spatial discontinuities in the environment to drive growth cone steering and, in particular, to accurately interpret numerous cues simultaneously, the growth cone requires a "navigation" system that translates multiple environmental directions through

Rho-family GTPases to locally modulate the dynamics of the cytoskeletal machinery including F-actin retrograde flow and F-actin guidance of MTs, in order to introduce spatial bias for steering the growth cone in the right direction (Lowery et al., 2009).

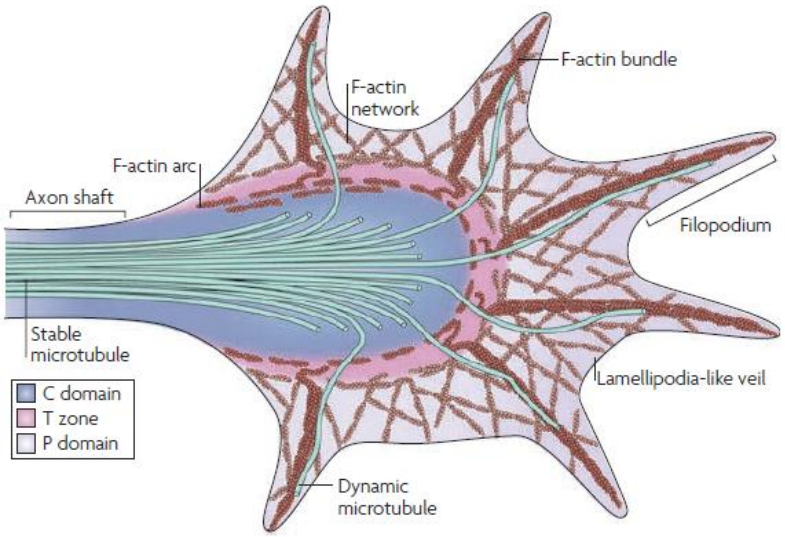

Figura 8. Growth cone structure. P domain contains (i) long, bundled actin filaments that form filopodia and (ii) mesh-like branched F-actin networks forming lamellipodia-like veils. C domain is formed by stable, bundled MTs, organelles, vesicles and stable actin bundles. T zone sits at the P-C domains interface, where contractile actomyosin structures lie perpendicular to F-actin bundles and form a hemicircumferential ring. (Adapted from Lowery et al., 2009).

1.3.2 PNS INJURY

Peripheral nerve injury leads to loss of neuronal communication along sensory and motor nerves between the CNS and the peripheral organs and depending on site of injury this can severely impair the quality of life of a patient (Arslantunali et al., 2014). Injuries are most commonly attributable to direct mechanical trauma, and less frequently, surgical resection secondary to tumour excision. However, the PNS has an intrinsic ability for repair and regeneration and such capacity relates to age of patient, mechanism of injury and in particular to the proximity of the injury to the nerve cell body; indeed often the nerve gaps are too big to be naturally regenerated (Faroni et al., 2014).

Reinnervation of denervated targets can be achieved by regeneration of injured axons or by collateral branching of undamaged axons in the proximity. However, often such mechanisms do not provide a complete functional recovery, especially after severe injuries. Neuronal response and axon regeneration imply complex interactions among different cell types as well as changes in the expression of many molecules. Failure in axon regeneration after peripheral nerve injury may depend on decreased intrinsic properties of neurons, absence of neurotrophic factors, or presence of inhibitory factors (Hsu et al., 2013). The withdrawal of target-derived neurotrophic support leads to profound changes in gene and protein expressions whose balance determines if the neuron survives and attempts regeneration or undergoes apoptosis (Reid et al., 2009). If regeneration is promoted, the distal stump of the injured nerve undergoes a series of molecular and cellular changes known as Wallerian degeneration. Within a few hours, both the axon and the myelin in the distal stump degenerate and macrophages migrate to the site of injury and contribute to debris clearance. In the first 24 hours, Schwann cells proliferate and switch from a myelinating to a regenerative phenotype and exhibit up-regulation of several molecules that assist the parallel degenerative and regenerative processes. In particular, the denervated Schwann cells downregulate structural proteins such as myelin basic protein and myelin-associated glycoprotein, whilst they upregulate L1-CAM, Neural-CAM, glial fibrillary acidic protein and many growth factors such as nerve growth factor (NGF), brain-derived neurotrophic factor (BDNF), glial-derived neurotrophic factor (GDNF), basic fibroblast growth factor (bFGF) and neurotrophin 3 (NT-3). Once debris is removed by the combined action of macrophages and Schwann cells, these latters align to form columns. This in turn provides a permissive environment rich in trophic factors, enabling guided axonal regeneration (Scheib et al., 2003; Faroni et al., 2014). Distal to the injured site, there are many obstacles for the regenerating axon to overcome prior to successfully reinnervate the target organ. Misdirection towards the wrong target reduces functional outcome even when the number of regenerated axons is

good; however, this is checked by "pruning" of growth cones that do not reach the correct target or lose support of their endoneurial tubes. Lack of neuronal contact in the distal stump leads to chronically denervated Schwann cells which downregulate growth factors and enter a dormant state, unable to support axonal progression. Similarly, the denervated target organ is exhausted of trophic factors, muscle fibres atrophy and satellite cells undergo apoptosis. These responses bear a significant impact on functional recovery following proximal nerve injuries (Fig. 9A) (Faroni et al., 2014).

1.3.3 CNS INJURY

CNS axons do not regenerate appreciably in their native environment. Several glycoproteins in the native extracellular environment (myelin) of the CNS are inhibitory for regeneration. The physiological response to injury in the CNS is also different compared to that of the PNS. After injury in the CNS, macrophages infiltrate the site of injury much more slowly compared to infiltration in the PNS, delaying the removal of inhibitory myelin. This largely depends on the blood-spine barrier, which limits macrophage entry into the nerve tissue to just the site of injury, where barrier integrity is weakened. In the case of spinal cord injury , cell adhesion molecules in the distal end of the injured nerve are not upregulated appreciably as they are in the PNS, limiting macrophage recruitment. Finally, astrocytes proliferate in a manner similar to that of Schwann cells in the PNS, but become "reactive astrocytes" producing glial scars that inhibit regeneration (Fig. 9B) (Schmidt et al., 2003).

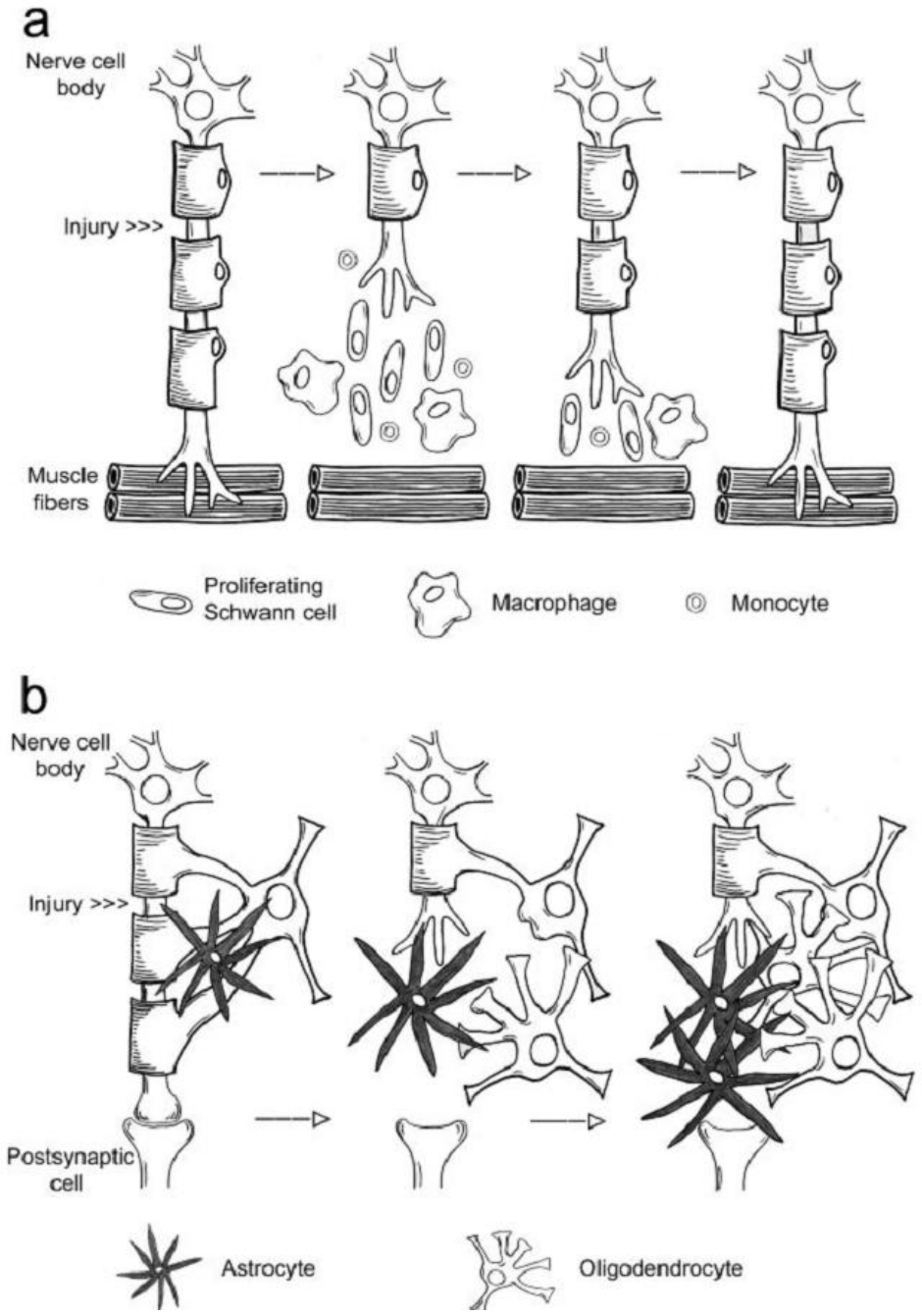

Figure 9. Responses to axotomy in the PNS and spinal cord. (A) In the PNS, support cells aid neuronal regeneration. Proliferating Schwann cells, macrophages, and monocytes work together to remove myelin debris, release neurotrophins, and lead axons toward their synaptic targets, resulting in restored neuronal function. **(B)** In the CNS, however, the few neurons that survive axotomy attempt regeneration and subsequently meet an impenetrable glial scar composed of myelin and cellular debris, as well as astrocytes, oligodendrocytes, and microglia. Fibroblasts, monocytes, and macrophages may also be present in the glial scar. Consequently, regenerating neurons in the spinal cord are blocked from reaching their synaptic target. (Adapted from Schmidt et al., 2003).

1.3.4 CURRENT CLINICAL APPROACHES FOR TREATING NERVE INJURIES

For peripheral nerve injury, treatments typically consist of either direct end-to-end surgical reconnection of the damaged nerve ends or the use of an autologous nerve graft. Suturing the ends of the two nerve ends together can repair small defects or gaps in the nerve. For longer nerve gaps, this approach is not desired because any tension introduced into the nerve cable would inhibit nerve regeneration. Thus, for a larger nerve defect, an autologous nerve graft that is harvested from another site in the body is used to span the injury site (Fig. 10A). Disadvantages of this technique include loss of function at the donor site and the need for multiple surgeries.

The development of therapies for spinal cord injury (SCI), traumatic brain injury (TBI), and other pathologies affecting CNS is more challenging due to the inhibitory environment that the injured axon has to face. Some attempts has been done attacking the inhibitory factors that suppress axonal regeneration. Active research is indeed focusing in the development of therapeutics able to counteract the myelin-associated inhibitors (e.g. LINGO1, NgR, Nogo, MAG). Various studies, both *in vivo* and *in vitro*, showed the ability of such therapeutics to suppress the inhibitory activity of glial scarring at the site of the injury and hence they are promising candidates for overcome the CNS injured axon inability to regenerate (GrandPre et al., 2002; Cho et al., 2012; Mi et al., 2013).

Furthermore, CNS axons have the ability to regenerate into PNS grafts and various groups have observed long distance regeneration with this approach (David et al., 1981; Tom et al., 2009). Within peripheral nerve grafts, parallel columns of Schwann cells surrounded by basal lamina render excellent guidance to regenerating axons. However, harvesting autografts is limited by tissue availability and donor site morbidity, and the alternative acellularized allografts fail to support axonal regeneration (Hurtado et al., 2011).

Treatment with growth factors showed the ability to promote neuronal survival and axon regeneration *in vitro*, but such a strategy is clinically problematic, when

considering the side-effect profile, the timing and method of growth factor release and the unpredictable interactions between growth factors and heterogeneous neuronal population (Faroni et al., 2014). However, some attempts have been done by delivering growth factors at the injured site using various types of nanocarriers. Other regenerative approaches regard the transplantation of stem cells at the injured site to favour tissue reconstruction and axon regeneration by replacing damaged neural tissues. Some works showed the ability of transplanted cells to undergo neuronal differentiation and then substitute lost neuronal and glial populations (McDonald et al., 1999; Chow et al., 2000; Cizkova et al., 2007); other studies demonstrated instead that stem cells are able to support axonal regeneration thanks to their own trophic activity and to sustain axon remyelination by differentiating into glial cells (Cízková et al., 2006; Wright et al., 2011).

An alternative strategy could be the use of biomaterial scaffolds incorporating multiple cues to more closely mimic native environment, thus promoting neural induction, axonal regeneration and neuroprotection.

1.3.4.1 Nerve guidance scaffolds

Spinal cord injury or pheripheral nerve repair requires "bridging" the lesion with a matrix that provides a permissive environment, fills the tissue gap and, concomitantly, provides structural support for axonal regrowth and functional reconnection. When the nerve graft is not possible, a valid alternative could be the development of nerve conduits able to guide the regenerating axons across the gap to connect with the distal end (Fig. 10B). Only then will signal transduction occur (Xu et al., 2014). An ideal nerve conduit needs to be biocompatible, flexible, neuroinductive, able to conduct electrical stimuli, tear resistant and sterilizable (Verreck et al., 2005). A number of materials have been proposed for use in neural tissue engineering. These include biodegradable, either natural or synthetic, as well as non-biodegradable polymers. Among the

biomolecules, the most studied and used are polyesters (poly(3-hydroxybutyrate) and poly (3-hydroxybutyric acid-co-3-hydroxyvaleric acid)), proteins (silk, collagen, gelatin, fibrinogen, elastin, and keratin), and polysaccharides (hyaluronic acid, chitin and alginate). Although aforementioned molecules are potentially able to sustain regeneration, their use is greatly limited by batch-to-batch variation and possibility to induce immunogenic reactions (Schmidt et al., 2003; Pego et al., 2012; Arslantunali et al., 2014). Synthetic polymers are attractive alternatives, as many of them are biocompatible and can elude the host immune response; moreover, their mechanical properties can be controlled and they can be processed in various forms to enhance tissue ingrowth. Many polymers, such as poly(L-lactic acid) (PLLA), poly(glycolic acid) (PGA), poly(lactic acid-co-glycolic acid) (PLGA), poly(ε -caprolactone) (PCL), polyurethanes (PUs), tri-methylene carbonate-co-ε-caprolactone, poly(D,L-lactide-co-ε-caprolactone), methacrylate-based hydrogels, polystyrene, silicone, and poly(tetrafluoroethylene), have already been used to create neural scaffolds (Schmidt et al., 2003; Pego et al., 2012; Arslantunali et al., 2014). PLLA for example is already FDA approved for use in tissue engineering application (Schmidt et al., 2003) and used as nerve conduit to promote regeneration of sciatic nerves and spinal cord in animal models (Evans et al., 1999; Oudega et al., 2001). In recent years, importance of the alignment in nerve guide conduits was understood, and conduits endowed with topographical cues as grooves and electrospun fibres were developed to direct the outgrowth of elongating neurites (Li et al., 2008; Liu., et al 2010). Hurtado et al, for example, developed a conduit formed by aligned electrospun PLLA fibres that successfully promote the regeneration of spinal nerves after a complete spinal cord transection (Hurtado et al., 2011). Moreover, as an electrically conducting tissue, the scaffold should likewise be able to conduct an electrical signal. In a recent study, PLLA was blended with polypyrrole (PPy) to produce a conducting nerve conduit; *in vitro* studies showed PC12 cell differentiation was improved when cells were seeded onto such conduits while *in vivo* studies demonstrated that these conductive

conduits behave like autologous nerve graft in repairing rat sciatic nerve defect suggesting that conducting materials have a great potential for nerve tissue regeneration (Xu et al., 2014).

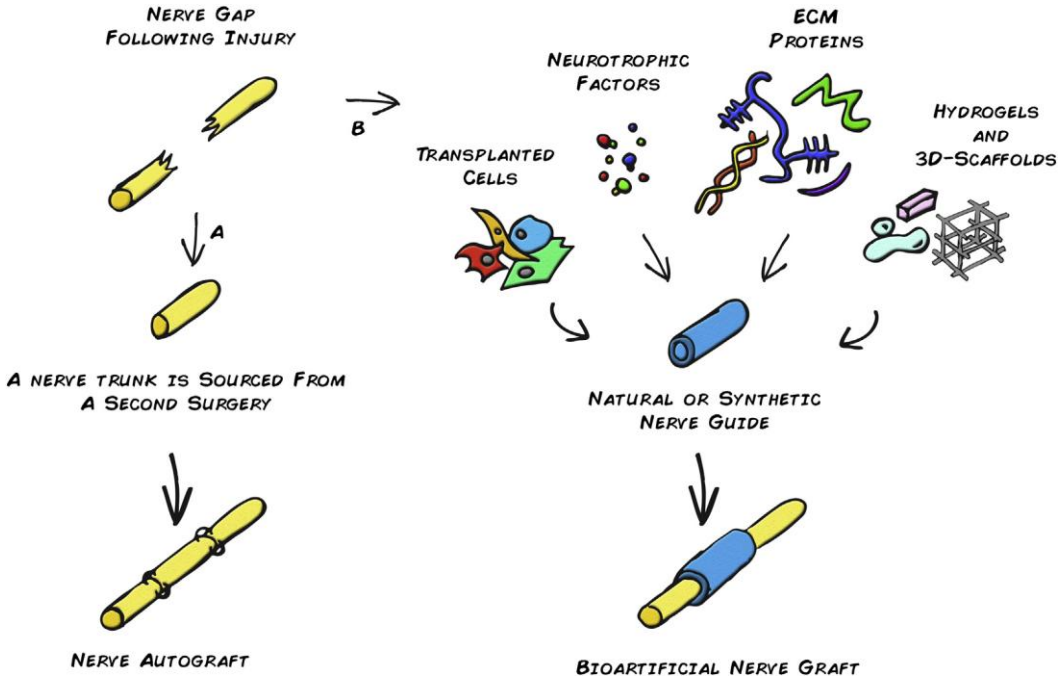

Figure 10. Bioartificial nerve graft for nerve repair. Autograft **(A)**. Artificial nerve graft that consists in nerve guide which could be enriched with several factors to enhance axonal regrowth **(B).** (Adapted from Faroni et al., 2014).

1.3.4.2 Biomaterials for brain repair

The objective of brain tissue engineering is to repair, replace, and regenerate tissue at the damaged site in order to re-establish functionality at both the cellular and organ levels. For these reasons, bioactive scaffolds are produced with the aim to provide a microenvironment that could facilitate survival, proliferation, differentiation, and connectivity of transplanted and/or endogenous cells. Many strategies have been developed so far to promote regeneration after brain injury, of which some require the implantation of scaffolds at the injured site in order to retrieve endogenous neural progenitors favouring their differentiation. Other strategies are based on implanting scaffolds to encourage the elongation of existing axons and - when massive cell lost occurs

- to use scaffolds for delivering stem cells at the injured site hence promoting a more rapid connectivity. A range of scaffolds including hydrogels, self-assembling peptides, and electrospun nanofibre scaffolds have been investigated as candidates for neural tissue engineering within the brain. It is essential for these scaffold that the surface properties are optimized to support endogenous or implanted cells and to possibly provide guided axonal growth (Pettikiriarachchi et al., 2010). Electrospun scaffolds are really interesting for such applications as their fibrillar architecture is mimetic for ECM topography and their large surface area to volume ratio and porosity can facilitate cell and axon penetration, neurite contact guidance as well as diffusion and waste of nutrients (all factors known to enhance scaffold–tissue integration). It is noteworthy that aligned fibrous scaffolds prepared by electrospinning are able to orient neurite growth whereas random organization promote neurite penetration (Nisbet et al., 2009). As for peripheral and spinal nerve conduits, various natural and synthetic polymers have been explored to develop electrospun scaffolds; a recent study demonstrates for example that PCL electrospun scaffold loaded with BDNF mimetic implanted toward the subventricular zone of rats mobilizes endogenous neuroblasts that are able to infiltrate the scaffold and differentiate (Fon et al., 2014). Great attention has been given to electroactive materials which can facilitate communication between neurons in the brain: for example, PCL and PLLA nanofibrous scaffolds were coated with PPy to form conductive sheaths and dorsal root ganglion cells were shown to extend longer neurite when subjected to electrical stimulation (Xie et al., 2009). Similar results were obtained by culturing PC12 cells onto a scaffold formed by electrospun PLLA fibres coated with PPy (Lee et al., 2009).

1.3.4.3 Nanostructured scaffolds for neural tissue engineering

A main problem with PPy and other conductive polymers is that their conductivity may change under harsh environment (Chao et al., 2009). For this

reason, CNTs are being increasingly used for developing neural regenerating scaffolds. It is expected that scaffold incorporated with CNTs can enable electrical stimulation and CNTs can be used into *in vivo* devices that could interact directly with neurons. All such unique CNT characteristics hold great technological promise for neuron related medical applications.

1.4 CARBON NANOTUBES (CNTS)

Since their discovery in 1991 by Iijima, CNTs have attracted wide interest in most fields of science and engineering due to their unique physical and chemical characteristics. These properties allow them to be used in a wide range of applications. The major areas of CNTs research are the polymer composites and biomedical devices including scaffold for regenerative medicine, biosensors, cell tracking and drug delivery carriers.

CNTs are cylindrical nanostructures whose simplest geometry is that of a single-walled nanotube (SWCNT). Here, a single graphene sheet (one-atom thick layer of carbon atoms arranged in a regular hexagonal pattern) is rolled up and closed at each end by a hemispherical fullerene cap; SWCNT diameters typically range between 0.8 and 2 nm with a tube length that can be many millions of times longer. Multi-walled nanotubes (MWCNT), on the other hand, are composed of numerous (by two up to hundreds) layer of graphene wrapped concentrically. Depending on the number of layers, MWCNTs have a larger diameter that can reach 100 nm (Sucapane et al., 2009).

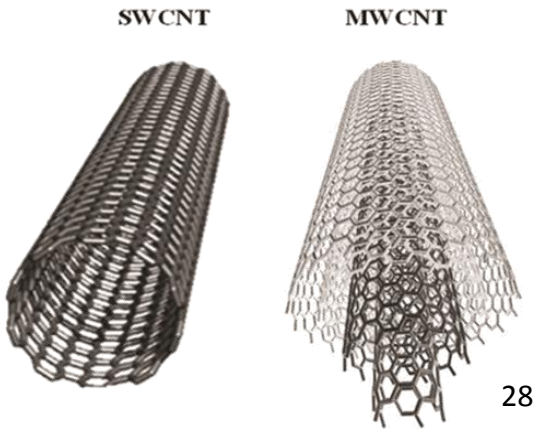

Figure 11. Schematic diagrams of single-walled carbon nanotube (SWCNT) and multi-walled carbon nanotube (MWCNT). SWCNTs consist of a single graphene sheet rolled up into a cylinder (left figure); MWCNTs consist of multiple concentric cylindrical shells of graphene sheets (right figure). (Adapted from Choudhary et al., 2011).

1.4.1 CNT-BASED SCAFFOLDS FOR NEUROLOGICAL APPLICATIONS

CNTs are attractive candidates for developing scaffolds to be used in neurological applications thanks to their morphology and nanoscale dimensions, their tunable electrical conductivity, their mechanical properties, and chemically modifiable surface.

1.4.1.1 CNTs nanotopography favours cell adhesion and neuronal differentiation

CNT structural features and dimensions resemble the smallest neuronal processes and many components of neuronal extracellular environment as proteins of the ECM (e.g. collagen), ion channels, signaling proteins and cytoskeletal elements (Fabbro et al., 2013).

Indeed, it has been found that such CNT nanoroughness - that matches the size of the neural environment roughness - contributes to anchor the neuronal cells. It was shown that, when seeded onto a CNT film, neuronal processes entangle around CNT nanostructures improving the binding of their membranes to the CNT surface (Sorkin et al., 2009). Furthermore, neuronal growth cones were shown to establish tight contacts with the CNT surface, and these strong interactions allowed the neurons to spread and interact with one another (Zhang et al., 2005).

CNTs - thanks to their chemical properties and enhanced surface area provided by a needle-like shape - have a good capacity to adsorb adhesion proteins from the serum, such as e.g fibronectin and laminin (Khang et al., 2007; Chao et al., 2010; Stout et al., 2012). Therefore, when cells grow onto CNT-based scaffold, they show enhanced capacity to form focal adhesions by clustering integrin molecules and hence, increased cell adhesion (Kim et al., 2012). In addition to favouring adhesion, CNT-based capacity to adsorb proteins results in trapping growth factors produced by the cells during their differentiation and this in turn

creates a storage site that can progressively release such growth factors during cell maturation, in a "signal-buffered" environment suitable for long term neuronal differentiation (Chen et al., 2013). At a glance, CNT ability to mimic neural environment topography and to retain proteins and growth factors would help and enhance cell adhesion, growth and neuronal differentiation.

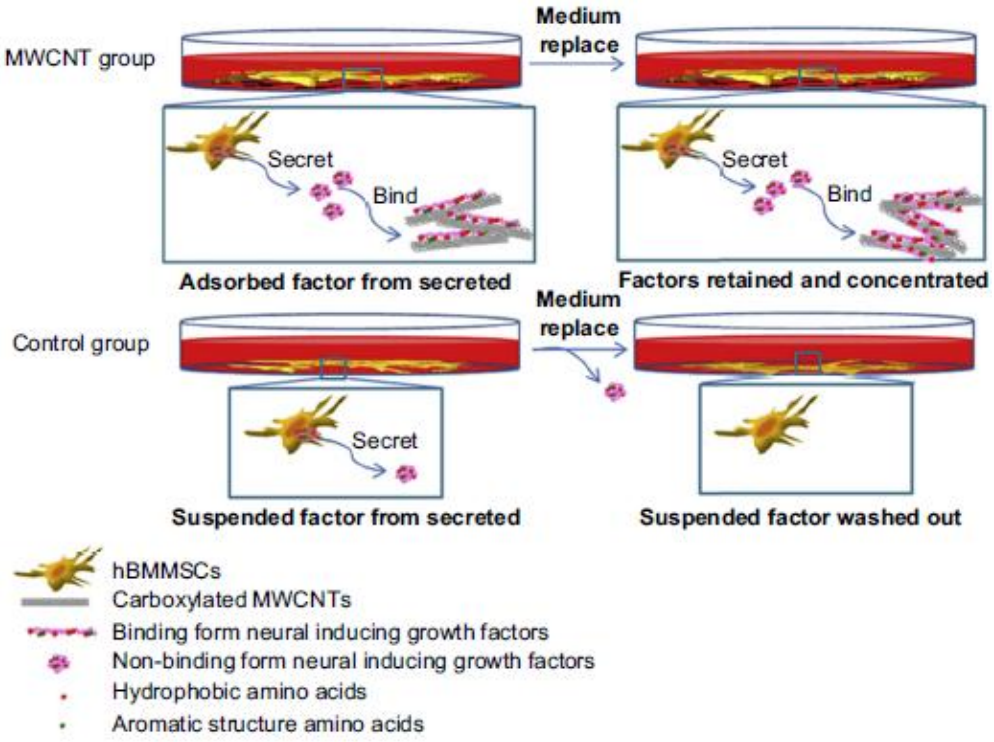

Figure 12. MWCNT film trap neural growth factors which are secreted from the cells. In contrast, these proteins in the control group cannot be kept but are washed out every time the medium is replaced. (Adapted from Chen et al., 2013)

1.4.1.2 CNT functionalization improves the scaffold properties

CNTs can be functionalized by covalent or non-covalent chemistry to improve their solubility in organic solvents, to modify their surface charge or to attach biologically active molecules able to promote neuronal cell adhesion and differentiation.

CNTS are highly hydrophobic and may contain residual impurities such as amorphous carbon and metallic nanoparticles; however, the surface

functionalization of CNTs by chemically attaching organic functional groups helps the CNT materials in becoming biocompatible and improves their solubilization in organic solvents for obtaining more homogeneous material. Two main paths are usually followed for the functionalization of CNTs: (i) attachment of organic moieties to the carboxylic groups that are formed by oxidation of CNTs with strong acids or (ii) direct bonding to the surface double bonds. Such strategies have been explored to engineer CNT surfaces by attaching bioactive molecules mediating specific biological responses (Saifuddin et al., 2013).

Such bioactive molecules can be linked to CNT surfaces also through non covalent functionalization, which is based on weak forces (van der Waals, hydrophobic or π-π interactions) unable to retain for long periods the interacting molecules. However, non covalent functionalization does not affect CNT charge and interacting molecules can adsorb to the external sides of nanotube, but also the adsorption to the internal side is possible (endohedral functionalization) (Hirsch et al., 2002).

The first use of CNT substrate for neuro-interfacing applications was reported by Mattson and colleagues, who cultured embryonic rat hippocampal neurons onto a coverslip coated with MWCNTs. Such a study demonstrated that pristine MWCNT substrates promoted cell adhesion while blocking neurite outgrowth. However, the non-covalent functionalization with 4-hydroxynonenal(4-HNE),a molecule promoting neurite elongation, showed a great increase in the number of neurite per cell and total neurite length (Mattson et al., 2000). Therefore the CNT functionalization resulted to be a valid method to improve scaffold performance. Later, Hu et co-workers studied the effect of surface charge modification: the MWCNT substrate charge was modified by functionalization with carboxyl groups, poly-m-aminobenzene sulfonic (PABS) acid or ethylenediamine (EN) to create negatively, zwitterionic or positively charged CNTs, respectively. Improved neurite elongation and branching were found when cells were seeded onto positively charged CNT scaffolds, according to the known preference of neuronal cells for positive substrates such as poly-lysine (Hu et al.,

2004). Therefore, manipulation of CNT surface charge can be successfully used to tune neurite outgrowth. Covalent functionalization with bioactive molecules was also explored; Matsumoto at al., covalently functionalized MWCNTs with NGF and BDNF and used them to culture embryonic chick dorsal root ganglion (DRG) neurons. DRG neurite outgrowth on modified MWCNTs was comparable to that seen with soluble NGF and BDNF in culturing media; therefore, such study indicated that CNT covalent functionalization with biomolecules allows the attached factors to maintain their bioactivity (Matsumoto et al., 2007).

1.4.1.3 CNTs incorporation in polymer scaffolds supports cell growth and maturation

CNTs are among the toughest and strongest nanomaterials; moreover, they are flexible and can be easily combined with both natural and synthetic polymers in developing scaffolds able to support neuronal cell adhesion and growth.
The incorporation of CNTs into polymeric scaffolds can be used to ameliorate the polymer scaffold characteristics:

- CNT can reinforce polymeric scaffold mechanical properties; indeed it has been shown that, increasing the percentage of incorporated CNTs, the scaffold toughness and tensile strength also increase (Kharaziha et al., 2014). Therefore, the CNT percentage within the scaffold can be modulated in order to mimic the ECM mechanical properties of the tissue of interest;

- CNTs can reduce the polymer electrical resistance. Indeed, it has been shown that, due to the CNT needle-like shape and high aspect ratio, their percolation threshold (the critical concentration where a transition from non-conducting to conducting state occurs) in polymer matrix composites is achieved at low concentrations ranging

from 0.0025 to 4 wt% . This allows for the modulation of the polymer electrical properties, without changing other important aspects as processability (Lizundia et al., 2012);

- CNTs feature a nanoscale meshwork within the polymer scaffolds and this could be of help to cell adhesion, as cells prefer rough surfaces (Bareket-Keren et al., 2013).

Different type of composites have been developed by combining CNT with polymers; for example, Jin and collaborators demonstrated that MWCNT-PLCL scaffolds showed improved adhesion, proliferation and neurite outgrowth of PC-12 cells (Jin et al., 2011). The *in vivo* studies using CNT-polymer devices are still very few, but a very recent report from Yu et al., showed that MWCNT-enhanced electrospun collagen/PCL conduit promote regeneration of sciatic nerve defects in rats and prevent muscle atrophy without invoking body rejection or serious chronic inflammation (Yu et al., 2014). Furthermore, Ahn and colleagues reported that CNTs chemically tethered onto the surface of aligned phosphate glass microfibers (PGFs) were successfully placed into three-dimensional poly(l/d-lactic acid) (PLDLA) tubes. After implantation of a CNT–PGF nerve conduit into the 10 mm gap of a transected rat sciatic nerve, the number of regenerating axons crossing the scaffold, the cross-sectional area of the re-innervated muscles and the electrophysiological findings were all significantly improved by interfacing with CNTs, thus demonstrating an effective role for CNTs in nerve regeneration (Ahn et al., 2015).

1.4.1.4 CNT conductivity boosts neuronal electrical signaling and differentiation

CNTs are electrically conductive and their conductivity is stable in biological environment (Chen et al., 2009). Therefore, their inherent electrical conductivity can mimic the features of the electrically conductive nervous tissue promoting neuronal maturation and excitability.

Lovat and co-workers found hippocampal neurons grown onto a MWCNT grid to show an enhanced network activity compared to those seeded onto control glass coverslips. The authors suggested that the increase in the efficacy of neural signal transmission may be due to the specific properties of CNT conductivity, able to provide a pathway allowing direct electrotonic current transfer, which in turn results in charge redistribution along the surface of the membrane. (Lovat et al., 2005). Similar results were obtained by using a substrate of SWCNTs for culturing hippocampal neurons: in this case very tight contacts between CNTs and neuronal membrane were shown by scanning electron microscopy (Fig. 13), hence supporting the hypothesis that improved neuronal electrical signals depends on CNT properties rather than on difference in neuronal survival or morphology (Mazzatenta et al., 2007). A further study clearly showed by transmission electron microscopy that CNTs can pinch neuronal membranes; when such neurons are forced to fire, CNT substrates strongly impact on single-cell regenerative electrical properties possibly due to electrical shortcut between adjacent dendritic compartments mediated by the conductive substrate (Cellot et al., 2009). Therefore, this study suggests a direct electrical coupling between CNTs and neuronal membranes. It was shown that other substrates for neuronal growth, mimicking either conductivity or nanoroughness of CNTs, are not able to enhance dendritic regenerative ability, thus suggesting that both properties are necessary for CNT substrates to influence neuronal activity (Cellot et al., 2009). Moreover, it was demonstrated with hippocampal neurons that SWCNT substrates can promote *de novo* formation of synapses characterized by an

improved efficacy (Cellot et al., 2011). CNTs scaffolds were also tested with three-dimensional cell cultures: in a study performed with spinal cord explants, beside the increase of fibres outgrowing the spinal tissue and the high growth cone activity, an increased synaptic efficacy was revealed even in neurons located at as far as 5 cell layers from the cell substrate interactions (Fabbro et al., 2012). Beside electrical signaling, the conductivity of CNT scaffolds can be modulated in order to control cell differentiation. Malarkey and co-workers studied SWCNT scaffolds with different conductivities and the same nonoroughness and found that rat hippocampal neuron neurite outgrowth changes depending on narrow ranges of conductivity (Malarkey et al.,2009). Therefore, the conductivity of the scaffold - modulating both neuronal differentiation neuronal electrical signaling - can be finely tuned to enhance scaffold performance.

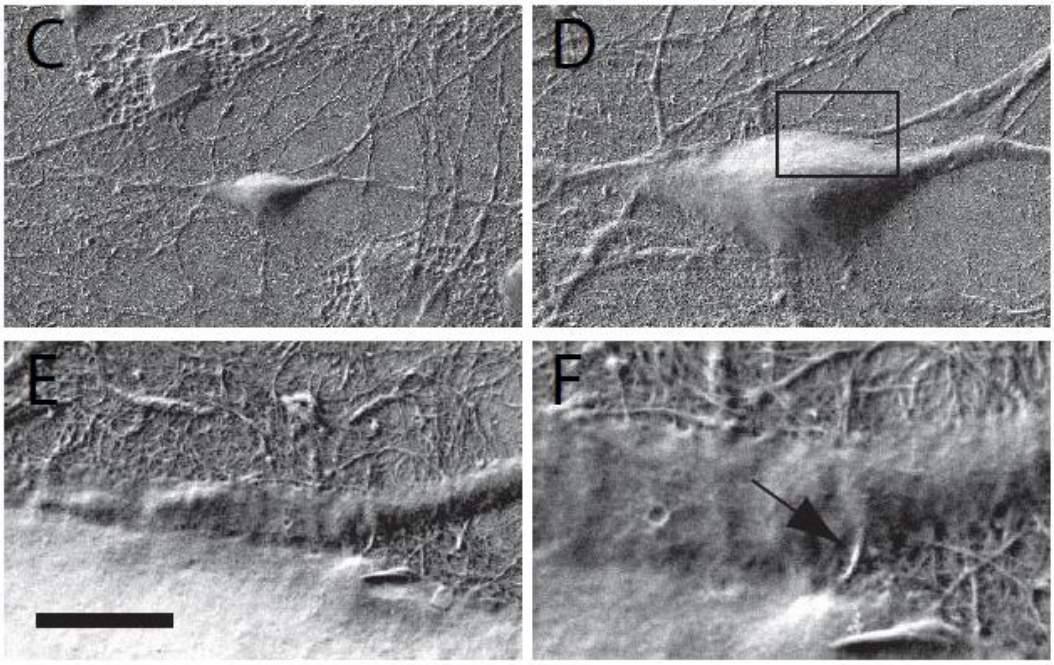

Figure 13. SEM images of cultured hippocampal neurons on SWNTs. (C, D) Subsequent micrographs at higher magnifications of neurons grown on SWNT. **(E, F)** Details of the square in **(D)** showing the interaction between neuronal membrane and SWNT. Scale bar (in E): C, 25 μm; D, 10 μm; E, 2 μm; F, 450 nm. (Adapted from Mazztenta et al., 2007).

1.4.1.5 CNT substrates can be used to electrically stimulate neurons

CNT-based scaffolds can also be used to stimulate cultured neurons; indeed, it was shown that the application of a current through the CNT substrates resulted in an inward transmembrane current that was indistinguishable from those induced by direct patch-clamp electrode-mediated depolarizing voltage steps (Liopo et al., 2006; Gheith et al., 2006). The effects of electrical stimulation through CNT scaffolds were analyzed: Huang and colleagues used a SWCNT rope as a substrate to cultivate and electrically stimulate NSCs and demonstrated that electrical stimulation boosted NSCs towards differentiated neurons in the early culture stage, when compared to conventional tissue culture plates via the analysis of neuronal gene and protein expressions (Huang et al., 2012). Landers et al. showed that, even when incorporated into polymer electrospun scaffolds, SWCNTs can be exploited to electrically stimulate cells, and the authors noted and enhanced NSC differentiation ability after electrical stimulation (Landers et al., 2014). Cho et al. demonstrated that electrical stimulation of PC-12 cell through a CNT/collagen composite can strongly improve neurite extension (Cho et al., 2010). Therefore, electrical stimulation through CNT-based matrixes can directly carry electrical current to control neuronal differentiation and neurite extension. This could be of benefit for developing novel neural electrodes and for enhancing and controlling cell behaviours in an electrically driven way.

CNTs have been successfully explored as coating material for metal electrodes. CNT coating enhanced both recording and electrical stimulation of neurons in culture, rat motor cortex and monkey visual cortex respect to bare metal electrodes. This improvement was due to reduced electrode impedance and increased charge transfer. Therefore, CNT-coated electrodes are expected to favour the development of long-lasting brain–machine interface devices (Keefer et al., 2008).

However, the major step toward implantable neuro-prosthetics applications is the development of flexible multi-electrode arrays (MEAs). Recently, a flexible

MEAs based entirely on CNT technology - where both the conducting traces and the stimulating electrodes consist of conducting CNT films embedded in a polymeric support - have been developed and showed a great suitability for high-efficacy neuronal stimulation applications (David-Pur et al., 2014).

1.4.1.6 CNTs can act as guidance cues for neurite outgrowth

Morphological guidance of regenerating axons is necessary to facilitate the formation of an effective neural network. CNT patterns have been shown to act as guidance cues for axonal growth, hence demonstrating a good potential in clinical applications .

Zhang et al., used a combination of microlithography and chemical vapor deposition to engineer patterned vertical MWCNT substrates. They found that neurons preferentially adhered to MWCNT patterns and growth cones were attached to the CNT surface, allowing the neurons to spread along patterns and interact with one another (Zhang et a l., 2005). Park and colleagues developed patterns of CNTs onto the biocompatible polymer polyimide (PI) by means of self-assembly monolayers (SAMs) and microcontact printing techniques. Such patterns were used for culturing hNSCs, showing that cells preferentially adhere in correspondence of the CNT patterned surfaces, and that CNT geometries can be modulated to tune both cell nuclei localization and neurite extension along the CNT patterns. Interestingly, the authors showed that such control on cell polarization can be obtained at single cell level (Park et al., 2011). Also when CNT are combined to other materials, it is possible to obtain some kind of control on neurite directionality; for instance, Jin et al. used CNT for coating aligned electrospun PLCL nanofibers and cultured DRG neurons and PC-12 cells; such coating could improve the outgrowth of neurites along the scaffold fibres (Jin et al., 2011).

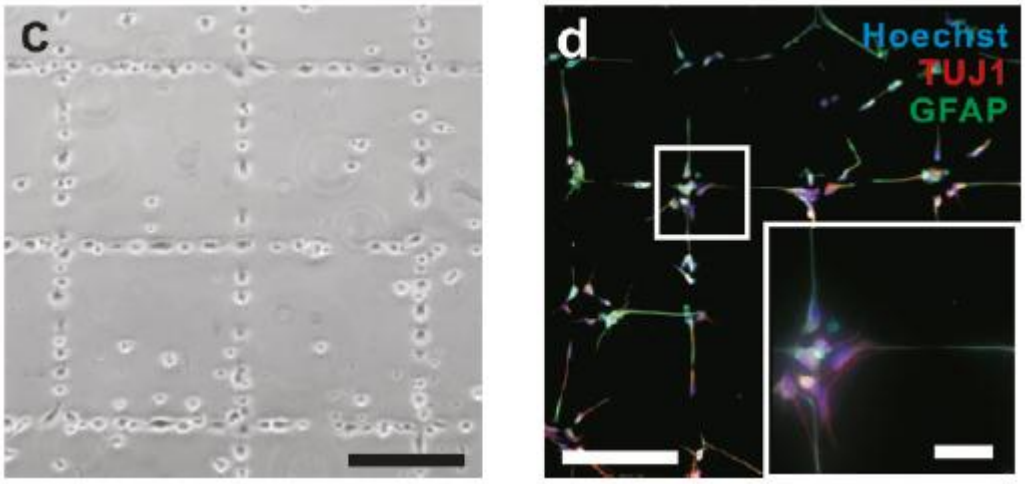

Figure 14. hNSC growth and differentiation on biocompatible and flexible PI substrate with CNT pattern. Phase contrast image of selective hNSC adhesion on CNT patterns on PI after cell seeding. Scale bar represents 200 μm **(c)**. Immunofluorescence image of the differentiated hNSCs on CNT patterns on PI (TUJ1 for neural cells and GFAP for astroglial cells). The inset shows the magnified image of the region marked by the white solid square. Scale bar represents 200 μm, and that of the inset represents 50 μm. It should be noted that the orientation-controlled neural networks were constructed along the CNT patterns on the PI membrane **(d)**. (Adapted from Park et al., 2011).

Thanks to their conductivity stable in biological environment and able to boost neuronal electrical signaling, their nanotopographical features resembling neuronal processes and the possibility to be conjugated with bioactive molecules and polymers, CNTs show the great potential to be used as implants where long-term extracellular molecular cues for neurite outgrowth are necessary. Furthermore, their nanometer dimensions, low impedance and high conductivity allow their use to develop stimulating electrodes to replace lost neuronal functions. Therefore, CNTs seem to be at the meeting point between neural regeneration strategies and neural prosthetics and further open up new avenues for biomedical applications.

1.4.2 CNT CYTOTOXICITY

The CNT cytotoxicity is still a debated issue and mainly concerns with types, functionalization and doses of CNTs being employed and the cell populations

tested. Pristine CNTs are water insoluble and packed in bundles or aggregates in aqueous solutions. They usually have impurities, typically amorphous carbon, graphite nanoparticles, and transition-metal catalyst particles that have been shown to create cytotoxicity both *in vitro* and *in vivo*:

- CNTs can penetrate the cells membranes, then being eliminated through renal excretion; for these reasons and thanks to their high loading capacity, CNTs have been widely investigated as drug delivery agents (Lacerda et al., 2008). However, depending on their length, CNTs can accumulate in the cytoplasm leading to cell death (Porter et al., 2007);

- insoluble pristine CNTs form bundles or aggregates in aqueous solutions. It was reported that, after intraperitoneal administration in mice, SWCNT bundles above 10 μm in length may induce granuloma formation (Kolosnjaj-Tabi et al., 2010);

- transition-metal catalyst may induce the formation of oxygen reactive species (ROS) with oxidative stress (Pulskamp et al., 2007).

The problem with impurity and insolubility has now been alleviated using a number of purification techniques and a wide variety of noncovalent and covalent methods for CNT functionalization. This strongly improved CNT level of biocompatibility (Cui et al., 2010). Therefore, it is very important to optimize type, doses, length and functionalization of CNTs being employed for each specific application.

1.5 PROTEINS INVOLVED IN NEURITE OUTGROWTH

1.5.1 L1CAM

Neural L1 cell adhesion molecule (L1CAM) plays a pivotal role in correct CNS development in humans, as it is involved in several activities important to CNS maturation, including neurite outgrowth, adhesion, fasciculation, migration, myelination and axon guidance. L1CAM promotes these cellular activities by interacting with a diverse group of CAMs, ECM molecules and signaling receptors through homo- and heterophilic interactions involving its extracellular region. L1 is composed of six immunoglobulin (Ig)-like domains and five fibronectin (Fn) type-III repeats in the extracellular region, a single pass transmembrane region and a short cytoplasmic tail. Tertiary structure of L1 is as yet unsolved; however, it is likely that the first four Ig domains Ig1-Ig4 exist in a dynamic equilibrium between extended and folded (horseshoe) conformations similar to that of the related proteins hemolin and axonin-1. L1 is exposed at the surface of both differentiating and differentiated neurons as well as on glial cells and it binds to a diverse set of molecules, sending intracellular signals through its cytoplasmic region (Kenwrick et al, 2000; Haspel et al., 2003). Two soluble forms of the L1 extracellular domain can be generated by proteolytic cleavage within the third Fn repeat or between the fifth one and the transmembrane region. Such soluble forms are able to promote neurite elongation by “conditioning” the extracellular matrix (Kalus et al., 2003; Maretzky et al., 2005). In particular, neurite outgrowth is triggered by homophilic binding in *trans* occurring between two L1 molecules that activate fibroblast growth factor receptors (FGFR) (Kenwrick et al., 2000). Even though it has been demonstrated that the Ig1-Ig4 region is the minimal contiguous segment necessary to mediate homophilic binding (Gouveia et al., 2008), a larger segment encompassing Ig1-Ig6 is needed to reproduce the biological potency of native L1 (Haspel et al., 2000; De Angelis et al., 2002).

Interestingly, a particular 14 amino acid long region was mapped within the 2nd Ig domain (Ig2) as a key fragment necessary for the initial interaction between two L1 molecules. Zhao et al., in 1998 produced this region as a synthetic peptide (called L1-A: 178-HIKQDERVTMGQNG-191) and demonstrated its capacity to mediate adhesion. In particular, they mixed GST-Ig2-conjugated covaspheres with L1-A peptide before seeding onto a substratum coated with GST-Ig2 and L1-A was found to inhibit binding of covaspheres to substrate-coated GST-Ig2, possibly because of peptide competition for the homophilic binding between the two Ig2 domains. As a negative control, they used a number of designed mutants. One such mutant, R184A, is of special interest as it resulted in fully impaired activity (inability to bind to Ig2 domain), hence underling the importance of the conserved Arg residue in L1 homophilic binding (Zhao et al, 1998). It is noteworthy that mutations regarding Arg 184 are causative for CRASH (Corpus callosum hypoplasia, Retardation, Adducted thumbs, Spasticity and Hydrocephalus) syndrome and the most severe phenotype known is given R184Q substitution (De Angelis et al., 2002).

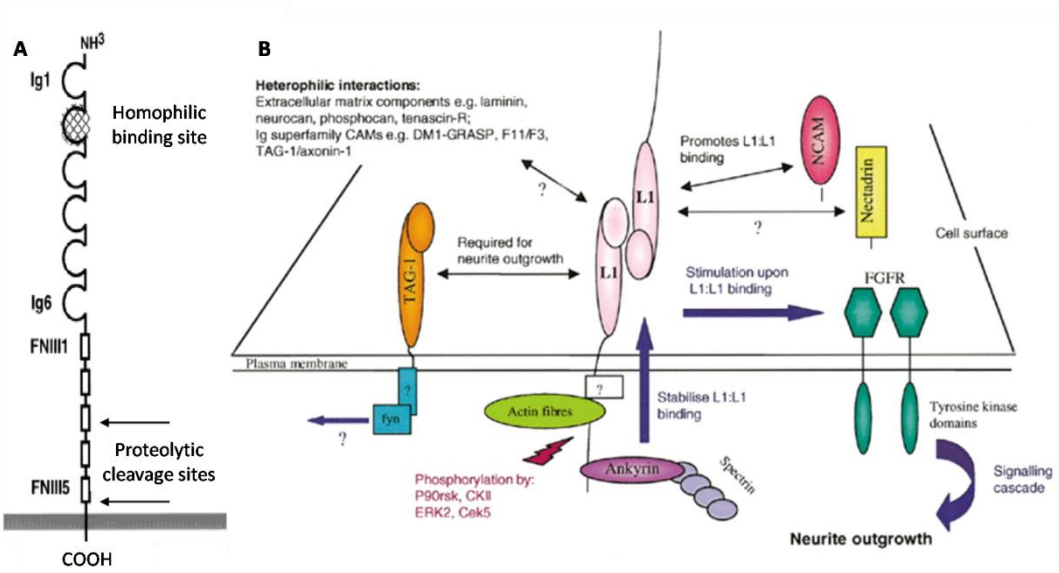

Figure 15. Schematic representation of L1 ectodomain and signaling activated by the homophilic binding. L1 ectodomain is composed by six Ig-like domains (Ig1–6) and five fibronectin type III domains (FnIII1–5). Proteolytic cleavages within repeat Fn3 and between Fn5 and the transmembrane region generate L1 ectodomain soluble forms **(A).** L1 homophylic binding is mediated by the Ig2 domain and activates FGFR stimulating neurite outgrowth **(B)** (adapted from Kamiguchiet et al., 1997 **(A)** and from Kenwrick et al., 2000 **(B)**).

1.5.2 LINGO1

Leucine rich repeat (LRR) and Ig-like domain containing Nogo receptor interacting protein (LINGO1) is a transmembrane protein that is selectively expressed in the CNS and plays an important role in neurite outgrowth control. LINGO1 is formed by 12 LRR motifs flanked by N- and C-terminal capping domains, one Ig-like domain, a transmembrane region and a short cytoplasmic tail. This latter contains an epidermal growth factor receptor (EGFR)-like phosphorylation site (Tyr 591). LINGO1 is highly conserved evolutionarily, with human and mouse orthologues sharing 99.5% identity (Mi et al., 2004; Llorens et al., 2008). LINGO1 forms at the neuron surface a complex with Nogo66-Receptor NgR1 (ligand binding subunit) and the neurotrophin receptor p75 (transducing subunit). NgR1/LINGO1/p75 complex interacts with Mag/NogoA/OMgp complex at the oligodendrocyte surface and inhibits neurite elongation by activating RhoA pathway (Mi et al., 2004). NgR1/LINGO1/p75 complex also interacts with neuronal NogoA, thus blocking neurite elongation and generating repulsion between neurites (Petrinovic et al., 2010). Moreover, LINGO1 can homophilically interact in *trans,* suggesting that LINGO1 molecules from adjacent neuronal and oligodendrocytic membranes might interact and inhibit oligodendrocyte final differentiation (Jepson et al., 2012). Furthermore, LINGO1 interacts with both EGFR and Tyrosine receptor kinase B (TRKB) inhibiting Akt signaling pathway and hence survival and neurite outgrowth (Inoue et al., 2007; Fu et al., 2010). Recent evidence shows that, despite LINGO1 extracellular domain is composed by twelve LRR and one Ig domain, this latter alone mediates homophilic binding and heterotypic interactions (Stein et al.; 2012). The LRR domain, instead, is mainly involved in homotetramerization and in hindering potential interactions with partners by the highly glycosylated concave faces of its extended, arc-shaped architecture (Mosyak et al., 2006). LINGO1 expression is high during embryo development to maintain the growing axons *en route* and away from uncorrect targets; its expression decreases during post-natal life but it is upregulated again

after injury to avoid regeneration (Mi et al., 2004). Furthermore, LINGO1 is involved in several CNS diseases: LINGO1 is an interacting partner of the amyloid precursor protein (APP) *in vivo* and cellular co-expression of LINGO1 with APP was found to augment the release of the αβ peptide, the presumed causative agent of Alzheimer's disease (Bai et al., 2008). Moreover, LINGO1 interacts with the APP only thanks to its Ig domain (Stein et al., 2011). LINGO1 seems to be involved also in Parkinson's disease (PD) and multiple sclerosis as its expression has been found elevated in the substantia nigra of PD patients (Inoue et al., 2007) and in oligodendrocyte progenitor cells from demyelinated white matter of multiple sclerosis post-mortem samples (Mi et al., 2013). *In vitro* and *in vivo* studies showed that LINGO1 inhibition (dominant-negative LINGO1 transmembrane form, soluble LINGO1-Fc; anti-LINGO1 antibodies) promotes neurite elongation, neuron and oligodendrocyte survival, axon regeneration, oligodendrocyte differentiation, remyelination and functional recovery (Mi et al., 2004; Ji et al., 2006; Inoue et al., 2007; Mi et al., 2013; Fernandez-Enright et al., 2014).

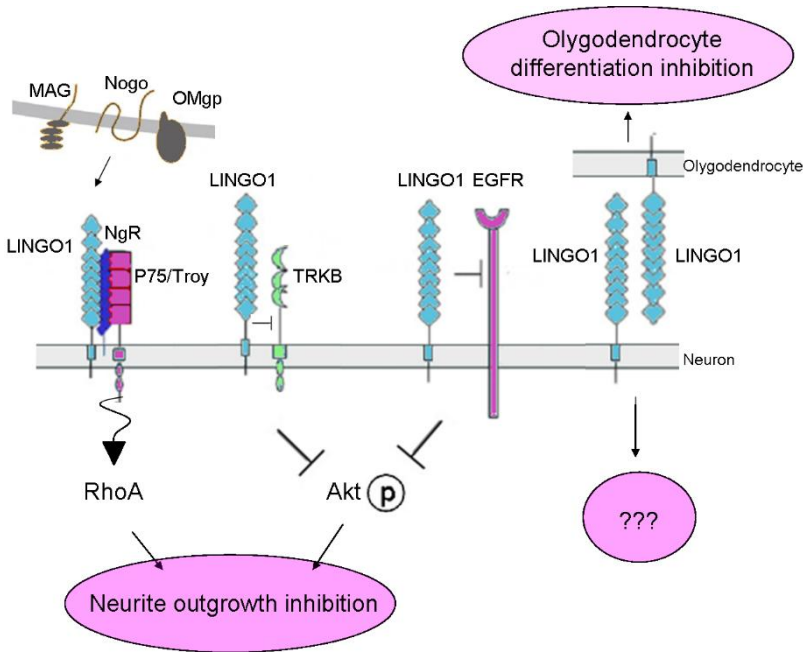

Figure 16. Signaling pathways for LINGO1 function. Neuronal NgR1/LINGO1/p75 complex interacts with Mag/NogoA/OMgp complex at the oligodendrocyte surface and inhibits neurite elongation by activating RhoA pathway. LINGO1 blocks TRKB and EGFR activation by inhibiting Akt signalling and neurite outgrowth. The homophilic binding between two LINGO1 molecules inhibits oligodendrocyte final differentiation, but effects at the neuronal level are still poorly understood.

Therefore, LINGO1 seems to be one of the molecules responsible for CNS neurons inability to regenerate and thus it represents an ideal candidate for therapeutic targets in neural dysfunctions because of its restricted tissue distribution.

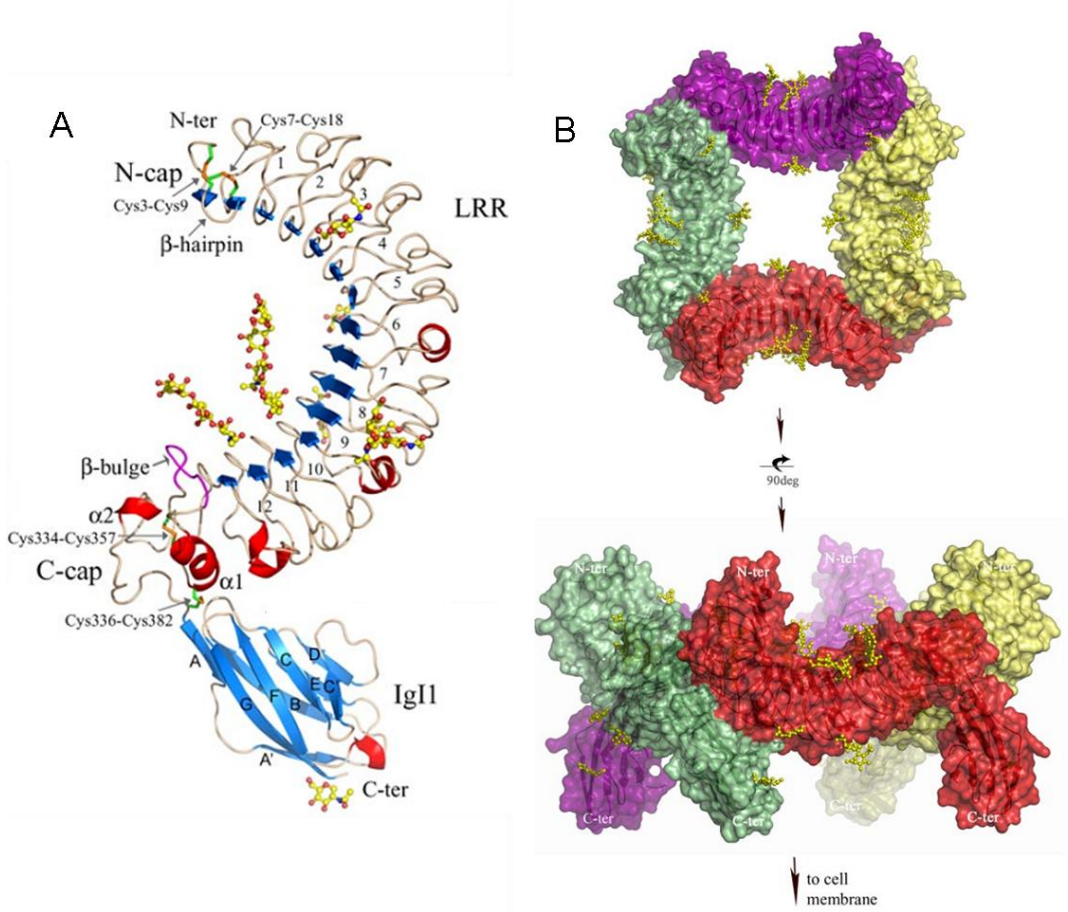

Figure 17. LINGO1 ectodomain structure. Ribbon diagram showing the overall architecture of the LINGO1 monomer, coloured according to secondary structure: beige, coil; blue, ß strand; red, α-helix. Disulfide bonds are shown in green, and N-linked carbohydrates are yellow **(A)**. View of the top and front surfaces of the LINGO1 tetramer, rendered in red, green, magenta, and yellow. The two views are related by 90° rotation with respect to the horizontal axis. Carbohydrate are shown as yellow sticks. The LRR modules interlock the ring head-to-tail, back-to-back and the Ig domains extend vertically. The bottom view illustrates the putative orientation of the tetramer relative to the cell surface **(B)**. (adapted from Mosyak et al., 2006).

1.6 STEM CELLS AND NEURONAL DIFFERENTIATION

1.6.1 STEM CELLS IN REGENERATIVE MEDICINE

Regenerative therapeutics using stem cells is a promising approach for the treatment of a variety of neurological diseases and both PNS and CNS injuries. Stem cells have multipotency to differentiate into specific lineages under different inducing conditions, making them a powerful tool for the regeneration of the biological function of injured tissues (Kim et al., 2012). It is well known that the interaction between stem cells and the extracellular microenvironment is critical in controlling stem cell differentiation. Control of cell fate determination can be achieved by creating a niche that mimics the ECM surface topography, mechanical properties, and chemical microenvironment (Chao et al., 2009). Concerning neuronal regeneration, it is important to ensure both complete neural induction of cells and morphological guidance of neurite outgrowth, thus facilitating the formation of an effective neural network (Park et al., 2011; Kim et al., 2012).

1.6.2 STEM CELLS FOR NEURAL REPAIR

Different types of stem cells have the potential to be exploited in neurological application. Embryonic stem cells (ESCs) are pluripotent stem cells that can be isolated from the blastocyst, an early-stage embryo. ESCs cells represented a promising source for cell transplantation because of their ability to differentiate into all somatic cell lineages, but their clinical use has remained somewhat hampered by the ethical implications of using human embryos. However, use of human induced pluripotent stem cells (iPSc) rather than ESCs begun to help overcome these issues. However, the tumorigenic potential of iPSCs remains a

great concern. Neural stem cells (NSCs) are thought to be an optimal cell source for the treatment of neurological disorders because of their potential to differentiate into cells of glial and neuronal lineage.However, there are ethical problems surrounding the use of foetal tissues associated with abortion and they are difficult to isolate from autologous brain biopsies. Mesenchymal stem cells (MSCs) are adult stem cells that are found mainly in the bone marrow; despite their mesenchymal origin, they showed the ability to differentiate into neurons under proper conditions and they offer the possibility of the autologous transplant (Wang et al., 2013). However, they are generally isolated from the iliac crest of the patient and therefore through a quite invasive method. A very valid alternative is represented by circulating multipotent cells (CMCs) thanks to their accessibility and the potential to differentiate into neurons (Di Liddo et al., 2012a-b).

1.6.2.1 Human circulating multipotent cells (hCMCs)

hCMCs are adult stem cells isolated by ficoll density gradient separation from human donor peripheral blood. hCMCs are mononucleated and have fibroblastic morphology during long term culture with a doubling population time of 48 hours over 31 passages; they show by flow cytometry immunophenotypical similarities to mesenchymal stem cells (CD105, CD166, CD73, CD29) and meso-angioblasts (CD34) (Di Liddo et al., 2012a). hCMCs have an intrinsic trophic activity able to establish a regenerative microenvironment at sites of tissue damage. Indeed, they secrete several cytokines and growth factors able to control their own proliferation and differentiation. hCMCs have been shown to be extremely sensible to changes in culture conditions that lead to sudden gene expression shifts and cell differentiation. They can be differentiated into progenitors for several mesenchymal tissues as adipocytes, osteoblasts, chondroblasts or muscle cells and; when treated with specific cocktails of growth factors, they are capable of neuronal differentiation as confirmed by immunoblot

analysis of the expression of TUBβ3 (Tubulin β III), MAP2 (Microtubule associated protein 2), NeuN (Neuronal nuclear antigen), SYP (Synaptophysin), Musashi, NCAM, dopamine transporter (DAT) and neurofilaments (NFM) (Di Liddo et al. 2012b).

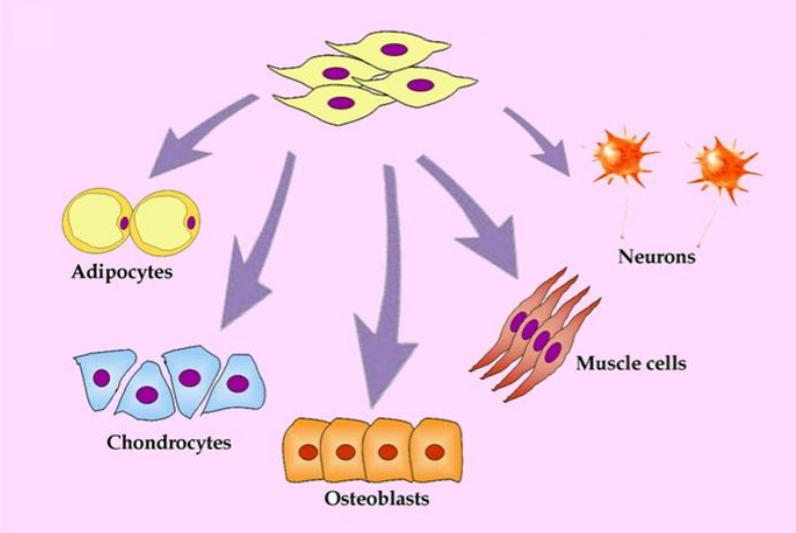

Figure 18. hCMCs differentiation into different cell types. hCMCs are isolated from peripheral blood and have the ability to differentiate into adipocytes, chondroblasts, osteoblasts, muscle cells and neurons under proper culture conditions.

The high degree of plasticity and the expression of a peculiar pattern of surface antigens not attributable to other defined adult stem cell populations, are consistent with the hypothesis that hCMCs belong to a new adult stem cell niche. These cells represent an attractive option for a wide range of regenerative medicine applications as hCMCs are (i) free from tumorigenisis risk sometimes associated to induced pluripotent stem cells (iPSCs), (ii) accessible, (iii) not subjected to ethical restrictions and (iv) a valid method to avoid rejection problems thanks to the autologous transplant.

1.6.3 NEURONAL MARKERS

Some of the markers that are generally analyzed to evaluate the differentiation of stem cells toward the neuronal lineage are the follows:

- Nestin is a class IV intermediate filament protein and a neural progenitor marker, therefore it is highly expressed in undifferentiated cells during nervous system development. After cell differentiation into neurons or glial cells, Nestin expression decreases and it is substituted by cell type-specific intermediate filament proteins like Neurofilament (neurons) and glial fibrillaracidic protein (GFAP) (astrocytes) (Dahlstrand et al., 1995).

- TUBβ3 is a class III specific β tubulin peculiar for neuronal cells expressed both in immature and mature neurons (including cells committed to a neuronal fate that are just post mitotic) (Zahir et al., 2009). TUBβ3 contributes to microtubule stability and has an important role in neuronal architecture formation and maintenance, neurite outgrowth, axon guidance and axonal transport (Tischfield et al., 2010).

- MAP2 is expressed mainly in neurons, but has also been detected in some non-neuronal cells such as oligodendrocytes and astrocytes. Its expression is very weak in neuronal precursors and then becomes strong after the expression of neuron-specific TUBβ3. MAP2 has a microtubule stabilizing activity and regulates microtubule networks in the axons and especially in the dendrites, determining their shape during neuron development. Moreover, MAP2 interacts with filamentous actin exerting a critical role in neurite initiation, during which networks of microtubules and filamentous actin are reorganized in a coordinated manner (Dehmelt et al., 2005).

- Vesicle associated membrane protein 7 (VAMP7) is a SNARE protein implicated in neurite elongation (Martinez-Arca et al., 2001). Indeed, VAMP7 is associated to vesicles involved in the transport of lipids and proteins from the Golgi apparatus to the extensions of plasma membrane generating neurites. One out of proteins carried by VAMP7-vescicles is neuronal L1CAM; since this protein is transported at the protruding sites of plasma membrane and exposed at the neuronal surfaces, it

homophilically binds to other L1 molecules from the adjacent cell membranes, thus stimulating neurite outgrowth (Alberts et al., 2003).

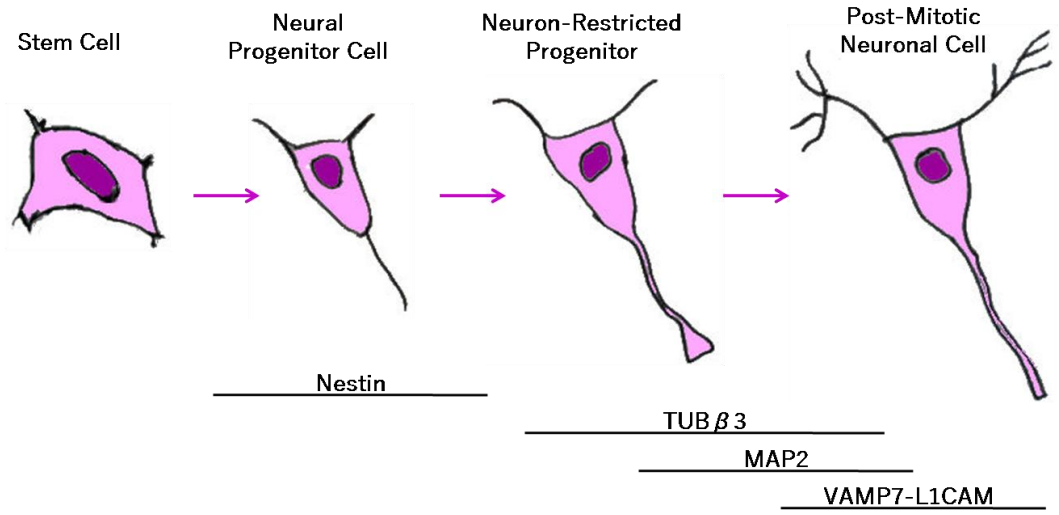

Figure 19. Appearance of neuronal markers during development. Nestin is highly expressed in neural progenitors cells, therefore in cells able to differentiate into neurons, oligodendrocytes or astrocytes. After neuronal commitment, Nestin expression decreases while neuron-restricted progenitor cells begin to express TUBβ3 and MAP2. During neuronal maturation, VAMP7 and L1CAM are also expressed.

1.6.4 STEM CELLS CULTIVATED ONTO CNT-BASED SCAFFOLDS

A number of scaffolds have been suggested to control cell adhesion, migration, proliferation, and differentiation for tissue engineering. Despite the unique abilities of cell patterning techniques, there are still some limitations in creating three-dimensional structures able to properly mimic ECM. Recently, a variety of nanomaterials including nanoparticles, CNTs, nanofibers and nanoscale-substrates have been developed to efficiently control dynamic cellular behaviour such as cell growth, migration and differentiation.

Indeed, it has been shown that both embryonic, mesenchymal and neural stem cells cultivated onto CNT-based scaffolds acquire the commitment towards neurogenesis when coupled with chemical soluble factors. Jan et al., in 2007

showed that mouse NSCs - when cultivated in differentiating medium - can then successfully differentiate into neurons, astrocytes, and oligodendrocytes with clear formation of neurites onto SWNT films. Chao et al., in 2010 showed that hESCs seeded onto a Poly(methacrylic acid)-grafted CNT scaffolds and treated with laminin are induced to express the neuron specific markers TUBß3 and Synapsin I while staminality marker Oct4 is decreased. Chen et al., in 2012 obtained almost the same results by seeding hESCs onto a silk-CNT composite coated with laminin: increased expression of Nestin and TUBß3 and enhanced axonal length demonstrated that hESCs differentiate in the presence of CNT better than onto silk-only composites or poly-L-ornithine coated coverslips. Kim et al., in 2012 showed that neuronal differentiation of human hMSCs cultivated in a neurogenic medium can be improved when seeding cells onto CNT sheets. Further works showed that stem cells can achieve neuronal commitment either in the absence of neuronal stimulating conditions: e.g., Shridharan et al., in 2009 cultivated hESCs onto a collagen/CNT matrix in the absence of inducing medium and showed that cell differentiation occurs toward the ectodermal lineage, as suggested by the strong expression of Nestin. Tay et al., in 2010 demonstrated that MSCs preferentially adhere in SWCNT covered coverlips respect to naked ones and cells showed a transient expression of Nestin and MAP2 genes while no upregulation of osteogenic markers were revealed, showing for the first time than the only CNT nanoroughness is of use to promote neuronal differentiation. Moreover, Chen et al., in 2013 showed that carboxylated MWCNT films deposited onto a collagen coated dish promotes hMSC neural differentiation through the upregulation of neural growth factors and trapping these neural growth factors to create a suitable environment for long-term neural differentiation. Furthermore, also Lee et al., in 2014 showed that CNT-collagen three dimensional cultures of rat MSCs promotes the expression of neural phenotypes and secretion of neurotrophic factors.

1.7 SH-SY5Y CELL LINE

SH-SY5Y cell line is a human catecholaminergic neuroblastoma derived from a thrice cloned subline SK-N-SH cells, which were originally established from a bone marrow biopsy of a neuroblastoma patient in the early 1970's. SH-SY5Y cells resembles immature neuroblasts in culture and are typically locked in an early neuronal differentiation stage, biochemically characterized by low presence of neuronal markers (Lopes et al., 2010). However, SH-SY5Y cells are able to acquire neuron-like phenotypes with neurite outgrowth and branches upon treatment with a variety of agents, including all-*trans*-retinoic acid (RA), phorbol ester, 12-O-tetradecanoylphorbol-13-acetate (TPA), BDNF, dibutyryl cyclic AMP (dBcAMP), purine, or staurosporine (Xie et al., 2010). The most widely used differentiating method is the treatment with RA which is an active metabolite of vitamin A. RA functions by binding to two families of nuclear receptors: the RA receptors (RARs) family (RARa, b and g), and the retinoid X receptors (RXRs) family (RXRa, b and g). Activated RAR heterodimerizes with RXR, then binding of RAR/RXR heterodimers to RA response element (RARE) results in transcriptional activation (Joshi et al., 2006). Indeed, RA treatment of SH-SY5Y cells stimulates the neurite outgrowth and a progressive length increase (depending on time of exposure); moreover, it also promotes the synthesis of neurospecific enzymes, neurotransmitters, changes in cytoskeletal markers and electrophysiologic modifications, as seen in normal neurons (Costantinescu et al., 2007). Therefore, SH-SY5Y share many biochemical and functional properties with neurons, hence representing a model system of special help in studying molecular mechanisms underlying neuronal differentiation. RA treatment also induces the expression of TRKB, which is the high affinity catalytic receptor for several neurotrophins, including BDNF. BDNF binding to TRKB activates pathways controlling cell differentiation (Edsjö et al., 2003). RA also plays a role in regulating transition from the proliferating precursor cell to post-mitotic differentiated cell; indeed, after *in vitro* treatment with RA, SH-SY5Y cells arrest in the G1-phase of the cell

cycle, DNA synthesis is inhibited and growth inhibition is detected 48 h after treatment (Costantinescu et al., 2007).

2. AIM OF THE PROJECT

Neural regeneration is a complex mechanism that can be aided by scaffolds able to recapitulate the features of the native tissue environment. The purpose of my thesis work has been to design and test scaffolds incorporating multiple cues in order to provide cells with information important for their growth and differentiation. In particular, my PhD project followed two main steps:

1) DEVELOPMENT OF THE BIOMIMETIC SYSTEM:

- Designing a freestanding scaffold made of carbon nanotubes (CNTs) dispersed in a poly-L-lactic (PLLA) matrix and testing its ability to support SH-SY5Y cell adhesion growth and differentiation;
- Designing peptides derived from specific L1 and LINGO1 motifs and testing their ability to induce SH-SY5Y differentiation;
- Combining scaffolds and peptides to further improve cell differentiation.

2) IMPROVEMENT OF THE BIOMIMETIC SYSTEM:

- Electrospinning of the CNT-PLLA matrix to further mimic neuronal extracellular environment;
- Mutagenesis of specific peptide amino acid residues for a preliminary characterization of their mechanism of action;
- Testing scaffolds and peptides with human circulating multipotent cells (hCMCs) in order to use a cell populations suitable for regenerative medicine applications and to evaluate if scaffolds and peptides are able to induce such stem population to differentiate toward the neuronal lineage.

3. METHODS

3.1 SCAFFOLD PREPARATION AND CHARACTERIZATION

3.1.1 CNT-PLLA SCAFFOLD

Commercially available MWCNTs (Sigma) were purified by two-steps treatment at high temperature, dispersion in aqueous HCl (37%), sonication and membrane filtration. MWCNTs were methoxyphenyl (PhOMe)-functionalized and dissolved with PLLA in chloroform under mild sonication. The resulting dispersion was drop-cast onto a glass dish to obtain the MWCNT-PhOMe@PLLA 1% scaffold. MWCNTs were characterized by micro-Raman spectroscopy, thermogravimetric analyses (TGA) and differential scanning calorimetry (DSC) analyses. Electrical resistance of the CNT-PLLA composite was measured by using a digital multimeter. For full methods, see Scapin et al, 2014.

3.1.2 ELECTROSPUN CNT-PLLA SCAFFOLD

The electrospun-CNT-PLLA (eCNT-PLLA) scaffolds were prepared using the same CNT-PLLA scaffold solution and processed with the electrospinning technique. Electrospinning was performed by passing the solution through an 18G needle at a flow rate of 0.03 ml/min, and applying an acceleration voltage of 18 kV, where a positive charge was applied to the solution, and the collector was electrically grounded at a working distance of 14 cm. The electrospinner was set up such that the needle was oriented vertically, and the fibre collector was placed directly underneath the needle. Fibres were collected onto 13 mm diameter

glass coverslips deposited onto a paper. The process was carried out at room temperature within a range of relative humidity (RH = 45–50 %).

All scaffolds were synthesized and characterized by prof. Menna group (Department of Chemical Sciences University of Padua).

3.2 PEPTIDE SYNTHESIS AND CHARACTERIZATION

LINGO1-A (467SAKSNGRLTVFPDG480), scrambled LINGO1-A_scr (TVFSRSKPLGNDGA), L1-A (178HIKQDERVTMGQNG191), scrambled L1-A_scr (IVDQGNREMGTKHQ), L1-A R184A (HIKQDEAVTMGQNG) and L1-A R 184Q (HIKQDEQVTMGQNG) peptides, and N-terminally fluoresceinated derivatives of L1-A and LINGO1-A were synthesized by the solid-phase method, purified to homogeneity (>98%) by reversed-phase high-performance liquid chromatography (RP-HPLC) and characterized by high-resolution mass spectrometry. The conformation of the peptides was analyzed by circular dichroism (CD) on a Jasco J-810 spectropolarimeter, equipped with a Peltier temperature control system. For full methods, see Scapin et al, 2014

All peptides were synthesized and characterized by prof. De Filippis group (Department of Pharmaceutical and Pharmacological Sciences University of Padua).

3.3 CELL CULTURE, DIFFERENTIATION AND EXPERIMENTAL DESIGN

3.3.1 SH-SY5Y

Exponential growing human neuroblastoma SH-SY5Y cells (Ross et al., 1983), were cultured with Dulbecco's Modified Eagle Medium/Nutrient Mixture F-12 (DMEM/F-12) GlutaMAX™ supplement (Invitrogen) supplemented with 10% heat-inactivated foetal bovine serum (FBS, Euroclone) and 25μg/ml gentamicin (Sigma) (growth medium), in humidified atmosphere of 5% of CO2 in air at 37 °C. Cultures were maintained by subculturing 900000 cells into 25 cm^2 flasks (Sarstedt) every 2 days (once they reached 90% confluence). Cell differentiation was induced by treating cells with all-*trans*-retinoic acid (RA, Sigma) at 10 μM concentration and lowering the FBS in the culture medium to 2% (differentiation medium) 24 h after seeding. In undifferentiated control samples, Dimethyl sulfoxide (DMSO) was added as equivalent amount (in which RA is dissolved). In experiments with peptides added to culture medium, cells were seeded in a 24-well plate (15000 cells/well) coated with gelatine (Sigma, porcine skin 0.005% in H2O milliQ)/poly-L-lysine (Invitrogen, 1μg/ml) solution. 24h after cell seeding (day 0), the growth medium was replaced by the differentiation medium; then, 24h after RA induction (day 1) peptides were added to the culture medium to asses if they can influence cell viability/proliferation and promote/inhibit neurite elongation. Peptides are not present in control samples. Cell viability and proliferation were assessed at all time points (days 0, 1, 2), while neurite lengths were measured 24 h after the peptides addition (day 2). In experiments with peptides adsorbed onto the substrate, peptides dissolved in gelatine solution were adsorbed onto the bottom of a 24-well plate prior to cell seeding (15000 cells/well). Culture wells coated with poly-L-lysine were used as control. 24 h after cell seeding (day 0), the growth medium was replaced by the differentiation

medium. Cell viability and proliferation were assessed at three time points (days 0, 1 and 4) or four time points (days 0, 1, 4 and 7) while neurite lengths were measured at day 4. In order to determine the percentage of adsorbed peptides, the fluorescein isothiocyanate (FITC)-conjugated version of peptides were used to coat well bottoms. Briefly, peptides were dissolved in a gelatine solution and incubated in a 24-well plate; then the fluorescence was measured with a plate reader (Ascent Fluoroscan, excitation 485 nm, emission 538 nm). Three hours after incubation, wells were washed 2 times with PBS and fluorescence was measured again in order to calculate the percentage of peptides adsorbed onto the wells. In experiments with cells seeded onto the scaffolds, PLLA and CNT-PLLA sheets were cut into round slices with 13 mm diameter to be well suited for positioning in 24-well plates. After sterilization by UV irradiation, PLLA and CNT-PLLA scaffolds were incubated for 3h with FBS and then cells (15000/well) were seeded onto their surfaces. 24 h after cell seeding (day 0), the growth medium was replaced with differentiation medium. Culture wells coated with poly-L-lysine were used as control. Cell distribution (between scaffold and well bottom) analysis was performed at day 0, cell viability and proliferation were assessed at days 0 and 2 and neurite lengths were measured at day 2. In experiments with cells growing onto CNT-PLLA scaffolds and treated with peptides, the CNT-PLLA scaffolds were incubated for 3 h with FBS and then cells (15000/well) were seeded on their surfaces. 24 h after cell seeding (day 0), the growth medium was replaced with differentiation medium and 24 h after RA induction (day 1) the peptides (1μM L1-A or LINGO1-A) were added to culture medium. Culture wells coated with poly-L-lysine were used as control. Cell viability and proliferation were assessed at days 0, 1 and 2, while neurite lengths were measured at day 2. In experiments with cells seeded onto the electrospun scaffolds, fibre covered coverslips were removed from the paper support to be well suited for positioning in 24-well plates. After sterilization by UV irradiation, ePLLA and eCNT-PLLA scaffolds were incubated for 3h with FBS and then cells (15000/well) were seeded onto their surfaces. 24 h after cell seeding (day 0), the growth

medium was replaced with differentiation medium. Culture wells coated with poly-L-lysine were used as control. Cell distribution (between scaffold and well bottom) analysis was performed at day 0, cell viability and proliferation were assessed at days 0 and 2 and neurite lengths were measured at day 2.

3.3.2 HUMAN CIRCULATING MULTIPOTENT CELLS (hCMCs)

hCMCs were isolated by ficoll density gradient separation from human donor peripheral blood and gently provided by prof. Di Liddo group (Department of Pharmaceutical and Pharmacological Sciences University of Padua). In experiments with cells seeded onto the scaffolds, CNT-PLLA sheets were cut into round slices with 13 mm diameter to be well suited for positioning in 24-well plates. After sterilization by UV irradiation, CNT-PLLA scaffolds were incubated for 24h in the culture medium. Then cells (12000/well) were seeded onto scaffold surfaces in complete growth medium (DMEM/F12 supplemented with 16.5% of heat-inactivated FBS and 50 U/ml penicillin - 50 μg/ml streptomycin). Cells were maintained in humidified atmosphere of 5% of CO2 in air at 37 °C. 24 h after cell seeding (day 1), the growth medium was replaced with differentiation medium (DMEM/F12 supplemented with 2% of heat-inactivated FBS, 50 U/ml penicillin - 50 μg/ml streptomycin and RA 10 μM). In undifferentiated control samples, DMSO was added as equivalent amount (in which RA is dissolved). Cells were maintained in culture for five days after cell seeding and analyses were performed at the following time points: cell proliferation, days 1, 3 and 5; morphological observations, day 1; qPCR experiments, days 1, 3 and 5; immunofluorecence, day5. In experiments with peptides added to culture medium, cells were seeded in 24-well plates (12000 cells/well) in complete growth medium. 24h after cell seeding (day 1), the growth medium was replaced by the differentiation medium; then, 24h after RA induction and the lowering of FBS (day 2) peptides (1 μM concentration) were added to the culture medium to asses if they can influence cell proliferation and differentiation. Peptides are not

present in control samples. Cell proliferation was assessed at days 1, 3 and 5 while qPCR experiments were performed at day 3 and 5. In experiments with cells seeded onto the eCNT-PLLA scaffolds, fibre covered coverslips were removed from the paper support to be well suited for positioning in 24-well plates. After sterilization by UV irradiation, eCNT-PLLA scaffolds were incubated for 24h in the culture medium. Then cells (12000/well) were seeded onto scaffold surfaces in complete growth medium. 24 h after cell seeding (day 1), the FBS concentration was reduced to 2%. Morphological observations and qPCR analyses were performed at day 1.

3.4 ANALYSIS OF CELL VIABILITY/PROLIFERATION AND NEURONAL DIFFERENTIATION

3.4.1 CELL PROLIFERATION

Resazurin reduction assay was performed to quantify the metabolically active living cells and thus to monitor how do peptides and the scaffolds affect cell proliferation of the cell populations tested. The assay is based on reduction of the indicator dye, resazurin (not fluorescent), to the highly fluorescent resorufin (excitation 569 nm, emission 590 nm) by viable cells. Non-viable cells rapidly lose their metabolic capacity to reduce resazurin and, thus, do not produce fluorescent signals anymore. Briefly, the culture medium was substituted with 500 µL of resazurin solution (Resazurin Sigma 15 µg/mL in complete medium without phenol red) and cells were incubated for 4 h in dark at 37°C and 5% CO2. Then, 200 µL of resazurin solution were removed twice from each well and transfer to a 96 well plate (technical duplicates). Fluorescence, directly correlated with cell quantity, was read in a plate reader (Ascent Fluoroscan, excitation 540 nm, emission 590 nm). Background values from wells without cells were subtracted and average values for the duplicates calculated. Cell

proliferation was calculated from a calibration curve by linear regression using Microsoft Excel. Resazurin assay was also used for testing cell ability to adhere to the scaffolds. 24 h after cell seeding, scaffolds were removed from the original wells and positioned into clean ones. Both wells were incubated with resazurin solution to quantify the number of cells adherent to scaffold or to well bottom.

3.4.2 CELL VIABILITY

The CytoTox-ONE™ Homogeneous Membrane Integrity Assay (Promega) was used to quantify the lactate dehydrogenase (LDH) release by cells that lose membrane integrity. Briefly, 100 µL of culture medium were transferred to a new 96 well plate. 50 µL of the reaction solution from the kit, containing the detection dye and the catalyst were then added to culture supernatants and fluorescence was measured after 10 minutes in a plate reader (Ascent Fluoroscan, excitation 540 nm, emission 590 nm). Background values from wells without cells were subtracted and average values for the duplicates calculated. Cell death was calculated from a calibration curve by linear regression after 100% cell lysis of known cell quantities. Cytotoxicity was then calculated according to the following equation: Cytotoxicity (%) = (number of dead cells)/(number of dead cells + number of living cells) x100.

3.4.3 NEURITE LENGTH ANALYSIS (SH-SY5Y CELLS)

Neurite outgrowth was measured after staining the cells with calcein acetoxymethyl ester (Calcein-AM, Biotium), a non-fluorescent cell permeable compound that when hydrolyzed by intracellular esterases in live cells converts to the strongly green fluorescent calcein (excitation 490 nm, emission 539 nm). This staining is particularly useful to clearly detect, along their whole length, the neural processes and to visualize cells growing onto the black CNT-PLLA

scaffolds. Briefly, cells were incubated with calcein-AM (2 μM in HBSS, Hank's Balanced Salt Solution, Invitrogen) for 30 minutes in dark at 37°C and 5% CO2 and visualized under a fluorescent microscope (Leica DM4000b) using green fluorescent protein (GFP) filter. Each experiment was performed in duplicate (two wells per conditions). Five images/well were recorded (ten images for each condition), taken with a 20X objective. The first field was set to correspond to the centre of the well. Next fields were then selected following each of the four directions (N, S, W, E) from the first field. Neurite length was measured using LAS AF lite software (Leica) by tracing the trajectory of the neurite from the tip to the junction between the neurite and cell body. If a neurite exhibited branching, the measure from the end of the longest branch to the soma was recorded, then each branch was measured from the tip of the neurite to the neurite branch point. The neuritogenic properties were analyzed in terms of total neurite length/no. of cells (aggregate length of all cellular processes divided by cell number), no. of neurites/no. of cells, no. of branch points/no. of neurites, the percent of neurites longer than 100 μm, no. of growth cones/no. of cells. Only neurites longer than 50 μm were considered (Hu et al., 2004; Munnamalai et al., 2014).

3.4.4 hCMC MORPHOLOGICAL ANALYSES

Cells were stained with Calcein-AM and inspected under the Leica DM 4000b inverted microscope equipped with the GFP filter. Five images/well were recorded (ten images for each condition), taken with a 20X objective. Field selection was performed as reported above. The morphological analyses performed are: no. of polarized cell/no. of cells, total protrusion length/no. of cells, no. of protrusions/no. of cells, total diameter length/no. of cells. The length of each neurite-like protrusion was measured from the cell body edge to the tip of the protrusion. Any protrusion shorter than half the cell body diameter was not recognized as a neurite-like protrusion and therefore cells were not

considered as polarized (Huang et al., 2013). Cell diameter was considered as the longest distance between two edges in the cell body (major axis). Protrusion length and diameter were measured using LAS AF lite software (Leica).

3.4.5 SCANNING ELECTRON MICROSCOPY ANALYSIS

The morphology of eCNT-PLLA scaffold fibres was studied by scanning electron microscopy (SEM); eCNT-PLLA scaffolds were coated with a thin film of gold particles to improve scaffold conductivity. For the analysis of SH-SY5Y cells growing onto CNT-PLLA scaffolds, cells were fixed in 4% paraformaldehyde in phosphate buffered saline (PBS), dehydrated in solutions with increasing ethanol concentration, and air dried. Samples were then coated with a thin layer of gold particles and examined and photographed using a Jeol JSM-6490 SEM.

3.4.6 RNA EXTRACTION AND RETROTRANSCRIPTION

RNA from each sample was obtained after cell homogenization with TrizolTM reagent (Invitrogen), following the manufacturer's instructions. After complete dissociation of nucleoprotein complexes, phase separation was achieved with chloroform and centrifugation at 12000 g. RNA was precipitated from the aqueous phase with isopropanol and washed with 70% ethanol. The RNA was dried and dissolved in RNase-free water. RNA was retrotranscribed in cDNA using GoScriptTM Reverse Transcription System and oligo(dT) primers (Promega). Briefly, 4 μl of RNA were incubated with oligo(dT) primers for 5 minutes at 70 °C for allowing template denaturation and than chilled for 5 minutes in ice. Then, the RNA and the oligo(dT) primers were added to 15 μl of mix solution containing the GoScriptTM reverse transcriptase, MgCl2, PCR nucleotide mix, buffer and the ribonuclease inhibitor. Such reaction mix was then incubated for 5 minutes at 25°C (annealing), 60 minutes at 40°C (extension) and 15 minutes at 70°C

(retrotranscriptase inactivation). After retrotranscription, the integrity of cDNA was checked by control PCR (Polymerase Chain Reaction). The S13 gene was amplified as an housekeeping internal control.

3.4.7 REAL TIME RT-PCR (qPCR)

Gene expression was analyzed by two-step real-time RT-PCR. 1µl of cDNA was used for each qPCR reaction that was performed using Power SYBR® Green PCR Master Mix (Life technologies) in a final reaction volume of 20 µl. The thermal cycler (Rotor-Gene 3000 from Corbett Research) was set as follows: 9' at 95°C followed by 43 cycles consisting of 30" melting at 95°C + 30" annealing at 60°C + 35" extension at 72°C. All primers were tested for their amplification efficiency: the threshold cycle (CT) values of four cDNA dilutions were plotted against the logarithm of input amount of standard material, in order to generate a standard curve. Only those primers having comparable value of the slope were considered. At least three independent experiments were performed in triplicate, each qPCR reaction was run in duplicate (technical replicates) and each gene was run together with its own reference gene and a negative control. The gene encoding human ribosomal protein S13 was used as the housekeeping control for normalization (Vacca et al., 2011). The comparative CT method ($2^{-\Delta C^T}$) was used to quantify gene expression. Melting curve analysis was performed to ensure all transcripts under investigation would be represented by a single peak, as an index for specificity (melting ramp from 70 to 95°C). Data analysis was carried out using the Rotor-Gene software (version 6.1; Corbett). The following forward (F) and reverse(R) primers (SIGMA-Genosys) were used:

S13-F: 5'-TACAAACTGGCCAAGAAGGG-3';
S13-R: 5'-GGTGAATCCGGCTCTCTATTAG-3';
Nestin-F:5'-CAGGGGAGGACTAGGAAAAGA-3';
Nestin-R: 5'- GAGATGGAGCAGGCAAGAG-3';

TUBß3-F: 5’- AGGAAGAGGGCGAGATGTA-3’;

TUBß3-R: 5’- CAATAAGACAGAGACAGGAGCAG-3’;

MAP2-F: 5’- ATAGACCTAAGCCATGTG-3’;

MAP2-R: 5’ -GGGACTGTGTAATGATCTC-3’;

TRKB-F: 5‘-TAGATCCTGAGAACATCACCG-3’;

TRKB-R: 5‘-GGATCAGTTCAGACAAGTCAA-3’;

VAMP7-F: 5’-CACTGATGATGATTTTGAACG-3’;

VAMP7-R: 5’-CTGAGCTACCAGATCTATGTTTCT-3’;

L1 (neuronal)-F: 5’ CCCTGGAGAGTGACAACG-3’;

L1 (neuronal)-R: 5’ CCTGGACTCCACTATTCTAGGG-3’;

LINGO1-F: 5’ TGGTGCTGCTGTTTCTCTG-3’;

LINGO1-R: 5’ CGTGTGTAGAAGGGTAGGGA-3’.

3.4.8 IMMUNOFLUORESCENCE

Five days after seeding, hCMCs were rinsed three times with PBS and then fixed with BD Cytofix™ Fixation Buffer (BD Biosciences) for 20 min at 4°C. hCMCs were then rinsed three times with PBS, permeabilized with 0.2% Triton in PBS for 30 min at room temperature and incubated in blocking solution (5% FBS in PBS) for 30 min at room temperature. hCMCs were then incubated for 1 hour at room temperature with primary antibodies diluted in blocking solution. Mouse anti-neuron specific β-III tubulin (1:200, MAB 1637 Millipore) was used as primary antibody. After 3 washes in PBS, cells were incubated for 1 hour at room temperature with secondary donkey anti-mouse antibody conjugated with Alexa Fluor-488 (Life technologies) at a 1:300 dilution. Nuclei were counterstained using Hoechst 33258 (Life technologies) for 5 min, and then washed three times with PBS. A small amount of PBS was left to keep well surfaces wet hence to avoid monolayer drying. Samples were inspected under the Leica DM 4000b inverted fluorescent microscope using the GFP (TUBβ3) and A4 (nuclei) filters. TUBβ3 and nuclei images were overlapped using LAS AF lite software (Leica).

3.5 BIOINFORMATIC ANALYSES

3.5.1 HOMOLOGY SEARCHES AND STRUCTURAL MODELING

Fold recognition searches were performed using Phyre 2 (Kelley et al., 2009), structural models were obtained by homology modeling using the Swiss model server (Guex et al., 1997). Structural superposition and analyses were performed using USFC Chimera software (Pettersen et al., 2004). Proteome-wide search for orthologous sequences of the L1 Ig2 and LINGO1 Ig domains were performed using corresponding sequences from the human proteins as probes for blastp runs at the blast NCBI server, using default settings, database limitation set to UniprotKB, taxonomic limitation set to Metazoa and excluding fragments (incomplete sequences).

3.5.2 PRIMER DESIGN

Each primer pair consists of specific forward and reverse primers derived from gene sequences contained in the NCBI Reference Sequence database. They were designed in order to produce a 250 bp amplicon crossing exon/exon boundaries whenever possible, to enable amplification of cDNA sequences and to prevent coamplification of genomic DNA. They all are standardized to work at the same temperature (60°C). L1 primers were designed to be specific for the L1 neuronal splicing isoform. Melting temperatures of PCR primers and possible occurrence of hairpins, self- and hetero-dimers was ruled out by Oligoanalyzer 3.1 (http://eu.idtdna.com/calc/analyzer) and the specificity was checked with primer-BLAST (http://www.ncbi.nlm.nih.gov/tools/primer-blast/).

3.6 STATISTICAL ANALYSES

Statistical analysis was performed using paired Student's t test, and results were considered significant when $p < 0.05$. Values are expressed as mean ± standard error of the mean (M ± SEM).

4. RESULTS

4.1 SET UP AND VALIDATION OF A POLYMER-CNT SCAFFOLD

Dispersion of CNTs into a biocompatible polymer matrix can help to generate a freestanding and implantable device (Gheith et al., 2005). Combination of a biocompatible polymer and a conductive nanostructure is expected to boost neuronal growth/differentiation by coupling polymer features (biocompatibility, processability, low cost, implantability) and CNT properties (mimicking of the topography of neural environment and conductivity). We chose PLLA as polymer matrix because of its biocompatibility and employment for neural tissue engineering applications (Yang et al., 2004; Koh et al., 2008; Gertz et al., 2010). Among the plethora of available CNTs, we chose MWCNTs because of high conductivity and shape mimicking nanoscale features of the extracellular matrix. We purified commercial MWCNTs to remove heavy metal impurities, which may result cytotoxic (Furtado et al., 2004). Moreover, to improve dispersibility, we functionalized the MWCNTs through addition of the diazonium salt of 4-methoxyaniline (Salice at al., 2012; Salice et al., 2014). We determined, according to a previously reported approach (D'Este et al., 2006), a degree of functionalization (see supplementary file) of 1/97. Characterization of MWCNTs by TGA analysis and micro-Raman spectroscopy is shown in Fig. 20. The resulting CNT derivatives, soluble in chloroform, were used to prepare a polymer nanocomposite made of 1% w/w MWCNTs dispersed into a PLLA matrix by solvent evaporation (Fig. 20C). Raman spectroscopy, TGA and DSC confirmed CNTs to be well dispersed in the scaffold (Fig. 20D-E-F). The electrical resistivity of the nanocomposite scaffold is around 130 kΩ with respect to >2000 kΩ of the pristine PLLA; in addition, it shows features compatible with a free-standing

polymer film as required for implantable scaffolds. Indeed, we compared CNT-PLLA and PLLA scaffolds for both biocompatibility and neuritogenic properties. Calcein-AM staining revealed that SH-SY5Y cells can adhere and grow onto both CNT-PLLA and PLLA scaffolds and show homogeneous spreading (Fig. 21A). No difference in cell proliferation (Fig. 21B) and viability (Table 1) was observed when growing cells onto either poly-L-lysine or the scaffolds; however, as shown in Fig. 21C, cells better adhere to CNT-PLLA (~63%) than to PLLA alone (~39%). Furthermore, cells grown onto CNT-PLLA can be differentiated with RA as well as control samples and they present a total neurite length higher than samples grown onto PLLA (Fig. 21D). SEM images of cells cultured onto CNT-PLLA show a healthy morphology and the outgrowth of neurites attaching to the scaffold surface (Fig. 22). At high magnifications, the intimate contacts between the scaffold and neuronal membrane are evident (Fig. 22D). Furthermore, when compared to control cell cultures (poly-L-lysine substrate), cells grown onto CNT-PLLA show an increased number of long filopodia extending from the growth cone and making contacts with the scaffold, possibly depending on improved activity of growth cones in sensing topographical cues (Fig. 22G).

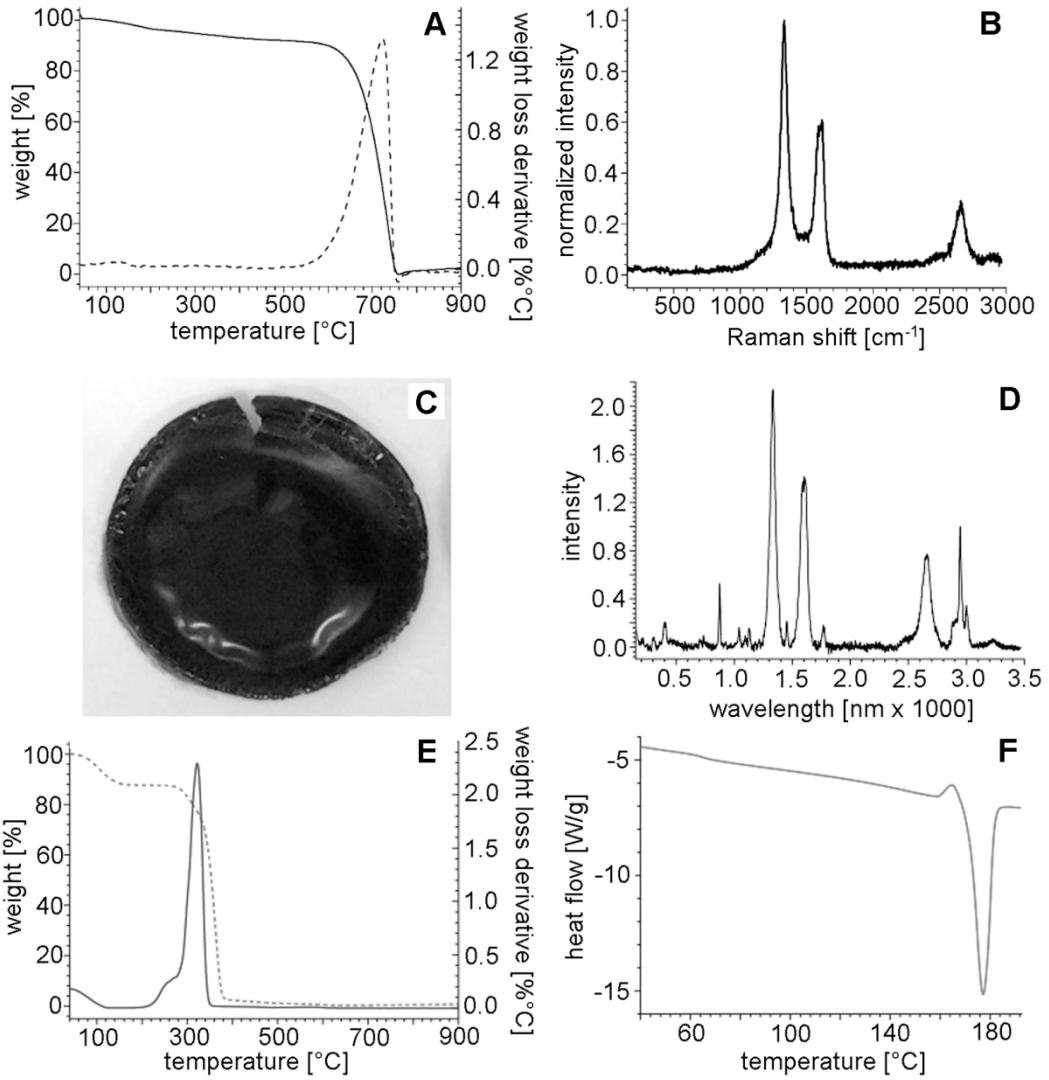

Figure 20. Scaffold characterization. TGA and micro-Raman analysis of MWCNT-PhOMe: Thermogram representing the residual weight (continuous line) and the weight loss derivative (dashed line) of the MWCNT-PhOMe measured under nitrogen atmosphere with a 10°C/min heating ramp **(A)**. Micro-Raman spectrum of the MWCNT-PhOMe sample (excitation line: 633 nm) **(B)**. CNT-PLLA scaffold characterization: Photograph of the PLLA@MWCNT-PhOMe 1% film **(C)**. FT-Raman spectrum of the PLLA@MWCNT-PhOMe 1% film (excitation line: 633 nm) **(D)**.Thermogram representing the residual weight (dashed line) and the weight loss derivative (continuous line) of the PLLA@MWCNT-PhOMe 1% film measured under nitrogen atmosphere with a 10°C/min heating ramp **(E)**. Differential scanning calorimetry (DSC) curve of the PLLA@MWCNT-PhOMe 1% film measured under nitrogen atmosphere with a 10 °C/min heating ramp **(F)** (Scapin et al., 2014).

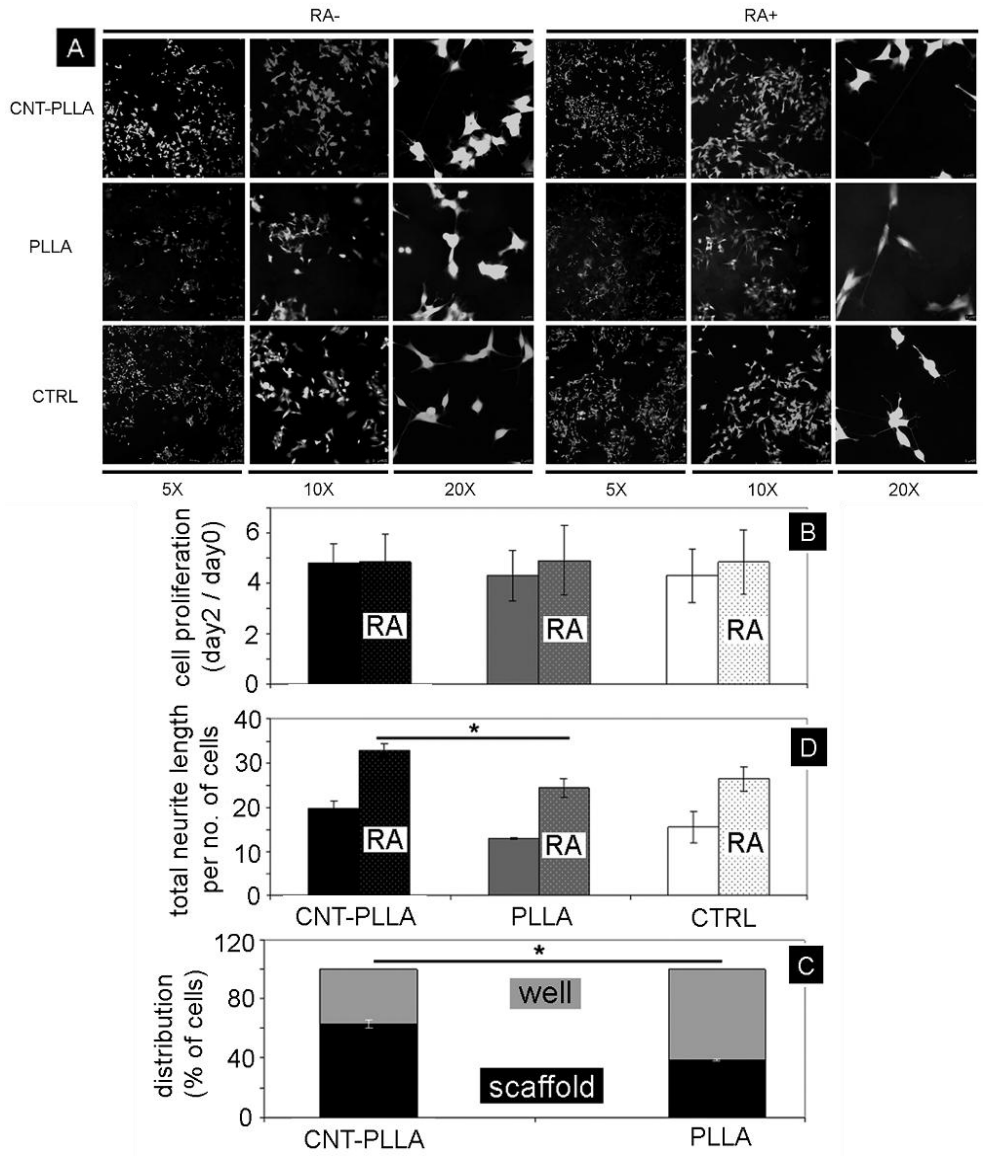

Figure 21. CNT-PLLA scaffold effect on SH-SY5Y cell adhesion, growth and differentiation. SH-SY5Y cells stained with Calcein-AM. Image magnification is reported **(A)**. Cell proliferation **(B)**, distribution **(C)** and differentiation **(D)**. Data represent the mean ± SEM of three independent experiments performed in duplicate. *shows significance at $p<0.05$ between cells seeded onto CNT-PLLA and PLLA. (Scapin et al., 2014).

% cell death	DAY0	DAY2	DAY2 RA
CNT-PLLA	14.71%	4.81%	3.82%
PLLA	14.23%	8.50%*	7.04%
CTRL	13.40%	2.84%	3.31%

Table 1. Percentage of cell death relative to three independent experiments performed in duplicate. * shows significance at $p<0.05$ between samples grown onto scaffolds and control cells (grown onto Poly-L-lysine).

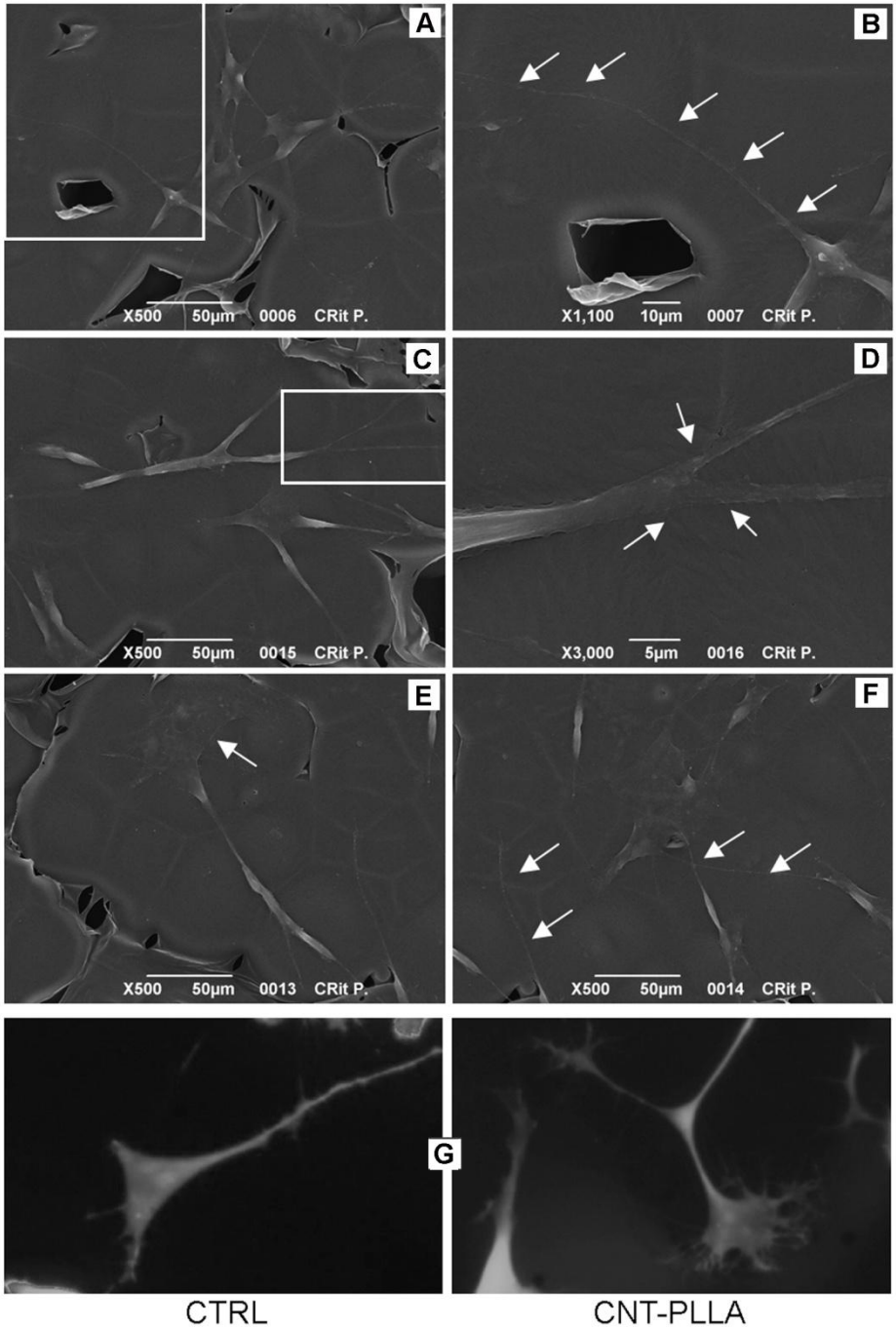

Figure 22. SH-SY5Y morphology when grown onto the CNT-PLLA scaffold.
(A to F) Scanning electron microscopy images of SH-SY5Y cells grown onto CNT-PLLA scaffolds. Scale bar: A, C, E, F = 50 μm; B = 10 μm; D = 5 μm. Panels B and D show details of the framed area in A and C, respectively. **(B, F)** Outgrowth of neurites attaching to the scaffold surface. At higher magnification **(D)** the intimate contacts between CNT-PLLA scaffolds and neuronal membrane are evident. **(E)** Growth cone morphology of cells growing onto the scaffolds. **(G)** Typical growth cones observed when cell differentiation is induced with RA. Cells were stained with calcein-AM. Image magnification is 32X (Scapin et al., 2014).

4.2 THE NEURITOGENIC PEPTIDES

4.2.1 IDENTIFICATION OF PEPTIDES DERIVED FROM L1 AND LINGO1

Cellular differentiation can be induced by synthetic peptides able to mimic differentiation signals. To this aim, peptides should correspond to interaction motifs likely to mediate such signals. In order to provide signals driving correct neuronal growth and differentiation, we started from the evidence that neuritogenesis and process guidance/elongation are driven by CAM proteins such as L1 (Alberts et al., 2003). In this work we tested biocompatibility and neuritogenicity of two peptides derived from L1 and LINGO1. The Ig2 repeat of the L1 ectodomain is involved in the homophilic binding and the interaction region corresponds to a 14-aminoacid long peptide named L1-A (Zhao et al., 1998). Therefore, we reproduced L1-A as a synthetic peptide for our experiments. Then, we searched for structural homologues of the L1 Ig2 repeat, to find further regulators of neural differentiation by homo/heterophilic interactions. Fold recognition search intriguingly identified the single Ig repeat of the LINGO1 ectodomain as the best structural template (99.7% confidence, 93% coverage). Given that identity between L1 Ig2 and LINGO1 Ig is 29%, we could use homology modeling method for obtaining a reliable model. Then, superposition (Fig. 23A) of the LINGO1 Ig template (Fig. 23B) and the L1 Ig2 model (Fig. 23C) revealed high structural similarity (RMSD = 0.65 Å). Intriguingly, the L1-A and aligned LINGO1 Ig sequence 467-480 (hereafter referred to as LINGO1-A), displayed high similarity. In particular, the two sequences share four identical amino acids and eight residues with similar physico-chemical properties (Fig. 23D). It has to be stressed that: (i) both LINGO1 and L1 are neural proteins involved in neurite outgrowth control, (ii) the LINGO1 Ig structure is quite similar to the L1 Ig2 domain, and (iii) the alignment between L1-A and LINGO1-A shows high conservation, including aminoacid positions relevant to L1 function (Zhao et al., 1998). Therefore, we produced LINGO1-A as synthetic peptide for our experiments. In order to distinguish among specific and unspecific effects, we

also synthesized the scrambled versions of the two peptides (L1-A_scr and LINGO1-A_scr). All peptides were produced by solid-phase synthesis and their chemical identities established by high-resolution mass spectrometry (Fig. 23E-F). As expected from both LINGO1-A and L1-A localization in flexible loop regions (see structural models in Fig. 23B-C), the conformation of the synthetic peptides in solution is essentially disordered as documented by the far-UV CD spectra resembling those typical of an unfolded polypeptide chain (Brahms et al., 1980) (Fig. 23G-H). Given that (i) L1-A was only investigated about its involvement in L1-L1 homophilic interactions (i.e. its role in cellular signaling was not determined) (Zhao et al., 1998) and (ii) LINGO1 Ig domain alone both mediates homo- and heterophilic interactions (Stein et al., 2012), but its binding region has not been identified yet, we decided to test the two peptides using the SH-SY5Y cell system to asses if (i) L1-A can trigger neurite elongation and (ii) LINGO1-A can regulate neural differentiation as well.

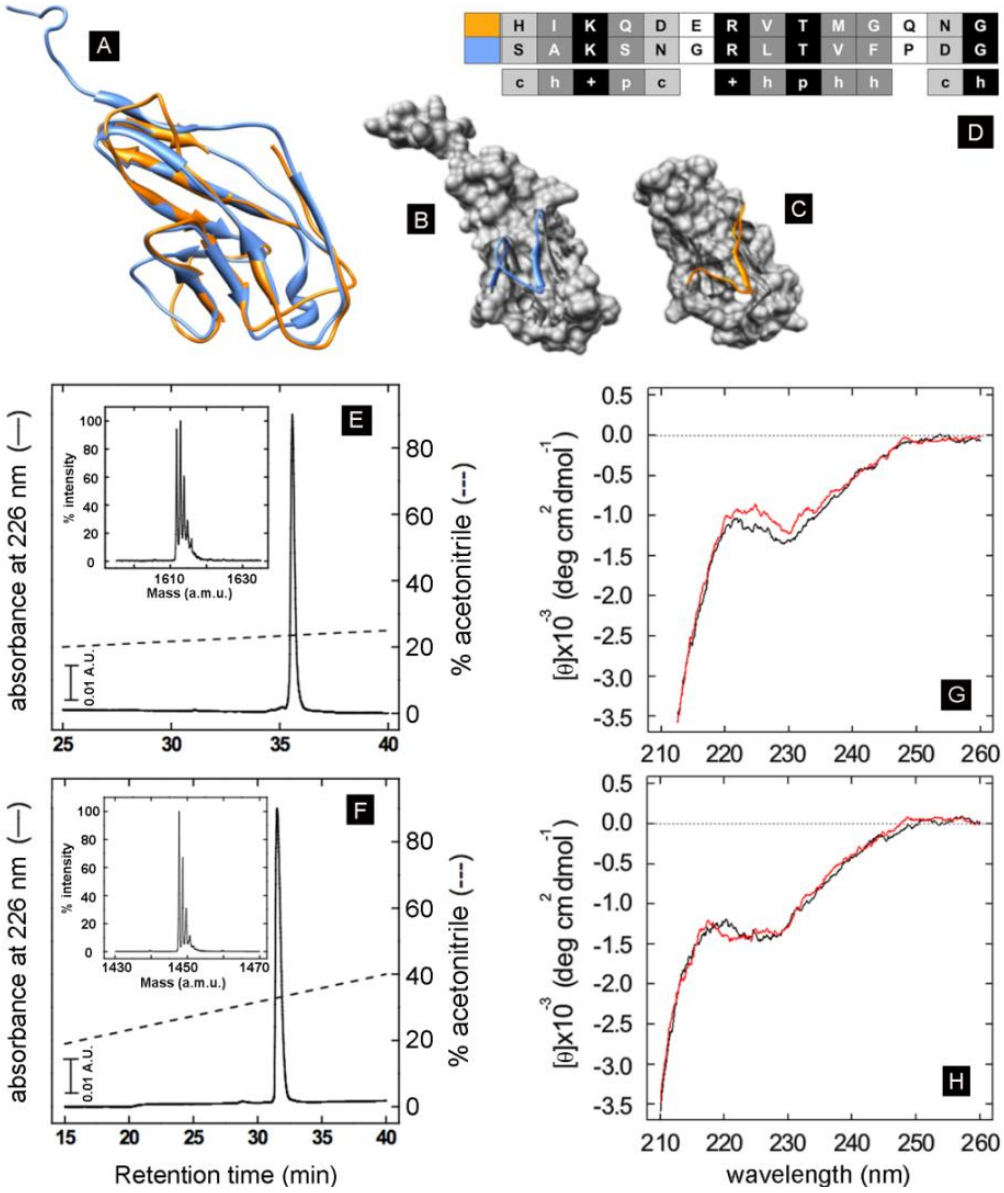

Figure 23. L1-A and LINGO1-A identification and characterization. (A) Superimposition between LINGO1 Ig domain (Blue) and L1 Ig2 domain (Orange). **(B)** LINGO1-A region (blue) and **(C)** L1-A region (orange) localization within the LINGO1 Ig and L1 Ig2 domains (gray) respectively. Models were obtained by UCSF Chimera software. **(D)** Alignment of L1-A and LINGO1-A peptide sequences. Black (identity), dark gray (same amino acid group), gray (compatible amino acid groups), white (different properties). Consensus code: c, compatible properties (polar and charged); h, hydrophobic; p, polar; +, positively charged. **(E, F)** RP-HPLC analysis of purified L1-A **(E)** and LINGO1-A **(F)** peptides by a C18 column eluted with an acetonitrile-0.078% TFA gradient (---) **(Inset)** Deconvoluted ESI-TOF mass spectrum of RP-HPLC purified peptides. The estimated molecular masses of L1-A (1611.79 ± 0.02 a.m.u.) and LINGO1-A (1447.72 ± 0.02 a.m.u.) peptides is in agreement with the theoretical values: 1611.78 and 1447.74 a.m.u., respectively. **(G, H)** Far-UV circular dichroism spectra of LINGO1-A **(G)** and L1-A **(H)** derivatives. All spectra were recorded at 25°C in PBS. L1-A and LINGO1-A spectra are in black; spectra from the corresponding scrambled peptides are in red. (Scapin et al., 2014).

4.2.2 L1-A AND LINGO1-A EFFECTS ON NEURONAL GROWTH AND DIFFERENTIATION

4.2.2.1 Peptides in solution

L1-A and LINGO1-A peptides were separately added to the medium at increasing peptide concentrations (0, 0.01, 0.1, 1, 10, 100 μM) to assess their effect on cell viability/proliferation and neuronal differentiation. As shown in Fig. 24A, both peptides do not alter cell proliferation with respect to control. Moreover, they are not cytotoxic as cell death in samples treated with the peptide is comparable to control (Table 2). Then, neuritogenic properties were analyzed and both peptides showed the highest effect on total neurite length at 1 μM concentration (Fig. 24B). In RA treated samples, L1-A addition increases total neurite length up to +~96%; in the absence of RA, the highest increase (+~115%) is mediated by LINGO1-A. In order to more precisely determine the optimal peptide concentration, a second series of experiments was performed narrowing dose response curves around 1μM peak. Data in Fig. 24C indicate 1 μM as the optimal concentration for both peptides. Then, the number of neurites per cell and the percentage of neurites longer than 100 μm were calculated. In order to aggregate the two set of experiments, only 0, 0.1, 1, 10 μM peptide concentrations were considered. Again, dose response curves reveal a bell-shaped pattern with the highest neuritogenic effect at 1 μM concentration (Fig. 24D-E). The number of neurites per neuron (Fig. 24E) follows the same trend as observed for the total neurite length: the highest effect is mediated by L1-A in RA induced samples (+~66%) or by LINGO1-A in the absence of RA (+~82%). The highest percentages of neurites longer than 100 μm (Fig. 24D) is found in samples treated with LINGO1-A (+~76%) and LINGO1-A RA (+~72%).

Given that both peptides mediated significant neuritogenic effects and according to established literature (Soroka et al., 2002), their scrambled versions (L1-A_scr

and LINGO1-A_scr) were used to discriminate among sequence specific mechanisms and effects unspecifically depending on amino acid composition. Scrambled peptides, like native ones, did not alter cell proliferation (Fig. 25A). In samples treated by scrambled peptides, values for total neurite length, number of neurites per neuron and percentage of neurites longer than 100 μm are comparable, or even lower than control (Fig. 25 B-C-D). Native peptides confirmed evidence from previous experiments, as the highest effect on total neurite length (Fig. 25B) and number of neurites per cell (Fig. 25C) is mediated by L1-A in RA-treated samples (+~88% total neurite length; +~71% neurites per cell) and by LINGO1-A in the absence of RA (+~82% total neurite length; +~44% neurites per cell). Furthermore, the highest percentage of neurites longer than 100 μm (Fig. 25C) is found in LINGO1-A treated samples (+~60% LINGO1-A, +~63% LINGO1-A RA). The neuritogenic effect of LINGO1-A and L1-A used in combination is lower than individual peptides.

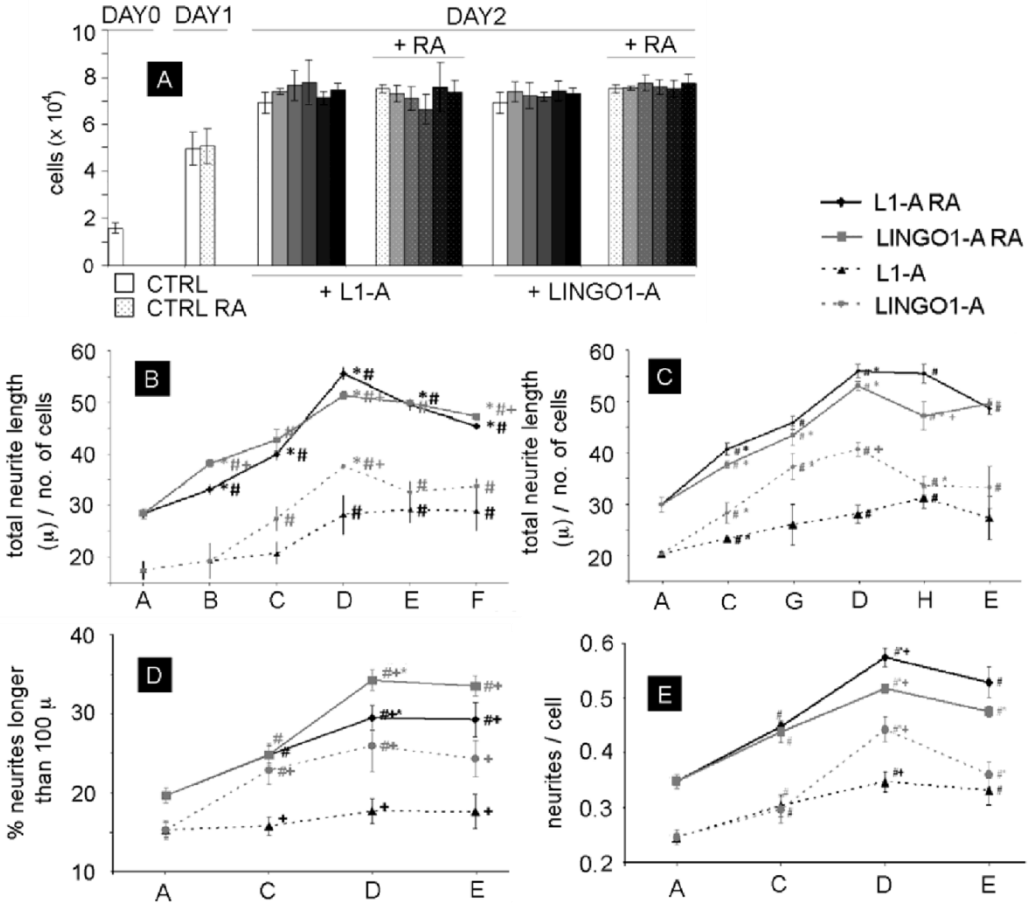

Figure 24. Effect of peptides added to the culture medium on SH-SY5Y cell proliferation and differentiation. Proliferation **(A)**, total neurite length **(B, C)**, neurites longer than 100 µm **(D)** and neurites per cell **(E)** from SH-SY5Y cells treated with increasing peptide concentrations in the absence or presence of RA. **(A)** White bars, control without peptides; other bars, the darker the colour the higher the peptide concentration following this gradient (0.001, 0.1, 1, 10, 100 µM). **(B to E)** Peptide concentrations: A, no peptide; B, 10 nM; C, 100 nM; D, 1 µM ; E, 10 µM; F, 100 µM; G, 316 µM; H, 3.16 µM. Data represent the mean ± SEM of three **(A, B, C)** and six **(D, E)** independent experiments performed in duplicate. # shows significance at $p<0.05$ between cells treated with peptides and the control without peptides. * shows significance at $p<0.05$ between samples 1X and sample 0.1X. + shows significance at $p<0.05$ between samples treated with L1-A and LINGO1-A at the same concentration. (Scapin et al., 2014).

% cell death	0 µM	0.01 µM	0.1 µM	1 µM	10 µM	100 µM
L1-A	2.44%	2.19%	2.42%	2.05%	2.29%	2.34%
LINGO1-A	2.44%	2.25%	1.99%	2.30%	2.31%	2.52%
L1-A RA	2.12%	1.87%	2.03%	1.98%	1.99%	2.00%
LINGO1-A RA	2.12%	2.04%	1.84%	1.89%	1.96%	1.96%

Table 2. Percentage of cell death relative to three independent experiments performed in duplicate.

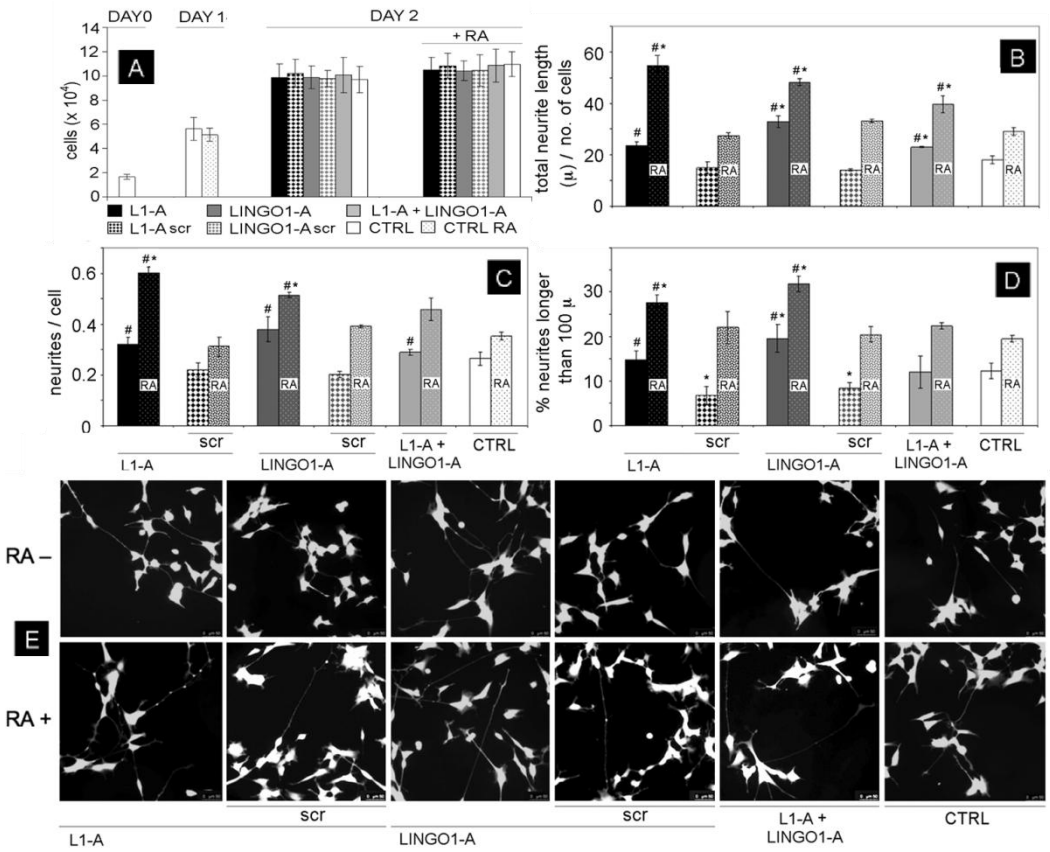

Figura 25. Effect of scrambled peptides (1 μM) added to the culture medium on SH-SY5Y cell proliferation and differentiation. Proliferation **(A)**, total neurite length **(B)**, neurites per cell **(C)**, neurites longer than 100 μm **(D)** and representative microscopy fields **(E)** from SH-SY5Y cells treated with 1 μM peptides or their scrambled versions in the absence or presence of RA. Data represent the mean ± SEM of three independent experiments performed in duplicate. * shows significance at $p<0.05$ between samples treated with peptides and the control without peptides. # shows significance at $p<0.05$ between samples treated with peptides and samples treated with their scrambled version. SH-SY5Y cells in **(E)** are stained with Calcein-AM. Image magnification is 20X. (Scapin et al., 2014).

4.2.2.2 Peptides adsorbed onto the substrate

The two peptides were designed to be used as guidance cues, mimicking ectodomains that could be biologically active either in solution or exposed at the surface of cells supporting neuronal growth. Therefore, in order to assess variation of their effects when used in solution or adsorbed onto a substrate, L1-A or LINGO1-A (at 1 μM or 10 μM concentrations) were also used (individually or in combination) for coating well bottoms. The residual amount of peptides (prior to cell seeding) was found to be approximately 75% (calculated by coating the well bottom with the peptide FITC-versions and quantifying the residual fluorescent after washing). As shown in Fig. 26A-B, both peptides are confirmed to have no meaningful effect on cell proliferation. Similarly, absence of cytotoxicity is confirmed (Table 3). When deposited onto the substrate, peptides exert a good neuritogenic effect. In fact, in all peptide-treated samples, the total neurite length is improved with respect to control samples (Fig. 26C-D) and the highest neuritogenic effect is observed at 1 μM concentration. Experiments with scrambled peptides confirmed the sequence-dependent specificity observed with peptides in solution. In particular, no effect is observed on cell proliferation (Fig. 27A) and cell death (not shown). Concerning total neurite length, number of neurites per neuron and percentage of neurites longer than 100 μm, values for scrambled peptides are always comparable or lower than control (Fig.27B-C-D). Native peptides confirmed their neuritogenic potential as the total neurite length (Fig. 27B), the number of neurites per neuron (Fig. 27C) and the percentage of neurites longer than 100 μm (Fig. 27D) are improved by native peptides. Differently from experiments in solution, the effect of the two peptides in combination is comparable or higher than individual peptides, while difference among L1-A or LINGO1-A treated samples is less evident, possibly because of the prolonged culture time (i.e. four days after RA induction).

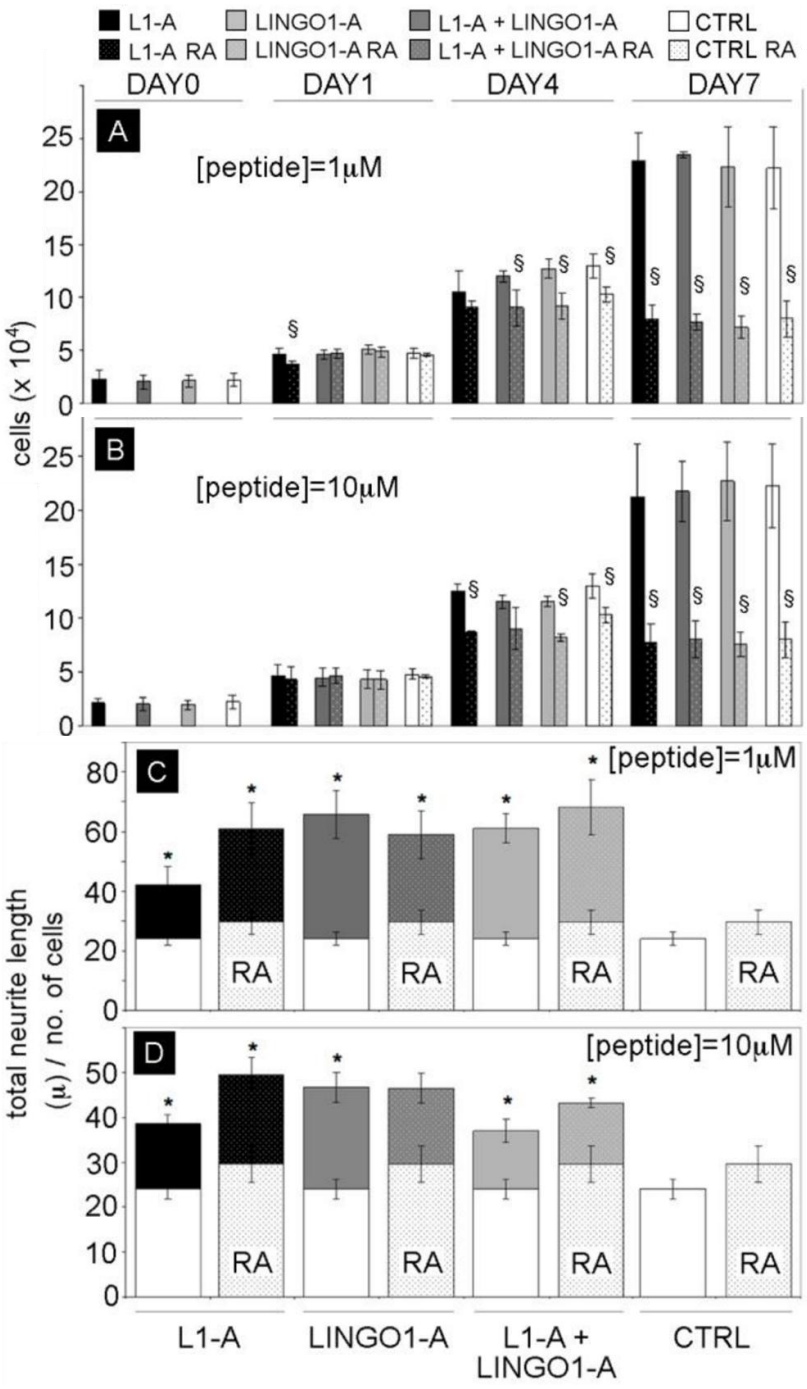

Figure 26. Effect of peptides deposited onto the substrate on SH-SY5Y cell proliferation and differentiation. Proliferation **(A, B)** and total neurite length **(C, D)** of SH-SY5Y cells seeded onto substrates coated with either 1 μM **(A, C)** or 10 μM **(B, D)** peptides. Data represent the mean ± SEM of three independent experiments performed in duplicate. § shows significance at $p<0.05$ between samples treated with RA and their respective untreated controls. * shows significance at $p<0.05$ between cells growing onto peptide substrate and the control (cells growing on poly-L-lysine). Incremental values compared to control are reported. (Scapin et al., 2014).

A

% cell death 1μM	L1-A	LINGO1-A	L1-A+LINGO1-A	PLL
DAY0	7.59%	7.41%	7.68%	7.68%
DAY1	6.44%	5.56%	5.02%	5.64%
DAY1 RA	6.91%	6.01%	5.67%	5.09%
DAY4	2.60%	1.76%	2.02%	2.80%
DAY4 RA	3.56%	3.27%	2.88%	3.29%
DAY7	2.54%	2.18%	2.13%	2.00%
DAY7 RA	3.75%	2.84%	2.66%	2.59%

B

% cell death 10 μM	L1-A	LINGO1-A	L1-A+LINGO1-A	PLL
DAY0	8.79%	10.42%	9.38%	7.68%
DAY1	5.66%	5.70%	5.67%	5.64%
DAY1 RA	4.67%	4.10%	4.60%	5.09%
DAY4	4.90%	4.40%	3.84%	2.80%
DAY4 RA	6.21%	5.70%	5.35%	3.29%
DAY7	2.49%	1.73%	1.99%	2.00%
DAY7 RA	2.93%	2.27%	3.54%	2.59%

Table 3. (A-B) Percentage of cell death relative to three independent experiments performed in duplicate.

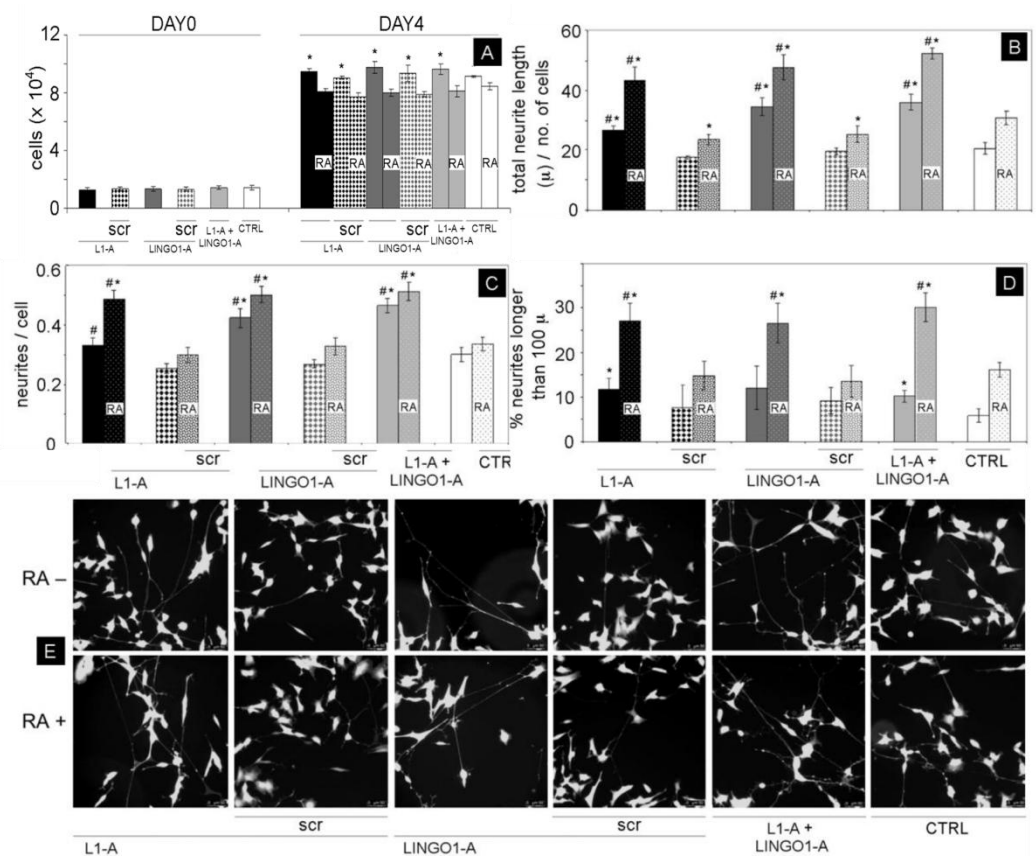

Figure 27.Effect of scrambled peptides (1μM) deposited onto the substrate on SH-SY5Y cell proliferation and differentiation. Proliferation **(A)** Total neurite length **(B)** neurites per cell **(C)**, neurites longer than 100 μm **(D)** and representative microscopy fields **(E)** from SH-SY5Y cells seeded onto substrates coated with 1 μM peptides or their scrambled versions in absence or presence of RA. Data represent the mean ± SEM of three independent experiments performed in duplicate. * shows significance at $p<0.05$ between cells growing onto peptide surface and the control (cells grown onto poly-L-lysine). # shows significance at $p<0.05$ between samples growing onto peptide surface and samples growing on their respective scrambled version. SH-SY5Y cells in **(E)** are stained with Calcein-AM. Image magnification is 20X. (Scapin et al., 2014).

4.3COMBINED EFFECTS OF THE CNT-PLLA SCAFFOLD AND NEURITOGENIC PEPTIDES ON NEURONAL GROWTH AND DIFFERENTIATION.

Separate characterization provided us with evidence that the CNT-PLLA scaffold is well suitable for neuronal culture and the peptides exert specific and important neuritogenic effects. Therefore, we performed experiments to determine if their combination could further promote neuronal differentiation. The scaffold+peptides combination neither altered cell proliferation nor cell death (Fig. 28A and Table 4), while showing instead evidence of synergy: total neurite length is significantly improved in RA induced samples treated by either L1-A or LINGO1-A when cells are grown onto the scaffold (Fig. 28B). Synergistic effect is also observed when cells are treated with L1-A in the absence of RA. Density of branch points per neurites and of neurites per cells were also determined and a synergistic effect is likely to occur as values for peptide and RA treated cells grown onto the scaffold are equal or higher than corresponding control samples (Fig. 28C-D). Synergistic effect can also be inferred when considering growth cone numbers. A growth cone was defined as a fan-shaped structure at the tip of a neurite, where the neurite began to increase in width (Abney et al., 1999; Dent et al., 2013). When used separately, neither peptides nor the scaffolds show meaningful effect (Fig. 28E), but when RA induced cells are simultaneously grown onto the scaffold and treated with the peptides, growth cone number is considerably increased (+~97% L1-A RA; +~49% LINGO1-A RA).

% cell death	L1-A	LINGO1-A	Ctrl
PLL	2.06%	2.15%	2.45%
CNT-PLLA	2.14%	2.43%	2.43%
PLL RA	1.61%	1.86%	2.18%
CNT-PLLA RA	2.33%	1.83%	1.55%

Table 4. Percentage of cell death relative to four independent experiments performed in duplicate.

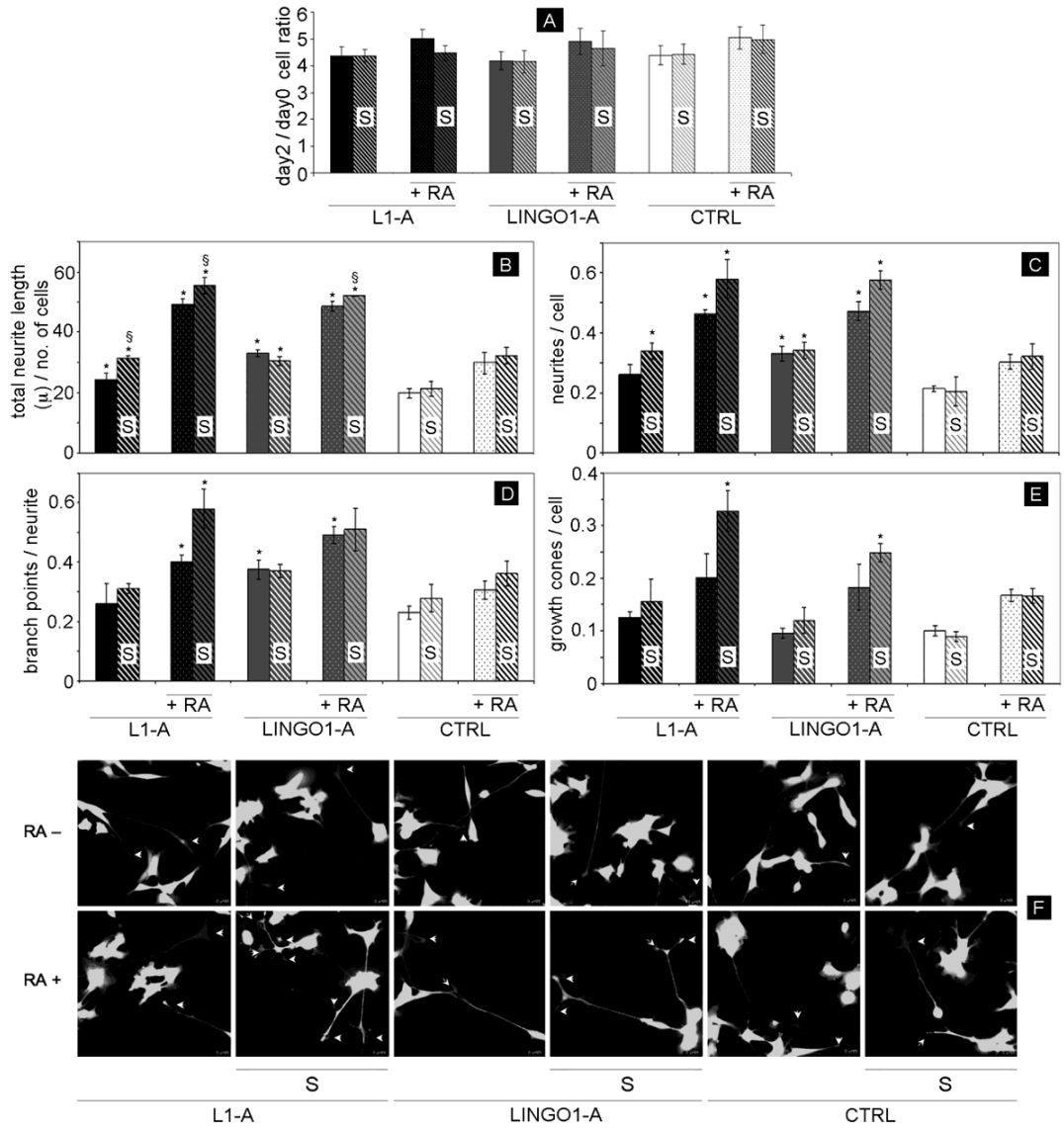

Figure 28. Comparison between SH-SY5Y cells seeded onto the CNT-PLLA scaffold (S) and control (poly-L-lysine coated wells) when treated with 1 μM peptides in the absence or presence of RA. Proliferation **(A)**, total neurite length **(B)**, neurites per cell **(C)**, branches per neurite **(D)**, growth cones per cell **(E)** and representative microscopy fields**(F)**. Data represent the mean ± SEM of three independent experiments performed in duplicate.*shows significance at $p<0.05$ between samples treated with peptides and their respective control without peptides. § shows significance between samples growing onto CNT-PLLA scaffold and control (poly-L-lysine coated wells). SH-SY5Y cells in **(F)**are stained with Calcein-AM. Growth cones are indicated by white arrows. Image magnification is 32X. (Scapin et a., 2014)

4.4 EFFECTS OF L1-A AND LINGO1-A PEPTIDES ON SH-SY5Y GENE EXPRESSION

The L1-A and LINGO1-A peptides showed a positive and specific effect in SH-SY5Y cell differentiation, but the understanding of their molecular mechanism of action could be of help to properly use them in clinical applications. Quantitative PCR analyses were performed in order to test which genes are upregulated after peptide administration and hence to get suggestions on the molecular pathway activated by the cells. 24 hours from peptide administration, Nestin upregulation occurs in samples treated with L1-A either in the presence or in absence of RA stimulation (Fig. 29A). Otherwise, TUBβ3 is upregulated in L1-A treated samples after RA stimulation and in LINGO1-A treated samples in the absence of RA stimulation (Fig. 29B). Effect on MAP2 expression is not so evident, except for a significant increase in LINGO1-A treated samples in the absence of RA induction (Fig.29C). VAMP7 and TRKB are upregulated both in L1-A and in LINGO1-A treated samples, either in presence or in the absence of RA stimulation (Fig. 29D,E); moreover, TRKB is strongly upregulated by RA treatment (Fig. 29E). Interestingly, TRKB is significantly more expressed in LINGO1-A treated samples than in L1-A treated samples, in the absence of RA induction (Fig. 29F). L1-A upregulates the expression of neuronal L1 either in presence or in absence of RA stimulation, suggesting the presence of positive feedback in L1 gene regulation (Fig.29G). In addition, L1-A treatment induces the expression of LINGO1 in the absence of RA stimulation (Fig. 29H). RA induced upregulation of L1 expression (Fig. 29G) and downregulation of LINGO1 expression (Fig. 29H) occurs in both peptide treated samples and controls.

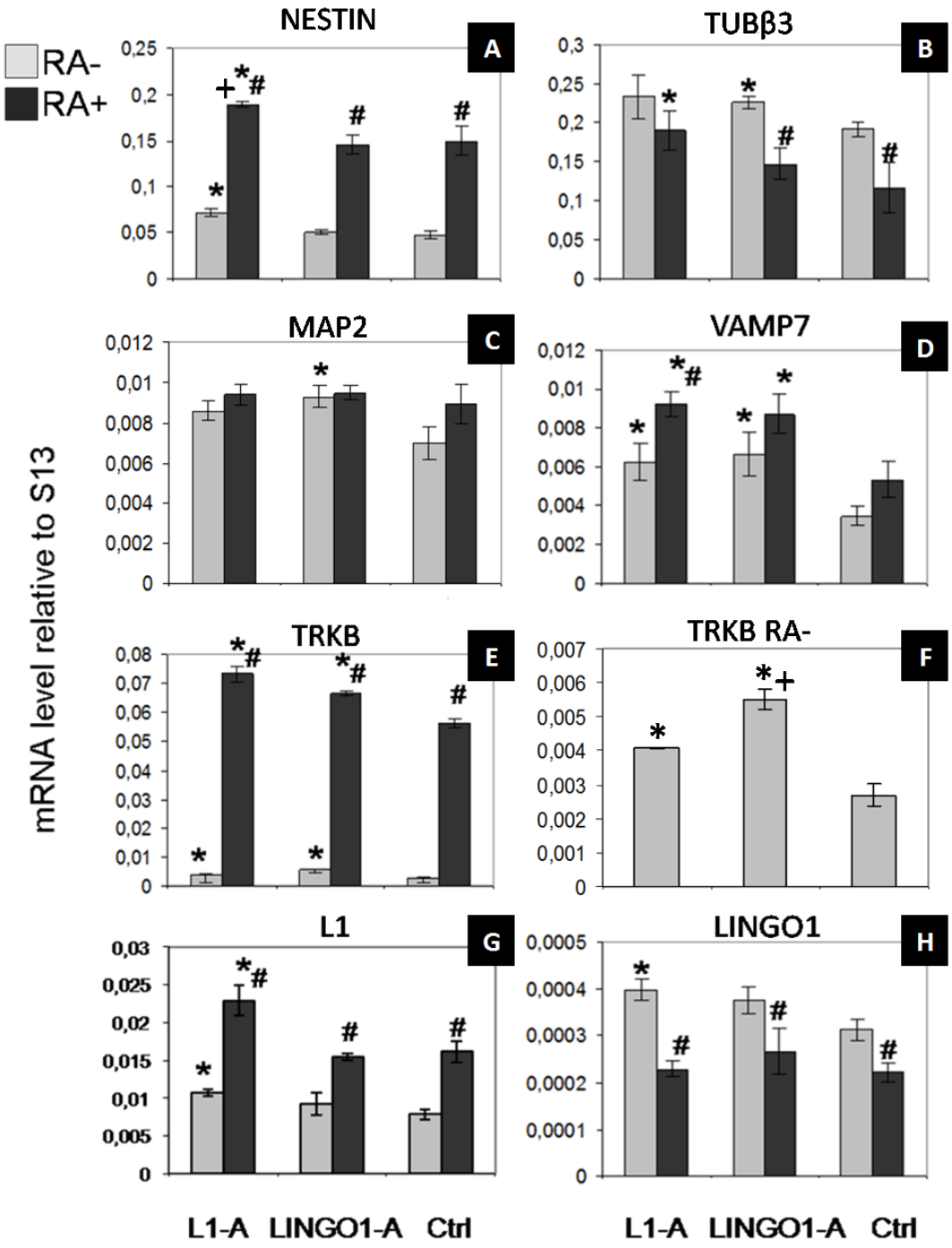

Figure 29. Effects of L1-A and LINGO1-A on neuronal marker expression. Nestin **(A)**, TUBβ3 **(B)**, MAP2 **(C)**, VAMP7 **(D)**, TRKB **(E)**, TRKB RA- **(F)**, L1 **(G)** and LINGO1 **(H)** expression profile of SH-SY5Y treated with peptides compared with untreated controls. Data are mRNA levels normalized to the expression of the housekeeping gene S13. At least three independent experiments were performed in triplicate and the real time PCR was run twice for each sample (technical duplicate). * shows significance at $p<0.05$ between peptide treated samples and control. # shows significance at $p<0.05$ between RA treated samples and their respective untreated controls. + shows significance at $p<0.05$ between L1-A treated samples and LINGO1-A treated samples.

4.5 PROTEOME-WIDE AND PRELIMINARY MUTATIONAL ANALYSIS OF THE PEPTIDES

We used the Ig2 domain of L1 and the Ig domain of LINGO1 as BLAST probes for collecting a dataset of mammals orthologues, and from the multiple alignment we analyzed the amino acid conservation for each position at the level of the peptide sequence. Such comparative analysis highlighted the seventh residue (Arg) in the peptide region as highly conserved. Intriguingly, it corresponds to Arg184 in L1CAM and its mutation to Gln is causative of the most severe CRASH syndrome phenotype (Jouet et al., 1994; De Angelis et al., 2002). Moreover, Zhao et al., showed that when replacing this Arg by Ala, the L1-A peptide is no longer able to bind to L1 Ig2 domain (Zhao et al., 1998). Given that the R184 position is likely crucial for homophilic binding and for a correct neurodevelopment as well, we decided to test the effect of both R184Q and R184A L1-A mutants on cell differentiation in our cell system. Comparison between mutant peptides, the wild type peptide and scrambled peptide (previously shown to have no neuritogenic effect) showed that R184A mutant completely lacks any neuritogenic effect, as values for total neurite length (Fig. 30A), number of neurites per cell (Fig. 30B) and percentage of neurites longer than 100 μm (Fig. 30C) are not meaningfully different from control samples (untreated or treated by scrambled peptides). Concerning R184Q mutant, it retains a very low neuritogenic activity, as indeed the total neurite length (Fig. 30A) and the number of neurites per cell (Fig. 30B) are higher than control samples, but significantly lower that wild-type peptide treated samples. Therefore, R184 position seems to be crucial for L1 function and we could provide the first direct link i.e. in the same cellular system between the role of R184 in homophilic binding (as demonstrated by Zhao et al, 1998) and relevance of the motif in neurodevelopment.

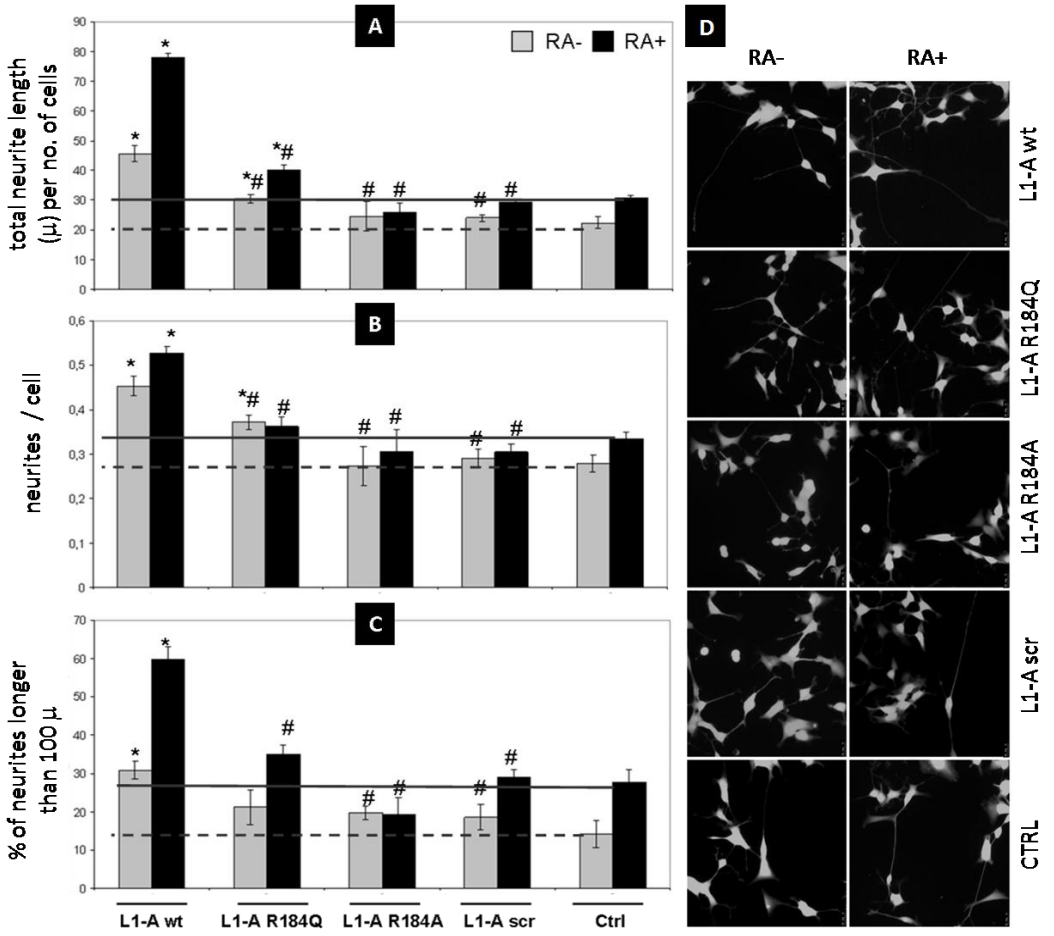

Figure 30. Analysis of the neuritogenic capacity of mutant L1-A peptides on SH-SY5Y cells. Total neurite length **(A)**, neurites per cell **(B)**, neurites longer than 100 μm **(C)** and representative microscopy fields **(D)**. Data represent the mean ± SEM of three independent experiments performed in duplicate. * shows significance at $p<0.05$ between samples treated with peptides and the control without peptides. # shows significance at $p<0.05$ between L1-A wild type and L1-A mutants/scrambled SH-SY5Y cells in **(D)** are stained with Calcein-AM. Image magnification is 32X**.**

4.6 eCNT-PLLA SCAFFOLD EFFECTS ON SH-SY5Y CELL ADHESION, GROWTH AND DIFFERENTIATION

We electrospun the CNT-PLLA matrix into fibres of submicron size with the aim to better mimic the neuronal processes and the collagenous component of the extracellular matrix. The electrospun CNT-PLLA matrix (eCNT-PLLA) was deposited onto a glass coverslip to help its usage as a scaffold for cell cultures. Scanning electron microscopy images of the randomly oriented electrospun CNT-PLLA fibres reveal a regular surface morphology with a diameter that range from 300 to 600 nm (Fig. 31A-B).

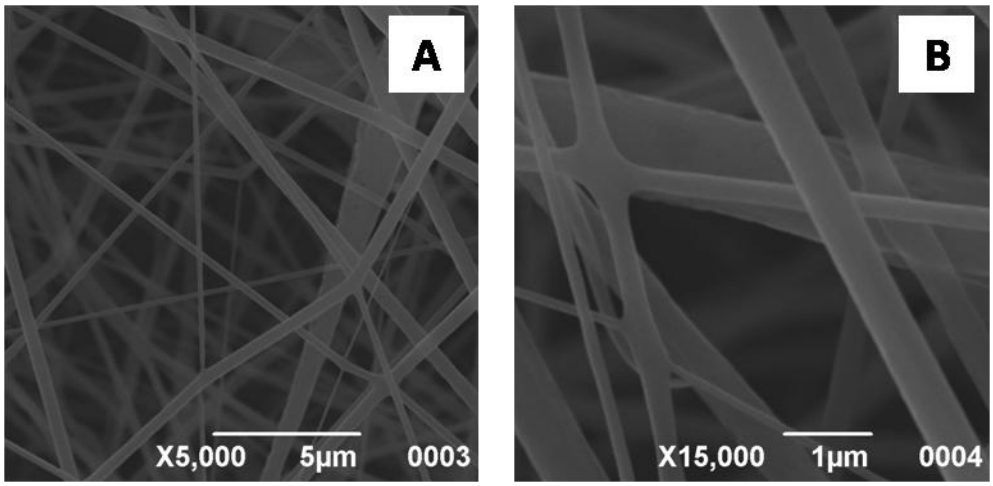

Figure 31. Scanning electron microscopy images of the eCNT-PLLA scaffold fibres. Scale bar: A = 5 µm; B = 1 µm.

Next, we compared eCNT-PLLA with a scaffold made of electrospun PLLA (ePLLA) and with the non-electrospun CNT-PLLA scaffolds for both biocompatibility and neuritogenic properties. As shown in figure 32A and table 5, no differences in cell proliferation and cell viability were revealed when growing cells onto the three different scaffolds or onto the poly-L-lysine coated control wells. However, cells better adhere onto eCNT-PLLA (~66%) than onto ePLLA (~53%). Furthermore, the total neurite length is significantly increased in samples seeded onto the eCNT-PLLA scaffolds either in presence or in absence of RA stimulation (Fig.33A). The number of neurites per cells is also significantly increased in samples grown onto

the eCNT-PLLA scaffolds (Fig 33B), but the analysis of the percentage of neurites longer than 100 µm reveals that such value is significantly lower in cells cultivated onto the eCNT-PLLA scaffolds compared to control and the non-electrospun CNT-PLLA scaffolds (Fig. 33C). Therefore, the eCNT-PLLA scaffolds promote the formation of new short neurites. Figures 34B-E-H show the SH-SY5Y cells with the cytoplasmic staining calcein-AM that is particularly useful to clearly detect, in all their length, the neuronal processes and to visualize cells growing onto the non-transparent eCNT-PLLA scaffolds. Figures 34A-D-G are the bright field images of the corresponding portion of the scaffold and figures C-F-I the superimposition of the fluorescent images with the corresponding bright field images. As indicated by the white arrows, the newly formed neurites elongate following the direction of fibre orientation; this indicates that cells are influenced by scaffold topography and it opens up the perspective to obtain a polarized neurite outgrowth upon fibre alignment.

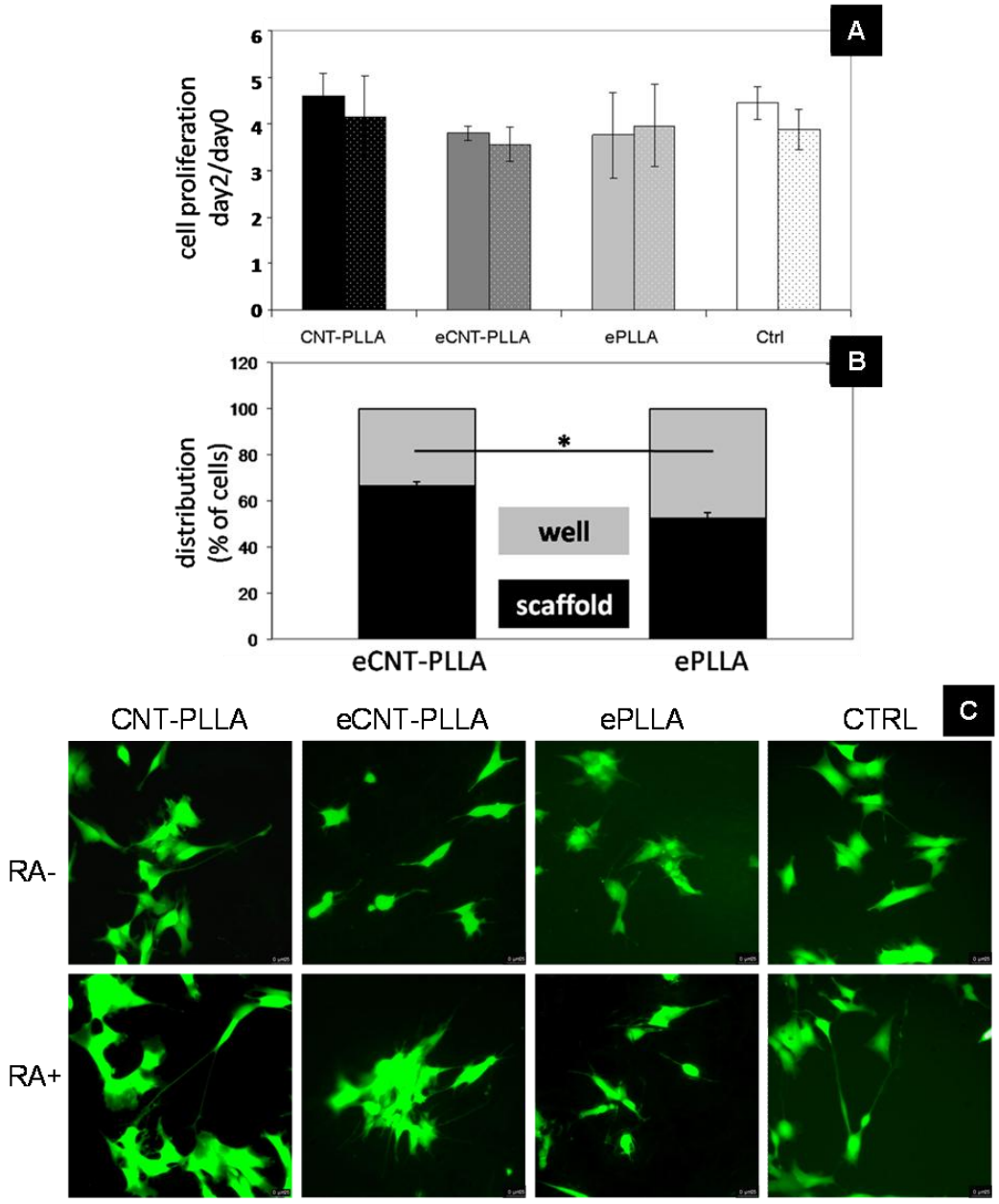

Figure 32. eCNT-PLLA scaffold effect on SH-SY5Y adhesion and growth. Cell proliferation **(A)** and cell distribution **(B)** and representative microscopy fields **(C)**. Data represent the mean ± SEM of three independent experiments performed in duplicate. *shows significance at $p<0.05$ between cells seeded onto eCNT-PLLA and ePLLA scaffolds. Dotted bars refer to the corresponding RA treated samples. cells in **(D)** are stained with Calcein-AM. Image magnification is 32X.

% of cell death	DAYO	DAY2	DAY2 RA
CNT-PLLA	18.06%	4.52%	4.06%
eCNT-PLLA	23.45%	7.48%	7.44%
ePLLA	22.01%	7.97%	7.59%
CTRL	19.59%	3.86%	3.34%

Table 5. Percentage of cell death relative to three independent experiments performed in duplicate.

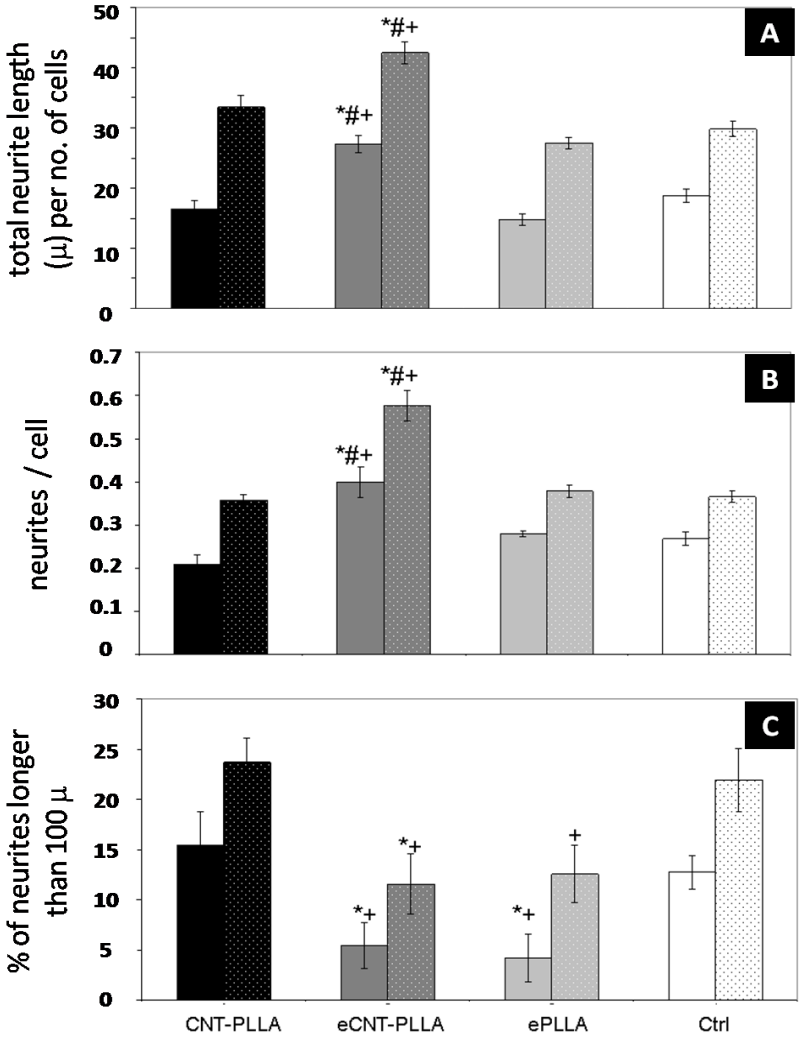

Figure 33. eCNT-PLLA scaffold effects on SH-SY5Y differentiation. Total neurite length **(A)**, neurites per cell **(B)**, neurites longer than 100 μm **(C)**. Data represent the mean ± SEM of three independent experiments performed in duplicate. *shows significance at $p<0.05$ between cells seeded onto eCNT-PLLA scaffolds and control (poly-L-lysine coated wells). #shows significance at $p<0.05$ between cells seeded onto eCNT-PLLA scaffolds and ePLLA scaffolds. +shows significance at $p<0.05$ between cells seeded onto CNT-PLLA scaffolds and eCNT-PLLA/ePLLA scaffolds. Dotted bars refer to the corresponding RA treated samples.

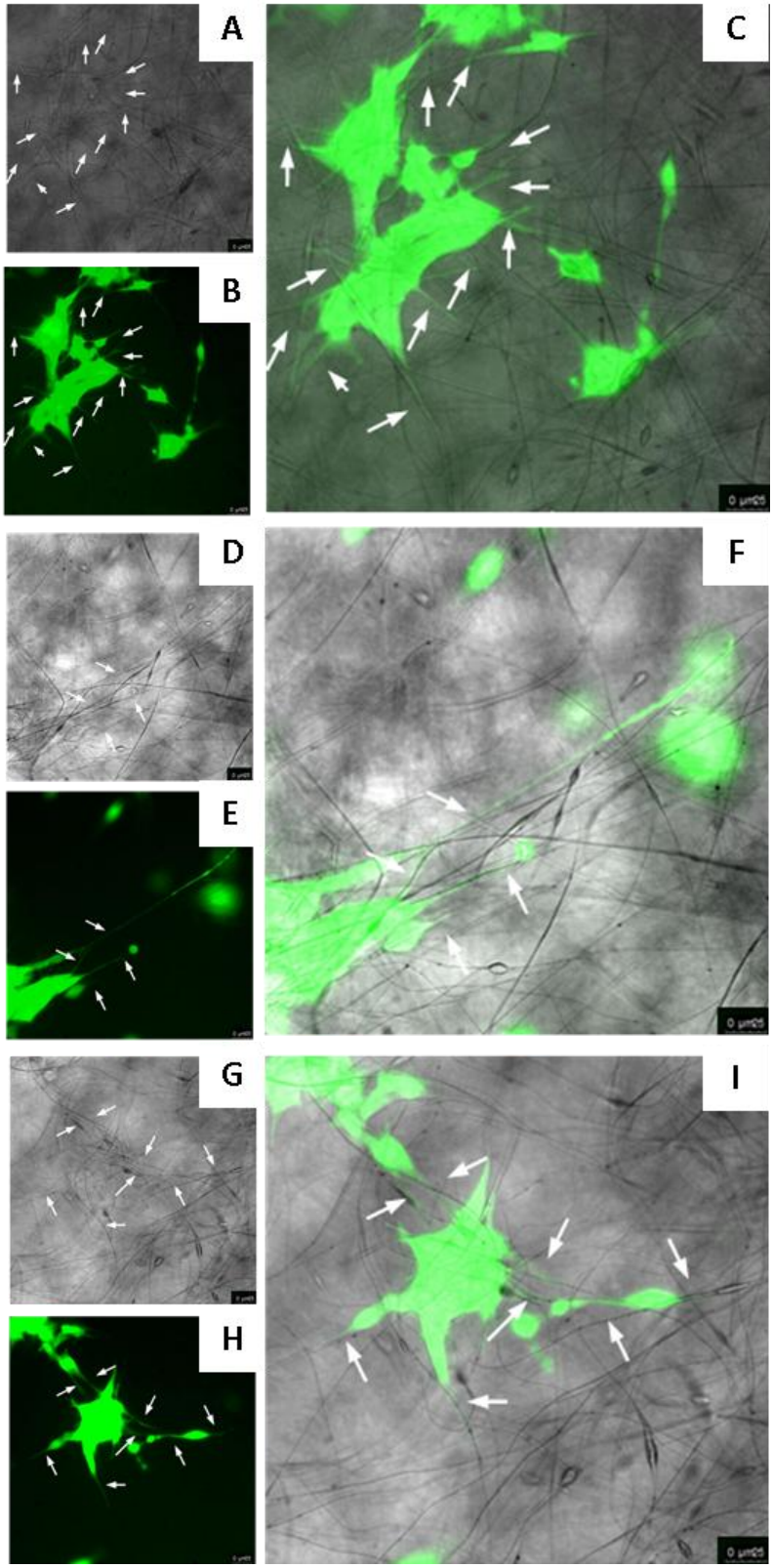

Figure 34. SH-SY5Y cells extend neurites following the scaffold fibre orientation. Bright field images of the eCNT-PLLA scaffold **(A, D, G)**, fluorescent images of RA treated SH-SY5Y cells stained with Calcein-AM **(B, E, H)**, superimposition of the two **(C, F, I)**. Arrows indicate neurites following the scaffold fibre orientation. Image magnification is 32X.

4.7 COMBINED EFFECTS OF THE eCNT-PLLA SCAFFOLD AND NEURTIOGENIC PEPTIDES ON NEURONAL GROWTH AND DIFFERENTIATION

Given that the eCNT-PLLA scaffolds resulted to be suitable for neuronal cell growth and they promote the formation of new neurites, cells were seeded onto their surfaces and treated with peptides added to culture medium to test if a synergistic effect between the two components occurs. The combination between scaffolds and peptides does not have effects on cell proliferation (Fig. 35A); furthermore, in almost all samples seeded onto the eCNT-PLLA scaffolds, the total neurite length is higher than in control (poly-L-lysine coated wells), except for L1-A treated samples after RA stimulation (Fig. 35B). The same trend is observed for the number of neurites per cell (Fig. 35C), but the percentage of neurites longer than 100 μm is higher in control samples than in cells grown onto the scaffolds (Fig. 35D). The only exception concerns cells cultivated onto the eCNT-PLLA scaffolds and treated with the LINGO1-A peptide after RA stimulation. In fact, in this sample the percentage of neurites longer than 100 μm reaches the value of its respective control (i.e., cells seeded onto poly-L-Lysine coated wells and treated with LINGO1-A) (Fig. 35D). Therefore, the LINGO1-A treated samples onto the eCNT-PLLA scaffolds show the highest number of neurites and the longest neurites, hence the highest level of cell differentiation as the scaffold induces the formation of new neurites and LINGO1-A promotes their elongation.

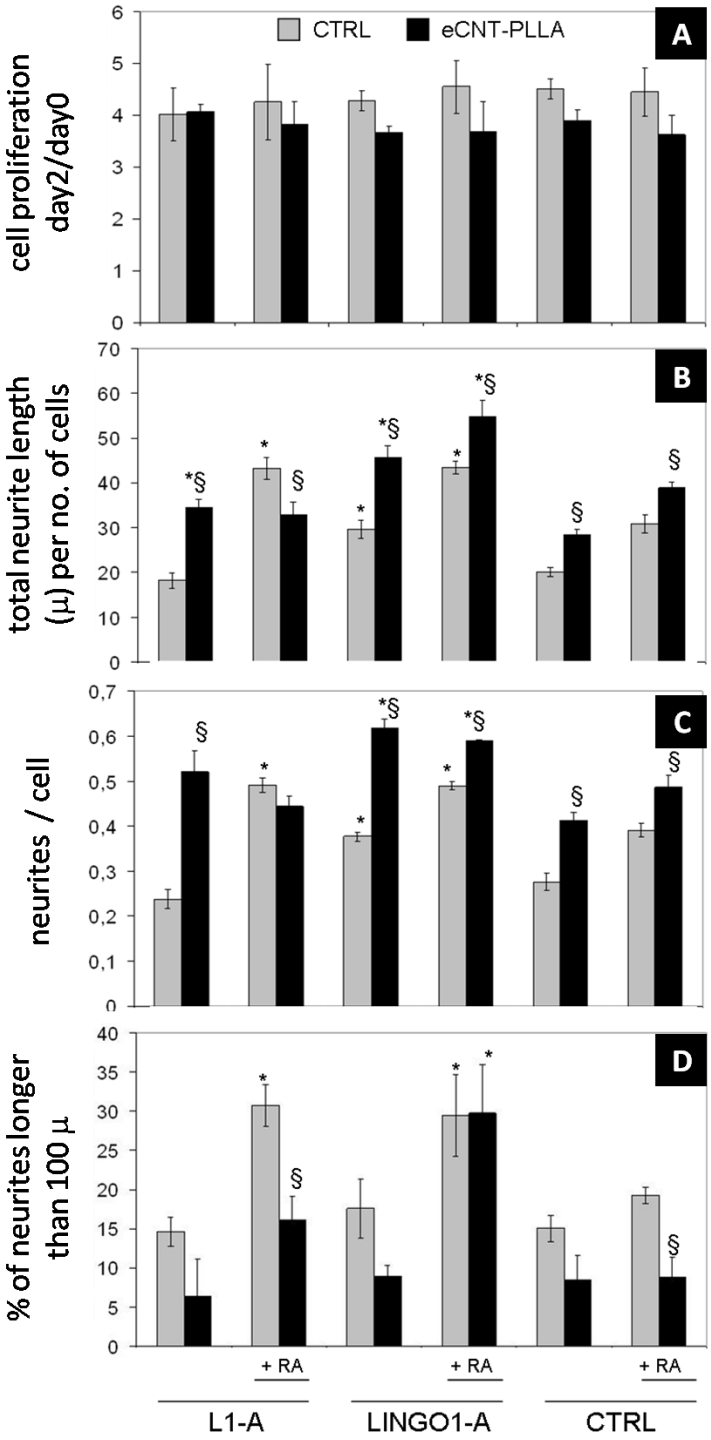

Figure 35. Comparison between SH-SY5Y cells seeded onto the eCNT-PLLA scaffold and control (poly-L-lysine coated wells) when treated with 1 μM peptides in the absence or presence of RA. Cell proliferation **(A)**, total neurite length **(B)**, neurites per cell **(C)**, neurites longer than 100 μm **(D)**. Data represent the mean ± SEM of three independent experiments performed in duplicate. *shows significance at $p<0.05$ between samples treated with peptides and their respective untreated controls. § shows significance between samples growing onto eCNT-PLLA scaffold and control (poly-L-lysine coated wells).

4.8 TESTING SCAFFOLDS AND PEPTIDES WITH A STEM CELL POPULATION

We developed a nanocomposite scaffold that combine the conductive and nanotopographical features of multi-walled CNTs (MWCNTs) with the freestanding biocombatibility of poly-L-lactic acid (PLLA). Such scaffold resulted to support adhesion, growth and differentiation of SH-SY5Y cells without exerting cytotoxic effects. Furthermore, the peptides derived from L1 and LINGO1 motives resulted to play a positive role in promoting SH-SY5Y differentiation and neurite extension. Therefore, after the setting up of the system with stabilized cell line as the SH-SY5Y cells, we decided to test our scaffolds and peptides with a physiological source of cells suitable for the regenerative medicine applications. We chose the human circulating multipotent cells (*h*CMCs) isolated from peripheral blood as they are autologous, accessible, not subjected to ethical restrictions and differentiable into neurons under proper conditions. All these characteristics make them the perfect source of stem cells exploitable for regenerative medicine applications. Our aim is to test the scaffolds and peptides with such cells in order to asses if the only features of scaffolds and peptides are able to induce cell differentiation toward the neuronal lineage without the use of growth factors that are traditionally used for the differentiation of stem cells into neurons.

4.8.1 CNT-PLLA SCAFFOLD EFFECTS ON hCMC ADHESION, GROWTH AND DIFFERENTIATION

We seeded hCMCs onto the CNT-PLLA scaffolds and after 5 days in culture, calcein-AM staining reveals these cells adhere and grow well onto the CNT-PLLA scaffolds, showing homogeneous spreading (Fig. 36A). No difference in cell proliferation was observed when seeding hCMCs onto either the scaffolds or the well bottoms, during the whole differentiation period (Fig. 36B). Furthermore,

the scaffold seems to influence cell morphology as, when seeded onto its surface, hCMCs show typical features of cells from the neuronal lineage like e.g. more fusiform cell bodies compared to the wide spread appearance of control cells, and neurite-like protrusions that are tipped with fan-shaped structures resembling growth cones (Fig. 37A). Indeed, the measurement of cell diameter shows that cell bodies are smaller when cells are seeded onto the CNT-PLLA scaffolds (Fig. 37B); in addition, more cells with a polarized appearance are counted onto the scaffolds with respect to controls (Fig. 37C). Finally, cells growing onto the scaffolds show a significant increase of total protrusion length and the number of protrusions per cell (Fig. 37D,E).

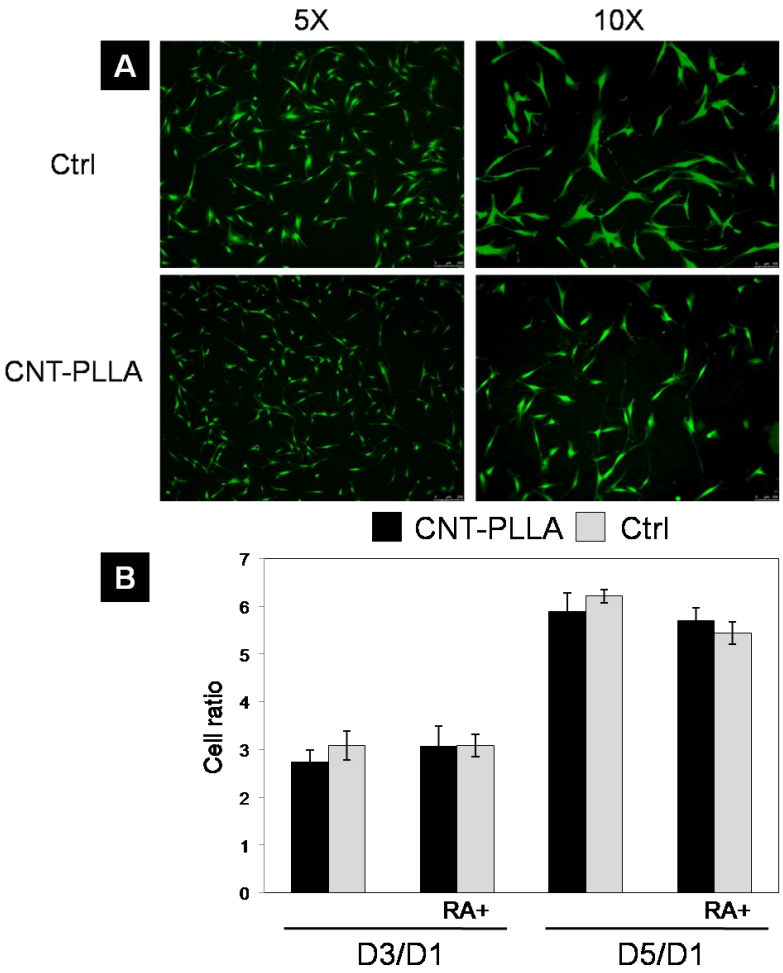

Figure 36. CNT-PLLA scaffold effect on hCMC adhesion and growth. hCMCs stained with Calcein-AM. Image magnification is reported **(A)**. Cell proliferation **(B)**. Data represent the mean ± SEM of three independent experiments performed in triplicate.

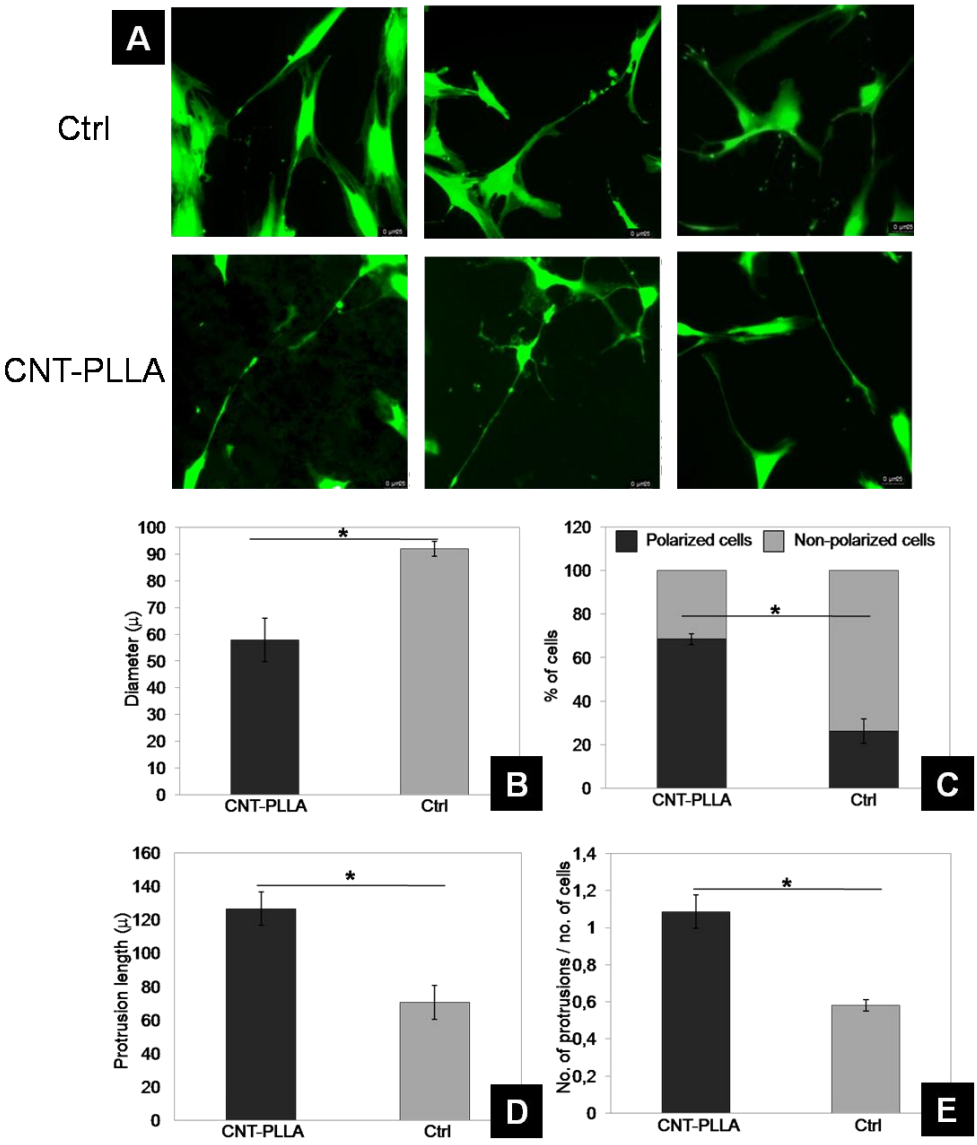

Figure 37. Effect of the CNT-PLLA scaffolds on hCMC morphology. hCMCs stained with Calcein-AM **(A)**. Mean cell diameter **(B)**, percentage of polarized cells **(C)**, total protrusion length **(D)**, number of protrusions per cell **(E)**. Quantification was performed 24 hours from cell seeding. Data represent the mean ± SEM of three independent experiments performed in duplicate.*shows significance at $p<0.05$ between cells seeded onto CNT-PLLA scaffold and control (well bottoms). Image magnification in **(A)** is 32X.

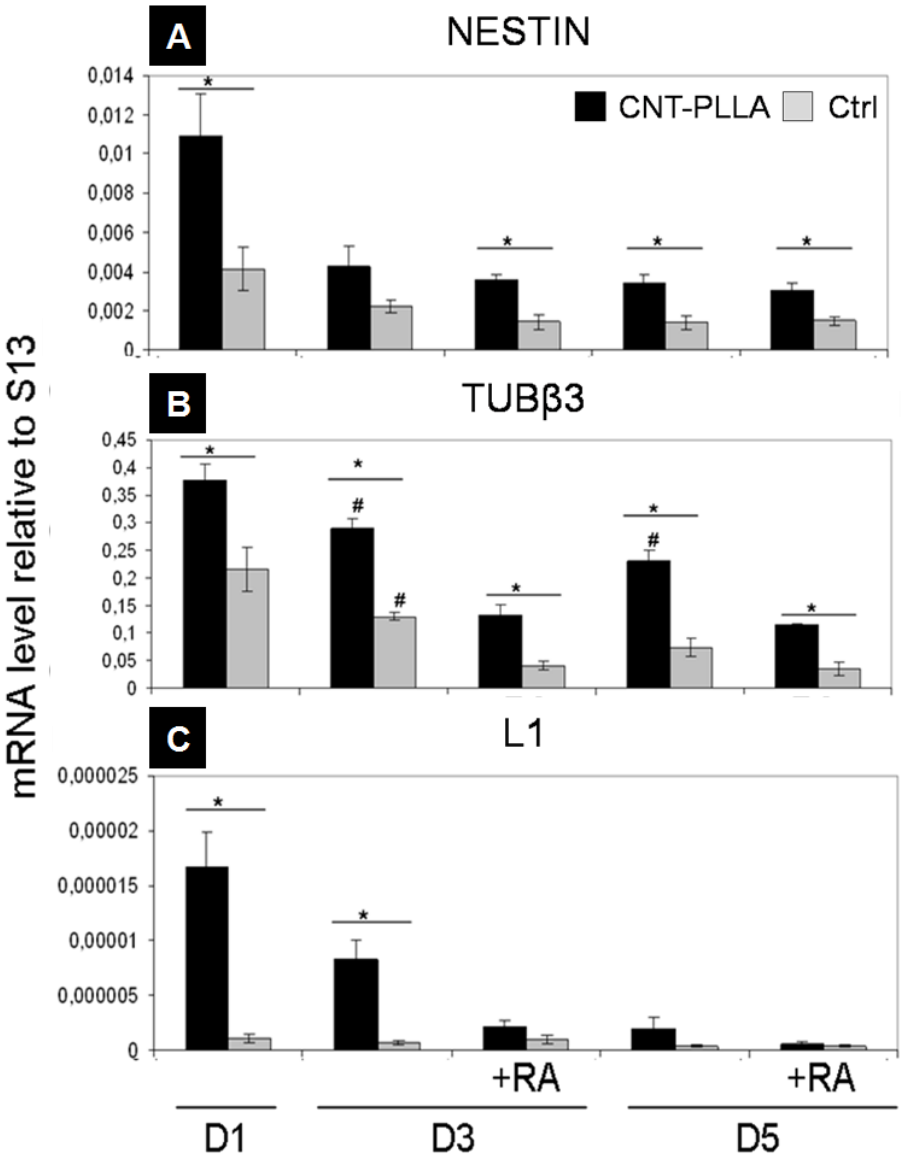

Figure38. Effects of the CNT-PLLA scaffolds on neuronal marker expression. Nestin **(A)**, TUBβ3 **(B)** and L1 **(C)** expression profile of hCMCs cultured on plates (control) and onto CNT-PLLA scaffolds. Data are mRNA levels normalized to the expression of the housekeeping gene S13. At least three independent experiments were performed in triplicate and the real time PCR was run twice for each sample (technical duplicate). * shows significance at $p<0.05$ between cells seeded on the CNT-PLLA scaffolds and the control.

qPCR analyses revealed a sudden change in gene expression soon after cell seeding onto the scaffolds. Nestin - a marker of neuronal precursors - is strongly upregulated after 24 hours from hCMCs seeding onto the scaffolds; then, its expression decreases with the maintenance in culture but it remains significantly higher than control cells (Fig. 38A). Neuronal L1 expression is upregulated on cells seeded onto the scaffolds and this is particularly evident within the first 72 hour from seeding in the absence of RA stimulation (Fig. 38C). TUBβ3 is a marker specific of cells that have acquired a neuronal commitment and it is highly upregulated soon after cell seeding onto the scaffolds, and its expression is higher than control during the whole differentiation period (Fig. 38B). The stimulation of cells with RA does not have a positive effect on TUBβ3 expression. TUBβ3 was also detected at the protein level by immunofluorescence, 5 days from cell seeding (Fig. 39A). As shown in Fig. 39B, approximately 77% of cells seeded onto the scaffold in the absence of RA stimulation are TUBβ3 positive, while in the presence of RA stimulation only ~ 37% of cells express TUBβ3. Otherwise, when grown onto the well bottom, the percentage of cells positive for TUBβ3 is strongly reduced (~23% RA-; ~7%RA+).

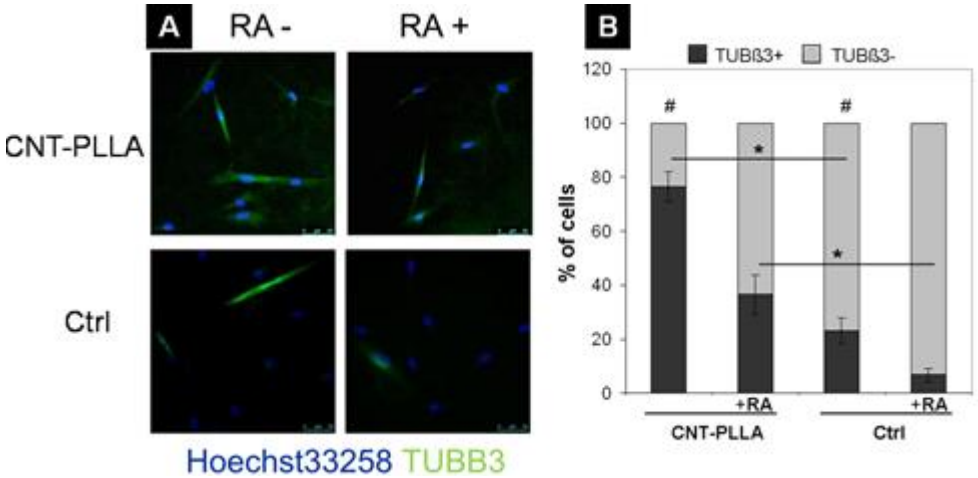

Figure 39. TUBβ3 expression detected by immunofluorescence. Immunofluorescence for TUBβ3 (green) in hCMCs after 5 days in culture. Nuclei are counterstained with Hoechst 33258 (blue) **(A)**. Quantification of TUBβ3 expression considered as the percentage of TUBβ3 positive cells in the total amount of cell counted **(B)**.Three independent experiment were performed in duplicate. * shows significance at $p<0.05$ between cells seeded on the CNT-PLLA scaffolds and the control (well bottoms). # shows significance at $p<0.05$ between cells treated with RA and their respective untreated control. Image magnification in **(A)** is 20X.

4.8.2 L1-A AND LINGO1-A EFFECTS ON hCMC GROWTH AND DIFFERENTIATION

We treated hCMCs with L1-A and LINGO1-A , and both peptides confirmed to be perfectly biocompatible as no meaningful difference was found with respect to untreated controls, either in the presence or absence of RA stimulation (Fig. 40A). The two peptides seem to influence cell morphology as (i) L1-A treatment elicits more fusiform cell body shape (compared to the wide spread appearance of control cells) and outgrowth of long protrusions that resembles neurites, while (ii) LINGO1-A treated samples show more rounded cell bodies and long neurite-like protrusions. Moreover, when cells are contemporarily induced with RA and treated with peptides, more arborized protrusions can be observed (Fig. 40B).

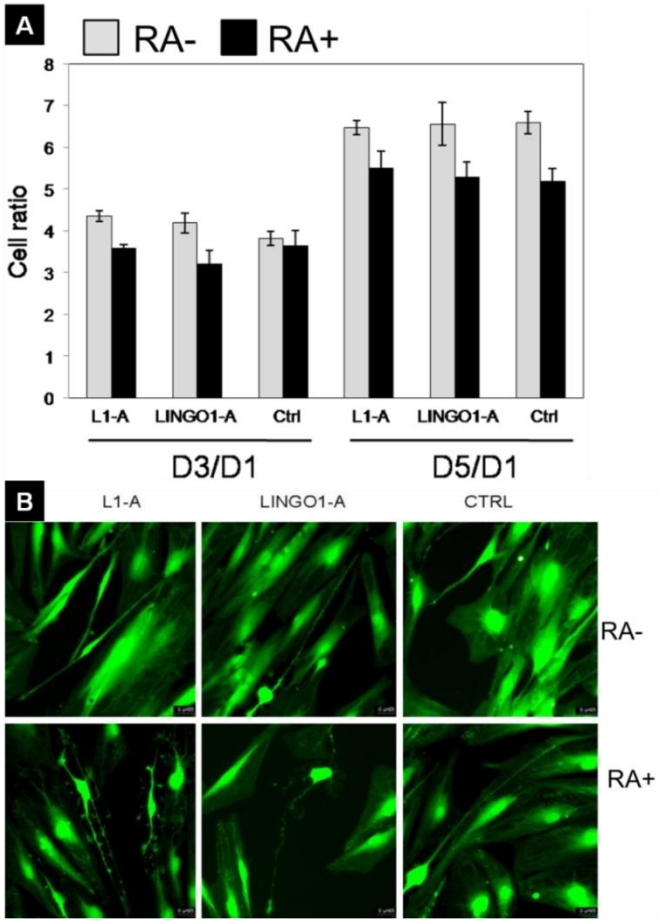

Figure 40. Peptide effects on hCMC growth and morphology. Cell proliferation. Data represent the mean ± SEM of three independent experiments performed in triplicate **(A)**. hCMCs stained with calcein-AM 24 hours after peptide administration, Image magnification is 32X **(B)**.

qPCR analysis show that L1-A and LINGO1-A peptides are able to influence the expression of markers typical of the neuronal lineage: Nestin and TUBβ3 are upregulated 24 hours from peptide administration in both L1-A and LINGO1-A treated samples in the absence of RA stimulation (Fig. 41A,B); MAP2 is a neuron-specific marker that resulted to be upregulated at day 3 in L1-A treated samples in the absence of RA stimulation and in LINGO1-A treated samples after RA stimulation. At day 5 we can notice an increment in the expression of this marker in both peptide treated samples after RA stimulation, but such incremental differences are not statistically significant from the control (Fig. 41C). VAMP7 - a vesicle associated membrane protein whose expression is high in neuronal cells - is crucial to the transport of lipids and proteins at the plasma membrane allowing neurite extension. We found that VAMP7 is upregulated in peptide treated samples either at day 3 and day5 in the absence of RA stimulation, while a strong upregulation of this marker happens in LINGO1-A treated samples after RA stimulation at day5 (Fig. 41D).

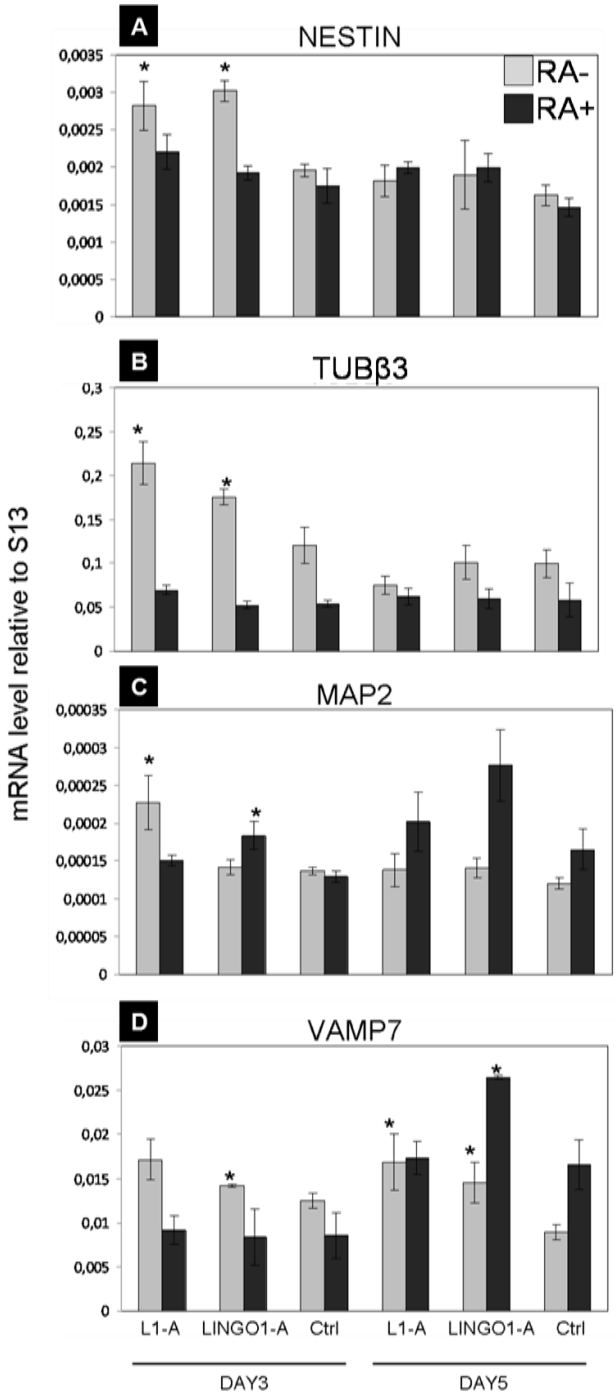

Figure 41. Peptide effects on neuronal marker expression. Nestin **(A)**, TUBβ3 **(B)**, MAP2 **(C)** and VAMP7 **(D)** expression profile of hCMCs treated with peptides and controls (untreated samples). Data are mRNA levels normalized to the expression of the housekeeping gene S13. At least three independent experiments were performed in triplicate and the real time PCR was run twice for each sample (technical duplicate). * shows significance at $p<0.05$ between peptide treated samples and the control.

4.8.3eCNT-PLLA SCAFFOLD EFFECTS ON hCMC ADHESION AND DIFFERENTIATION

hCMCs were tested also with eCNT-PLLA scaffolds, even in this case cells are able to adhere and grow onto scaffold surfaces. As previously shown for the CNT-PLLA scaffolds, also the eCNT-PLLA scaffolds influence cell morphology as cells show features typical of cells of the neuronal lineages (Fig. 42A). Such cells onto the scaffold present a reduced diameter size and fusiform cell bodies compared to the wide appearance of control cells (Fig. 42B). Moreover, more polarized cells are counted when cells are grown onto the eCNT-PLLA scaffold (Fig. 42C); indeed cells show very long neurite-like protrusions and present a total protrusion length and a number of protrusions per cell higher than control (Fig. 42D,E). Interestingly, hCMCs showed high sensitivity for scaffold topography: indeed, from the superimposition of the Calcein-AM stained cells and the bright field images of the corresponding portion of the eCNT-PLLA scaffold, we can notice that hCMCs extend protrusions following scaffold fibre orientation as shown by the white arrows (Fig. 43).

qPCR analyses, performed 24 hours after seeding, revealed the upregulation of Nestin, TUBβ3, MAP2 and VAMP7 neuronal markers (Fig. 44) and hence suggesting the neuronal differentiation program activation.

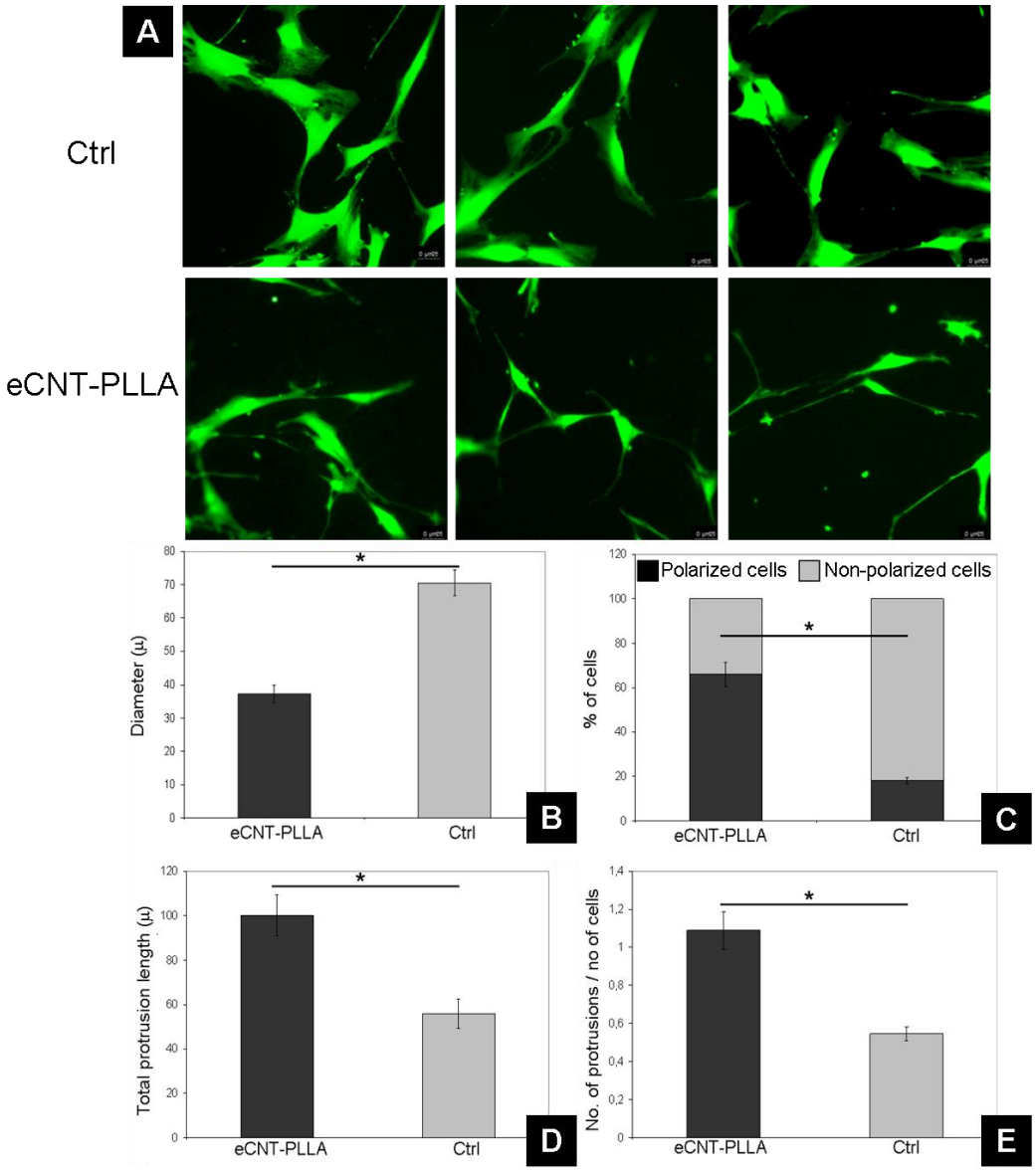

Figure 42. Effect of the eCNT-PLLA scaffolds on hCMC morphology.hCMCs stained with calcein-AM **(A)**. Mean cell diameter **(B)**, percentage of polarized cells **(C)**, total protrusion length (**D)**, number of protrusions per cell **(E)**. Quantification was performed 24 hours from cell seeding. Data represent the mean ± SEM of three independent experiments performed in duplicate. *shows significance at $p<0.05$ between cells seeded onto eCNT-PLLA scaffold and control (well bottoms). Image magnification in **(A)** is 32X.

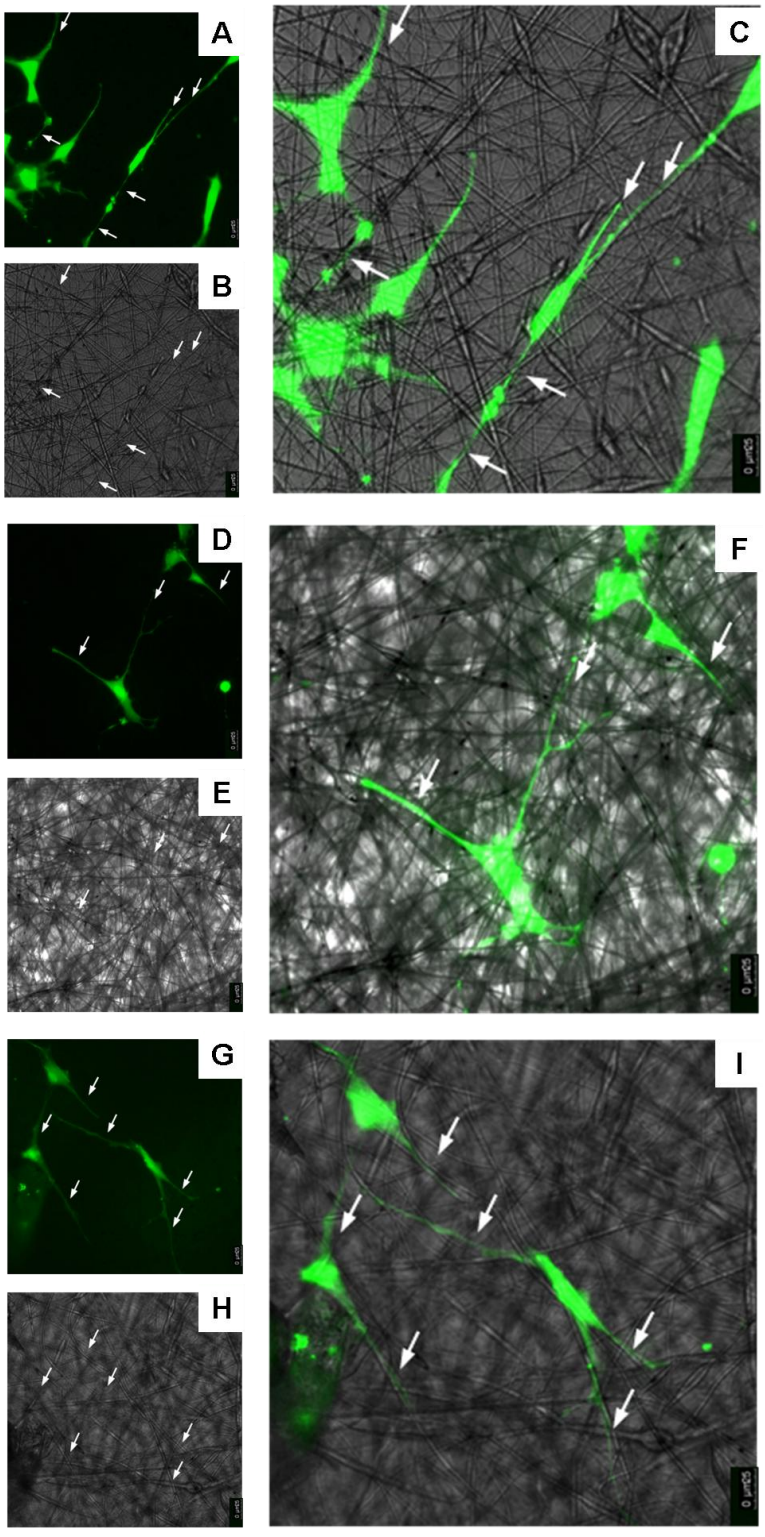

Figure 43. hCMCs extend protrusions following the scaffold fibre orientation. Fluorescent image of hCMCs stained with Calcein-AM **(A, D, G)**, bright field image of the eCNT-PLLA scaffold **(B, E, H)**, superimposition of cell fluorescent images and scaffold bright field images **(C, F, I)**. Arrows indicate protrusions following the scaffold fibre orientation. Image magnification is 32X.

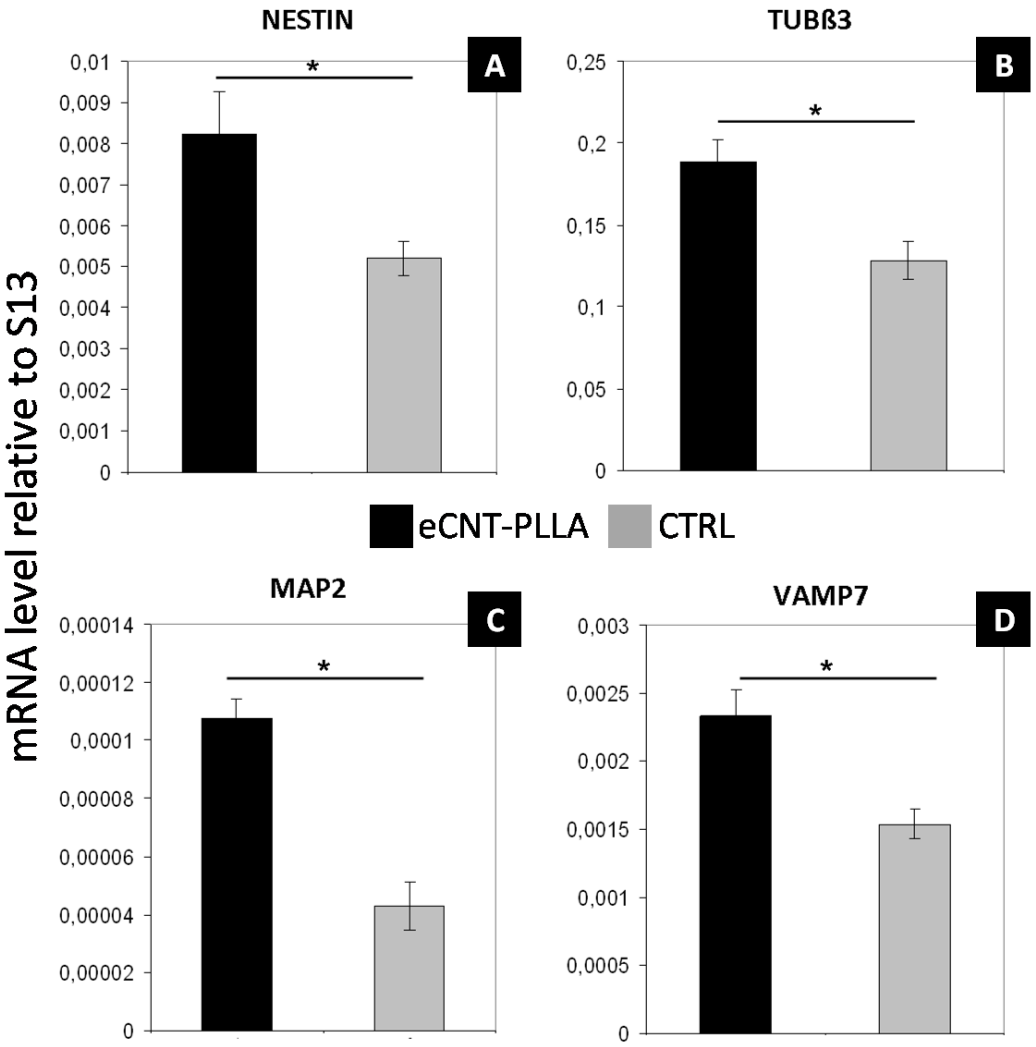

Figure 44. Effects of the eCNT-PLLA scaffolds on neuronal marker expression 24h cell seeding. Nestin **(A)**, TUBβ3 **(B)**, MAP2 **(C)** and VAMP7 **(D)** expression profile of hCMCs cultured on plates (control) and onto eCNT-PLLA scaffolds. Data are mRNA levels normalized to the expression of the housekeeping gene S13. Three independent experiments were performed in triplicate and the real time PCR was run twice for each sample (technical duplicate). * shows significance at $p<0.05$ between cells seeded on the eCNT-PLLA scaffolds and the control.

5. DISCUSSION

SH-SY5Y is a neuroblastoma cell line that shares many features with immature neuroblasts and hence shows characteristic of cells committed to the neuronal fate (Constantinescu et al., 2007). After RA treatment, several neuronal markers such as Nestin, VAMP7, TRKB and L1 are upregulated in SH-SY5Y cells, according to knowledge about RA mediated positive regulation on neuronal differentiation. Moreover, RA induced cell differentiation is confirmed by the increased number of long processes protrudring from treated cells. Therefore, SH-SY5Y cells represent a good model system to study neuronal differentiation *in vitro*.

The synthetic peptides L1-A and LINGO1-A - designed to mimic the neural environment by reproducing interaction motifs involved in guidance of neuronal processes - were confirmed to improve neuronal differentiation and thus are good candidates for functionalizing neural regeneration implants. In all experimental conditions, both L1-A and LINGO1-A showed full biocompatibility, neither exerting cytotoxic effects nor influencing cell proliferation, and their positive effect on neuronal differentiation (with 1 μM as optimal concentration) is sequence specific, as confirmed by control experiments with the scrambled peptides. Since the highest neuritogenic effects are mediated by L1-A and LINGO1-A (when added to the culture medium) in the presence or absence of RA induction, respectively, these peptides are likely to act through (at least partially) different pathways.

We showed that RA promotes neuronal L1 expression; indeed, RA also induces the degradation of the Repressor Element-1 Silencing Transcription factor (REST) (Singh et al.,2011), which in turn mediates transcriptional repression of neuronal L1. REST is highly expressed in SH-SY5Y cells to maintain them poorly differentiated (Mikulak et al., 2012); therefore, RA induction promotes L1 expression and L1-A is likely to encounter an increased number of homophilic

ligands on neuronal surfaces. Such binding is thought to be mimetic of the L1 homophilic binding and hence able to stimulate neurite outgrowth through the activation of intracellular signaling cascades (Kenwrick et al., 2000; Loers et al., 2005). Indeed, many neuronal differentiation genes are upregulated in RA induced samples after L1-A administration: Nestin and TUBβ3 expression is consistent with cytoskeleton rearrangements necessary for cell architecture changes during differentiation, VAMP7 upregulation allows the transport of proteins and lipids at the plasma membrane for neurite elongation, TRKB renders cells responsive to neurotrophins, while L1 augmentation suggests the presence of a positive feedback as the increase of putative ligands enhances endogenous L1 expression. It was previously demonstrated that L1 molecules are transported at the plasma membrane in VAMP7 vesicles and that L1 homophilic binding at the plasma membrane recruits VAMP7 vesicles for L1 recycling (Alberts et al., 2003). Therefore, in addition to recruit VAMP7 at the plasma membrane, the L1 homophilic binding might stimulate VAMP7 and L1 expression due to the involvement of these proteins in the establishment of a dynamic gradient of L1 adhesivity necessary for neurite elongation (Kamiguchi et al., 2000).

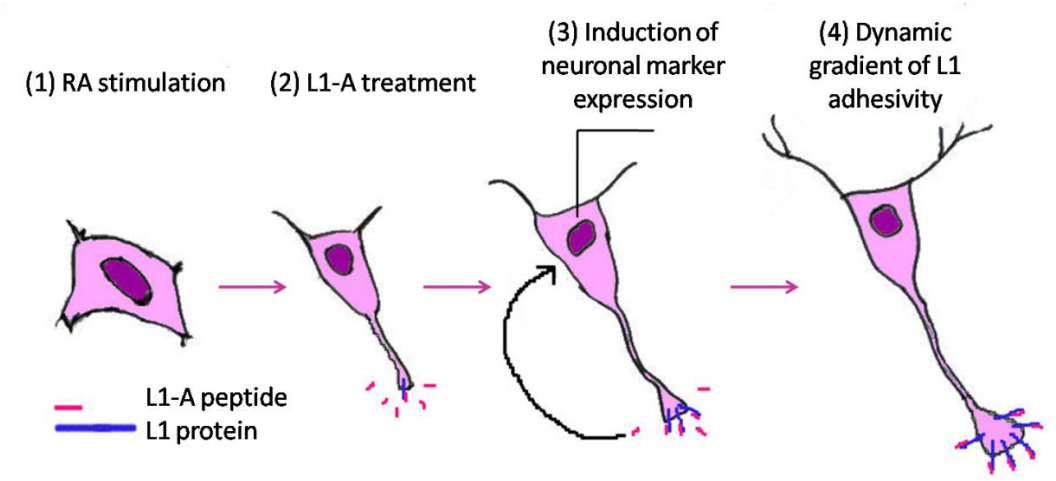

Figure 45. Proposed mechanism of action of L1-A peptide. (1) RA stimulation induces L1 endogenous molecule expression, **(2)** L1-A peptide binds to L1 endogenous molecules **(3)** inducing the expression of neuronal differentiation markers as TUBβ3, TRKB, VAMP7 and L1. **(4)** The upregulation of VAMP7 and L1 may be of help in the establishment of a dynamic gradient of L1 adhesivity necessary for neurite outgrowth.

Otherwise, we confirmed that RA downregulates LINGO1 expression (Puttagunta et al., 2011) and thus, in the absence of RA, the number of LINGO1 molecules at the neuronal surfaces is increased. When considering similarity between L1/L1-A and LINGO1/LINGO1-A systems, LINGO1 might interact with LINGO1-A peptide stimulating neurite outgrowth as suggested by the enhancement of neuronal differentiation markers expression as TUBβ3, MAP2, TRKB and VAMP7. In fact, homophilic binding between neuronal LINGO1 and oligodendrocyte precursor LINGO1 occurs and leads to oligodendrocyte final differentiation inhibition (Jepson et al., 2012). Even though effects at neuronal level are still unclear, this interaction could stimulate neurite elongation, because the axon needs to grow properly before being myelinated. Alternatively, LINGO1-A peptide could act by masking LINGO1 interaction site with the other members of the NgR1/LINGO1/p75 complex, with neuronal NogoA or with EGFR. This in turn would lead to non-functional complexes formation, blocking LINGO1 inhibitory effect on neurite elongation. These hypotheses are supported by evidences according to which LINGO1 mediates homo/heterotypic interactions through its Ig domain (Stein et al., 2012) and that when LINGO1 is inhibited neurite elongation is promoted (Mi et al., 2004; Ji et al., 2006; Inoue et al., 2007; Mi et al., 2013; Fernandez-Enright et al., 2014). In this work, LINGO1-A treated samples presented the highest percentage of neurites longer than 100 μm; increased number of such long neurites could depend on "inhibition of the inhibitory effect" as inhibition of repulsive forces can prevent their sprouting from parental neurites, favouring elongation. Moreover, the upregulation of TRKB in peptide treated samples suggests the possibility of TRKB signaling activation by peptides. Indeed, L1 homophilic binding is known to activate FGFR pathway (Kenwrick et al., 2000) leading to cAMP response element-binding protein (CREB) phosphorylation and TRKB expression (Deogracias et al., 2004; Ditlevsen et al., 2008). Otherwise, LINGO1 is known to interact with TRKB avoiding its phosphorylation and hence exerting negative effects on neuronal survival and differentiation (Fu et al., 2010). Therefore, LINGO1-A peptide could act by

masking LINGO1 interaction sites with TRKB, allowing TRKB activation and the initiation of a signaling cascade that leads to CREB phosphorylation and TRKB expression (Finkbeiner et al., 1996; Deogracias et al., 2004). Even when L1-A and LINGO1-A were used to coat wells prior to cell seeding, their positive effect on neuronal differentiation was confirmed.

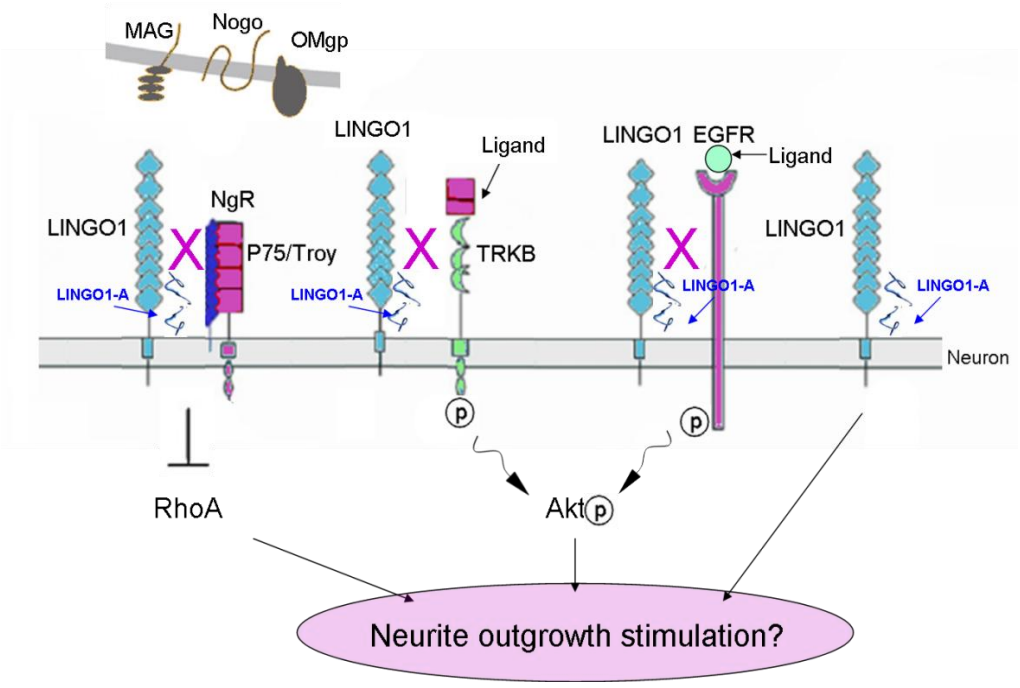

Figure 46. Proposed mechanism of action of LINGO1-A peptide. LINGO1-A peptide could act by masking LINGO1 interaction site with partners and hence blocking LINGO1 inhibitory effects on neurite outgrowth. LINGO1-A peptide might interact with LINGO1 endogenous molecules stimulating neurite outgrowth.

A proteome-wide search showed that the Arg at the seventh position in the L1-A and LINGO1-A peptide sequences is highly conserved in mammals and vertebrates; furthermore, mutations regarding this position in L1 protein (R184) are causative of neurological disorders (De Angelis et al., 2002) and able to impair the L1 homophilic binding (Zhao et al., 1998). We showed that L1-A R184A (Zhao mutation) peptide completely loses the neuritogenic effect when used to treat SH-SY5Y cells; while L1-A R184Q (CRASH mutation) peptide maintains a very low differentiating activity. Such results provide a unifying rationale for the role of the conserved motif in neuronal function and differentiation, as the same

position results to be crucial to both (i) adhesion, (ii) neuritogenesis and (iii) correct neuronal function. In fact:

i. Zhao and co-workers demonstrated that the L1-A peptide is able to inhibit the homophilic binding between two L1 Ig2 domains and identified this region as the homophilic binding site. Otherwise, the L1-A R184A mutant is unable to inhibit such interaction (Zhao et al., 1998);

ii. we showed that the L1-A peptide alone stimulates neurite outgrowth in SH-SY5Y cells and thus it seems to be mimetic of the entire Ig2 domain in promoting the homophilic binding (Scapin et al., 2014).

iii. R184Q mutation is causative for the CRASH syndrome, possibly depending on impaired L1 homophilic binding (De Angelis et al., 2002).

The low neuritogenic activity maintained by L1-A R184Q may depend on the compatible features of Arg and Gln (positively charged and polar); the R184A mutation has not been retrieved in CRASH syndrome patients and may be not compatible with life. Therefore, R184 position seems to be crucial for L1 function; however, it is noteworthy that in our scrambled peptide, Arg at seventh position is kept and this notwithstanding, sequence randomization at other positions also results in activity loss. Therefore, in addition to the conserved Arg, further positions are crucial to the binding motif, and our own data are in agreement with evidence that when keeping Arg184, mutation at position 2 (Ile) also results in CRASH syndrome (Ruiz at al., 1995).

The positive role played by CNTs in supporting neuronal growth and differentiation is suggested by recently published, excellent works (see Introduction). However, the limits of these systems also emerged (e.g., cytotoxicity of CNTs upon scaffold disaggregation). While immobilization of CNTs onto coverslips partially alleviate these problems (Mattson et al., 2000; Hu et al.,

2004; Lovat et al., 2005; Malarkey et al., 2009), such a strategy is not suitable for regenerative medicine purposes as coverslips are not implantable. Instead, nanocomposite CNT-PLLA scaffolds grant (i) full biocompatibility, (ii) good support of cell growth and differentiation and (iii) mechanical flexibility required for implant purposes. Moreover, the low percentage of purified CNTs within the scaffold reduces both costs and cytotoxicity by residual impurities, while preserving the ability of CNT-based scaffolds to support neuronal growth and differentiation.

Indeed, our data show that CNT-PLLA scaffolds support SH-SY5Y cell adhesion and differentiation better than PLLA alone. Moreover, L1-A and LINGO1-A exert improved neuritogenic properties when cells are cultured onto CNT-PLLA scaffolds and in some conditions their effect is enhanced by the CNT-PLLA scaffold itself. This effect is particularly evident when considering data about total neurite length, branch points per neurite and neurites per cell concerning cells cultivated onto the CNT-PLLA scaffold and treated with L1-A or LINGO1-A after RA induction. The combination of CNT-PLLA scaffolds, L1-A or LINGO1-A treatment and RA induction also promotes the formation of growth cones, likely because of an increased amount of cue types available for the cells in their environment.

Once the CNT-PLLA scaffolds are developed, the scaffold topography was further improved by including fibres through the electrospinning technique. Such novel electrospun eCNT-PLLA scaffolds show a regular surface morphology with a diameter that ranges from 300 to 600 nm; therefore, scaffold fibre diameters are within the diameter range of axons (from 0.08 to 20 µm) (Debanne et al., 2011) and of collagen fibrils (from 260 to 410 nm) (Dvir et al., 2011). The eCNT-PLLA scaffolds showed a good level of biocompatiblility with SH-SY5Y cell cultures and promoted cell adhesion and differentiation better than ePLLA alone. The presence of CNTs (whose diameter range from 6 to 30 nm) is thought to alter the nanotopography of scaffold networks providing sites for cellular anchorage and guiding cytoskeletal extensions (Lee et al 2014). Moreover, SH-SY5Y cells resulted

to be very sensible to scaffold topography as they are induced to extend more neurites compared to control cells. The newly formed neurites are shorter than those from control cell neurites; however, they elongate following fibre orientation and this responsiveness to scaffold topography is of particular interest because it opens up the perspective to obtain a polarized neurite outgrowth upon fibre alignment.

In addition, a synergistic effect was revealed between the eCNT-PLLA scaffold and LINGO1-A peptide as the scaffold induce le formation of new neurites and LINGO1-A promotes their elongation. This suggests a good starting point to develop next-generation scaffolds upon peptide functionalization.

After setting up the biomimetic nanosystem with SH-SY5Y cells, we decided to test our scaffolds and peptides with a more physiological source of cells, suitable for regenerative medicine applications. We chose hCMCs as these adult stem cells can be (i) easily isolated from peripheral blood and then (ii) differentiated into many cell types under proper conditions; moreover, they are (iii) suitable for autologous transplant without implying ethical restrictions. With this work we showed that features of our CNT-PLLA scaffolds and biomimetic peptides are able to provide these cells with neuronal commitment.

The CNT-PLLA scaffold resulted to be a good support for hCMCs adhesion and growth without exerting cytotoxic effects. When cultivated onto the CNT-PLLA scaffolds, cells show typical features of cells from the neuronal lineage, such as reduced size of cell bodies and polarized morphology with neurite-like protrusions tipped with fan-shaped structures that resemble neuronal growth cones. Soon after cell seeding, upregolation of typical genes from the neuronal lineage occurs: in particular, upregulation of Nestin indicates that cells are undertaking the differentiation pathway that leads to neural progenitor cells like neurons, oliogdendrocytes and astrocytes. However, upregulation of TUBβ3 and the neuronal form of L1 - that is evident 24 hours from cell seeding and maintained higher than control until the third (L1) and the fifth (TUBβ3) day of cultures - shows that some cells are acquiring a neuronal commitment. TUBβ3 is

revealed at the protein level in the majority (~77 %) of cells seeded onto the CNT-PLLA scaffolds in the absence of RA stimulation confirming the neuronal commitment acquisition since TUBβ3 is a marker specific of immature and post-mitotic neurons. Therefore the CNT-PLLA scaffolds seem to be able to confer a neuronal commitment to hCMCs only thanks to their own characteristics:

- the CNT component of the scaffold - whose nanoroughness matches the size of the finest neuronal processes (Fabbro et al., 2013) - is indeed thought to mimic the neural environment topography and therefore favouring cell adhesion, neurite extension and differentiation toward the neuronal lineage;
- CNTs are able to adsorb proteins and growth factors thanks to their chemical properties and enhanced surface area provided by their needle-like shape (Chao et al., 2010; Chen al., 2013). In addition, hCMCs produce cytokines and growth factors capable to control their own proliferation and differentiation. Therefore, the CNT-PLLA scaffold could retain proteins and growth factors produced by hCMCs acting as a reservoir of elements available for cells during their growth and differentiation.
- we previously showed that the CNT presence within the scaffold increases the scaffold conductivity (Scapin et al., 2014); therefore, the conductive properties of the scaffold could be responsible for cell differentiation maybe due to the formation of hybrid nanotube-cell unit (Mazzatenta et al., 2007). It is known in fact that electrical conductivity has a critical role in controlling neuronal cell growth and differentiation (Yamada et al., 2007; Gordon et al., 2009; Fabbro et al., 2013).
- Cell differentiation observed onto CNT-PLLA scaffolds is likely related to changes in cell shape. Indeed, cells onto the scaffold have polarized appearance and reduced size of cell bodies. Modulating cell shape might play a central role in directing the fate of differentiation, because it can influence nucleus shape affecting nuclear matrix proteins and focal

adhesion complexes and thus the expression of silent genes (Kim et al., 2012).

Other studies previously reported the ability of CNT-based scaffolds to modulate embryonic, mesenchymal and neural stem cells commitment towards neurogenesis when coupled to chemical soluble factors (Jan et al., 2007; Chao et al., 2010; Chen et al., 2012; Kim et al., 2012). Other works show instead that such cells can achieve a neuronal commitment either in absence of neuronal stimulating conditions when CNT films (Tay et al., 2010) and CNT-collagen scaffolds (Chen et al., 2013; Lee et al., 2014) are used. Therefore, our study confirms that the CNTs features are able *per se* to promote stem cell differentiation toward the neuronal lineage and highlights that a very low percentage of dispersed CNTs (1%) is sufficient to improve scaffold electrical properities and cell differentiation. Furthermore, our scaffold combines the nanotopographical and electrical characteristics of CNTs with the properties of PLLA. This synthetic, fully biocompatible polymer is not immunogenic hence more suitable than animal-derived collagen for developing implantable scaffolds. Moreover, the dispersion of CNTs in the PLLA matrix makes the scaffold flexibility suitable for properly shaping and well fitting into the injured site.

At least in our knowledge, the study presented in this thesis represents the first report on human adult stem cells derived from blood to be cultured onto CNT-based scaffolds and hence highlights hCMCs as a precious source of stem cells exploitable for such applications. hCMCs in fact present some advantages in comparison to other sources of stem cells: (i) when compared to hESCs, hCMCs are not subjected to ethical restrictions in that representing an autologous cell source; (ii) unlike iPSCs, hCMCs are free from tumorigenesis risk, (iii) they can be isolated in larger amounts than NSCs, (iv) they can be more easily isolated and in a less invasive way with respect to both NSCs (brain) (Rietze et al., 2006) and MSCs (mainly bone marrow) (Augello et al., 2010). Therefore, such CNT-PLLA scaffolds both (i) support cell growth onto a low cytotoxicity environment and (ii)

contain the instructions necessary to drive cell neuronal differentiation. Thanks to these characteristics, hCMCs could be transplanted to neuron injured sites onto the CNT-PLLA scaffolds that would promote their differentiation without the addition of soluble factors that are more difficult to administrate and pattern *in vivo* (Chen et al., 2013).

Concerning the biomimetic L1-A and LINGO1-A peptides, they were able to influence hCMC behaviour without altering cell proliferation. When added to culture medium, the peptides are able to influence cell shape as treated cell morphology is sharper than the wide spread appearance of control cells. Moreover, the two peptides induce the formation of long protrusions resembling neurites and stimulate the expression of neuronal cytoskeleton markers, such as Nestin, TUBβ3 and MAP2 that have an important role in neuronal architecture definition. Last but not least, the upregulation of VAMP7 is consistent with the enhancement of proteins and lipids transport at the plasma membrane for the neurite outgrowth initiation.

Moreover, hCMCs resulted to be sensitive to scaffold topography; indeed when seeded onto the eCNT-PLLA scaffolds both the cell bodies and the neurite-like protrusions were found to be stretched out and aligned along the scaffold fibres. In addition, qPCR analyses showed an upregualtion of neuronal marker genes attesting the differentiation program activation. Considering that - for an effective electrical signal transfer - transplanted cells not only have to differentiate but also need to be synaptically connected to neural networks, the possibility to control both cell differentiation and polarization through scaffold composition and topography could be of great help to clinical applications. Such results suggest the possibility to covalently functionalize the scaffolds with peptides, in order to enrich the spectrum of differentiating cues provided by the scaffolds and to more finely regulate cell differentiation and their spatial organization.

6. CONCLUDING REMARKS

In conclusion, we developed freestanding scaffolds that combine the biocompatible properties of PLLA (Yang et al., 2004) with the conductive, mechanical and topographical features of CNTs. Furthermore, designed L1-A and LINGO1-A peptides were confirmed to mediate positive effects on neuronal differentiation and, even though further studies are needed to clearly determine their mechanisms of action, they represent a promising tool for regenerative medicine. Indeed, replacement of recombinant proteins by biomimetic peptides reproducing only active motifs dramatically cuts costs, simplifies preparation and functionalization of scaffolds. Moreover, short peptides display increased stability and lower immunogenic potential with respect to entire proteins and protein domains (Chen et al., 2008). Our CNT-PLLA scaffold, used in combination with the peptides, demonstrates synergistic effects in supporting neuronal cell growth and differentiation and thus it is a good starting point for setting up next generation scaffolds upon peptide functionalization. Moreover, the hypothesis of LINGO1-A peptide ability to inhibit LINGO1 endogenous molecule function is of particular interest because a small synthetic peptide able to counteract the effect of inhibitory proteins is of potential wide applicability. In fact, in addition to being used in the development of scaffolds promoting neuronal regeneration after injury, it might also be of help in the treatment of some neurodegenerative diseases characterized by LINGO1 upregulation, like e.g. Parkinson's disease and Multiple Sclerosis (Inoue et al., 2007, Mi et al., 2013). Thanks to LINGO1 restricted tissue distribution and to LINGO1-A small size that allows its encapsulation into nanocarriers able to overpass the emathoencephalic barrier (Silva et al., 2007); LINGO1-A represents an interesting starting molecule for developing therapeutics to cure neural dysfunctions. Our experiments with L1-A mutant peptides confirm the important role of the highly conserved R184

residue for L1 function as it is crucial at the same time to adhesion, neuritogenesis and correct neurodevelopment. The shaping of the CNT-PLLA scaffold into fibres mimicking neuronal extracellular environment results in enhanced cell ability to form new neurites that elongate following the scaffold fibre orientation. Such micro/nano-scale sensitivity of cells to the scaffold topography is of great interest because it opens up the perspective to obtain a polarized neurite outgrowth upon fibre alignment. The polarized neurite outgrowth is a fundamental prerequisite for neural regenerating scaffold as the regenerating axon needs to be properly guided towards the correct target, improving the formation of an effective neural network. Moreover, the synergistic effect shown by eCNT-PLLA scaffolds and LINGO1-A peptide suggests that the scaffold functionalization with LINGO1-A peptide could provide substrates endowed with multiple cues able to stimulate both neurite sprouting and their elongation and highlight the importance of nanomaterials and micro/nanotechnology for developing devices to control cell behaviours with a micro/nano-scale sensitivity. Moreover,the scaffolds and the peptides resulted to be suitable for hCMCs cultures and to induce their entering the neuronal differentiation pathway.

Further improvements in the scaffold geometry and composition, functionalization with peptides and culture conditions are necessary to achieve the complete neuronal differentiation of cells and to control the neuron subtype obtained, but our system resulted to be a good starting point for setting up implantable scaffolds for autologous neuronal differentiation. In addition, such results highlight the high plasticity of hCMCs that, even if isolated from blood and thought to have a mesodermal origin, they are able to undergo neuronal differentiation, hence representing a precious source of adult stem cell with potential for neural tissue engineering applications. Future functional assessment ofsynaptic transmission and electrophysiological properties of cells onto the scaffolds will be of great interest. Moreover, coupling such scaffolds with electrical stimulation (which is readily achievable using CNT based

materials) can boost further analyses aimed at studying neuronal differentiation and has great potential in nerve injury repair as well as neuron prosthesis.

7. REFERENCES

Abney JR, Meliza CD, Cutler B, Kingma M, Lochner JE, Scalettar BA. Real-time imaging of the dynamics of secretory granules in growth cones. Biophys J. 1999;77(5):2887-95.

Abrams GA, Goodman SL, Nealey PF, Franco M, Murphy CJ. Nanoscale topography of the basement membrane underlying the corneal epithelium of the rhesus macaque. Cell Tissue Res. 2000 Jan;299(1):39-46.

Ahn HS, Hwang JY, Kim MS, Lee JY, Kim JW, Kim HS, Shin US, Knowles JC, Kim HW, Hyun JK. Carbon-nanotube-interfaced glass fiber scaffold for regeneration of transected sciatic nerve. Acta Biomater. 2015 Feb;13:324-34.

Alberts P, Rudge R, Hinners I, Muzerelle A, Martinez-Arca S, Irinopoulou T, Marthiens V, Tooze S, Rathjen F, Gaspar P, Galli T. Cross talk between tetanus neurotoxin-insensitive vesicle-associated membrane protein-mediated transport and L1-mediated adhesion. Mol Biol Cell. 2003 Oct;14(10):4207-20.

Arnold M, Cavalcanti-Adam EA, Glass R, Blümmel J, Eck W, Kantlehner M, Kessler H, Spatz JP. Activation of integrin function by nanopatterned adhesive interfaces. Chemphyschem. 2004 Mar 19;5(3):383-8.

Arslantunali D, Dursun T, Yucel D, Hasirci N, Hasirci V. Peripheral nerve conduits: technology update. Med Devices (Auckl). 2014 Dec 1;7:405-24. doi: 10.2147/MDER.S59124. eCollection 2014.

Augello A, De Bari C. The regulation of differentiation in mesenchymal stem cells. Hum Gene Ther. 2010 Oct;21(10):1226-38.

Bai Y, Markham K, Chen F, Weerasekera R, Watts J, Horne P, Wakutani Y, Bagshaw R, Mathews PM, Fraser PE, Westaway D, St George-Hyslop P, Schmitt-Ulms G. The in vivo brain interactome of the amyloid precursor protein. Mol Cell Proteomics. 2008 Jan;7(1):15-34.

Bareket-Keren L, Hanein Y. Carbon nanotube-based multi electrode arrays for neuronal interfacing: progress and prospects. Front Neural Circuits. 2013 Jan 9;6:122.

Berezin V, Bock E. NCAM mimetic peptides: Pharmacological and therapeutic potential. J Mol Neurosci. 2004;22(1-2):33-39.

Bhardwaj N, Kundu SC. Electrospinning: a fascinating fiber fabrication technique. Biotechnol Adv. 2010 May-Jun;28(3):325-47.

Brahms S, Brahms J. Determination of protein secondary structure in solution by vacuum ultraviolet circular dichroism. .J Mol Biol. 1980;138(2):149-178.

Brunetti V, Maiorano G, Rizzello L, Sorce B, Sabella S, Cingolani R, Pompa PP. Neurons sense nanoscale roughness with nanometer sensitivity. Proc Natl Acad Sci U S A. 2010 Apr 6;107(14):6264-9.

Cellot G, Cilia E, Cipollone S, Rancic V, Sucapane A, Giordani S, Gambazzi L, Markram H, Grandolfo M, Scaini D, Gelain F, Casalis L, Prato M, Giugliano M, Ballerini L. Carbon nanotubes might improve neuronal performance by favouring electrical shortcuts. Nat Nanotechnol. 2009 Feb;4(2):126-33.

Cellot G, Toma FM, Varley ZK, Laishram J, Villari A, Quintana M, Cipollone S, Prato M, Ballerini L. Carbon nanotube scaffolds tune synaptic strength in cultured neural circuits: novel frontiers in nanomaterial-tissue interactions. J Neurosci. 2011 Sep 7;31(36):12945-53.

Chao TI, Xiang S, Chen CS, Chin WC, Nelson AJ, Wang C, Lu J. Carbon nanotubes promote neuron differentiation from human embryonic stem cells. Biochem Biophys Res Commun. 2009 Jul 10;384(4):426-30.

Chao TI, Xiang S, Lipstate JF, Wang C, Lu J. Poly(methacrylic acid)-grafted carbon nanotube scaffolds enhance differentiation of hESCs into neuronal cells. Adv Mater. 2010 Aug 24;22(32):3542-7.

Chen CS, Soni S, Le C, Biasca M, Farr E, Chen EY, Chin WC. Human stem cell neuronal differentiation on silk-carbon nanotube composite. Nanoscale Res Lett. 2012 Feb 14;7(1):126. doi: 10.1186/1556-276X-7-126.

Chen H, Yuan L, Song W,Wu Z, Li D. Biocompatible polymer materials: Role of protein–surface interactions. Progress in polymer science 2008;33:1059-1087.

Chen YS, Hsiue GH. Directing neural differentiation of mesenchymal stem cells by carboxylated multiwalled carbon nanotubes. Biomaterials. 2013 Jul;34(21):4936-44.

Chew SY, Wen Y, Dzenis Y, Leong KW. The role of electrospinning in the emerging field of nanomedicine. Curr Pharm Des. 2006;12(36):4751-70.

Cho Y, Borgens RB. The effect of an electrically conductive carbon nanotube/collagen composite on neurite outgrowth of PC12 cells. J Biomed Mater Res A. 2010 Nov;95(2):510-7.

Cho, Y., Borgens, R.B., 2010b. The effect of an electrically conductive carbon nanotube/collagen composite on neurite outgrow th of PC12 cells. J. Biomed. Mater. Res. A 95A, 510–517.

Choudhary V, Gupta A. Polymer/Carbon Nanotube Nanocomposites, Carbon Nanotubes - Polymer Nanocomposites, Dr. Siva Yellampalli 2011 (Ed.), ISBN: 978-953-307-498-6.

Chow SY, Moul J, Tobias CA, Himes BT, Liu Y, Obrocka M, Hodge L, Tessler A, Fischer I. Characterization and intraspinal grafting of EGF/bFGF-dependent neurospheres derived from embryonic rat spinal cord. Brain Res. 2000 Aug 25;874(2):87-106.

Christopherson GT, Song H, Mao HQ. The influence of fiber diameter of electrospun substrates on neural stem cell differentiation and proliferation. Biomaterials. 2009 Feb;30(4):556-64.

Cirillo V, Guarino V, Alvarez-Perez MA, Marrese M, Ambrosio L. Optimization of fully aligned bioactive electrospun fibers for "in vitro" nerve guidance. J Mater Sci Mater Med. 2014 Oct;25(10):2323-32.

Cizkova D, Kakinohana O, Kucharova K, Marsala S, Johe K, Hazel T, Hefferan MP, Marsala M. Functional recovery in rats with ischemic paraplegia after spinal grafting of human spinal stem cells. Neuroscience. 2007 Jun 29;147(2):546-60.

Cízková D, Rosocha J, Vanický I, Jergová S, Cízek M. Transplants of human mesenchymal stem cells improve functional recovery after spinal cord injury in the rat. Cell Mol Neurobiol. 2006 Oct-Nov;26(7-8):1167-80.

Colangelo AM, Bianco MR, Vitagliano L, Cavaliere C, Cirillo G, De Gioia L, Diana D, Colombo D, Redaelli C, Zaccaro L, Morelli G, Papa M, Sarmientos P, Alberghina L, Martegani E. A new nerve growth factor-mimetic peptide active on neuropathic pain in rats. J Neurosci. 2008 Mar 12;28(11):2698-709.

Comisar WA, Hsiong SX, Kong HJ, Mooney DJ, Linderman JJ. Multi-scale modeling to predict ligand presentation within RGD nanopatterned hydrogels. Biomaterials. 2006 Apr;27(10):2322-9.

Constantinescu R, Constantinescu AT, Reichmann H, Janetzky B. Neuronal differentiation and long-term culture of the human neuroblastoma line SH-SY5Y. J Neural Transm Suppl. 2007;(72):17-28.

Cui HF, Vashist SK, Al-Rubeaan K, Luong JH, Sheu FS. Interfacing carbon nanotubes with living mammalian cells and cytotoxicity issues. Chem Res Toxicol. 2010 Jul 19;23(7):1131-47.

Curtis A, Wilkinson C. Nanotechniques and approaches in biotechnology. Trends Biotechnol. 2001 Mar;19(3):97-101.

Curtis A, Wilkinson C. Topographical control of cells. Biomaterials. 1997 Dec;18(24):1573-83.

Dahlstrand J, Lardelli M, Lendahl U. Nestin mRNA expression correlates with the central nervous system progenitor cell state in many, but not all, regions of developing central nervous system. Brain Res Dev Brain Res. 1995 Jan14;84(1):109-29.

David S, Aguayo AJ. Axonal elongation into peripheral nervous system "bridges" after central nervous system injury in adult rats. Science. 1981 Nov 20;214(4523):931-3.

David-Pur M, Bareket-Keren L, Beit-Yaakov G, Raz-Prag D, Hanein Y. All-carbon-nanotube flexible multi-electrode array for neuronal recording and stimulation. Biomed Microdevices. 2014 Feb;16(1):43-53.

De Angelis E, Watkins A, Schäfer M, Brümmendorf T, Kenwrick S. Disease-associated mutations in L1 CAM interfere with ligand interactions and cell-surface expression. Hum Mol Genet. 2002 Jan 1;11(1):1-12.

Debanne D, Campanac E, Bialowas A, Carlier E, Alcaraz G. Axon physiology. Physiol Rev. 2011 Apr;91(2):555-602.

Dehmelt L, Halpain S. The MAP2/Tau family of microtubule-associated proteins. Genome Biol. 2005;6(1):204.

Dent EW, Gupton SL, Gertler FB. The growth cone cytoskeleton in axon outgrowth and guidance. Cold Spring Harb Perspect Biol. 2011;1;3(3).

Deogracias R, Espliguero G, Iglesias T, Rodríguez-Peña A. Expression of the neurotrophin receptor trkB is regulated by the cAMP/CREB pathway in neurons. Mol Cell Neurosci. 2004 Jul;26(3):470-80.

D'Este M, De Nardi M, Menna E. A co-functionalization approach to soluble and functional Single-Walled Carbon Nanotubes. Eur J Org Chem 2006; (11): 2517-2522.

Di Liddo R, Bertalot T, Barbon S, Rajendran S, Gasparella M, Parnigotto PP, Conconi MT. Differentiative potential of fibroblast-like cells from human peripheral blood. National congress S.I.A.I. - Società Italiana di Anatomia e Istologia, Pistoia 2012a, Congress book.

Di Liddo R, Rajendran S, Bertalot T, Barbon S, Mandoli A, Conconi MT. Neuron-like cells arise in vitro from human circulating multipotent cells. 4th Intl. Congr. on Stem Cells & Tissue Formation, Dresden 2012b, Congress Book.

Ditlevsen DK, Owczarek S, Berezin V, Bock E. Relative role of upstream regulators of Akt, ERK and CREB in NCAM- and FGF2-mediated signalling. Neurochem Int. 2008 Nov;53(5):137-47.

Dvir T, Timko BP, Kohane DS, Langer R. Nanotechnological strategies for engineering complex tissues. Nat Nanotechnol. 2011 Jan;6(1):13-22.

Edsjö A, Lavenius E, Nilsson H, Hoehner JC, Simonsson P, Culp LA, Martinsson T, Larsson C, Påhlman S. Expression of trkB in human neuroblastoma in relation to MYCN expression and retinoic acid treatment. Lab Invest. 2003 Jun;83(6):813-23.

Engler AJ, Sen S, Sweeney HL, Discher DE. Matrix elasticity directs stem cell lineage specification. Cell. 2006 Aug 25;126(4):677-89.

Evans GR, Brandt K, Widmer MS, Lu L, Meszlenyi RK, Gupta PK, Mikos AG, Hodges J, Williams J, Gürlek A, Nabawi A, Lohman R, Patrick CW Jr. In vivo evaluation of poly(L-lactic acid) porous conduits for peripheral nerve regeneration. Biomaterials. 1999 Jun;20(12):1109-15.

Fabbro A, Prato M, Ballerini L. Carbon nanotubes in neuroregeneration and repair. Adv Drug Deliv Rev. 2013 Dec;65(15):2034-44.

Fabbro A, Villari A, Laishram J, Scaini D, Toma FM, Turco A, Prato M, Ballerini L. Spinal cord explants use carbon nanotube interfaces to enhance neurite outgrowth and to fortify synaptic inputs. ACS Nano. 2012 Mar 27;6(3):2041-55.

Faroni A, Mobasseri SA, Kingham PJ, Reid AJ. Peripheral nerve regeneration: Experimental strategies and future perspectives. Adv Drug Deliv Rev. 2014 Nov 14. pii: S0169-409X(14)00273-7.

Fernandez-Enright F, Andrews JL, Newell KA, Pantelis C, Huang XF. Novel implications of Lingo-1 and its signaling partners in schizophrenia. Transl Psychiatry 2014;4:e348. doi: 10.1038/tp.2013.121.

Finkbeiner S, Tavazoie SF, Maloratsky A, Jacobs KM, Harris KM, Greenberg ME. CREB: a major mediator of neuronal neurotrophin responses. Neuron. 1997 Nov;19(5):1031-47.

Fon D, Zhou K, Ercole F, Fehr F, Marchesan S, Minter MR, Crack PJ, Finkelstein DI, Forsythe JS. Nanofibrous scaffolds releasing a small molecule BDNF-mimetic for the re-direction of endogenous neuroblast migration in the brain. Biomaterials. 2014 Mar;35(9):2692-712.

Fu QL, Hu B, Li X, Shao Z, Shi JB, Wu W, So KF, Mi S. LINGO-1 negatively regulates TrkB phosphorylation after ocular hypertension. Eur J Neurosci. 2010 Mar;31(6):1091-7.

Furtado CA; Kim UJ, Gutierrez HR, Pan L, Dickey EC, Eklund PC. Debundling and dissolution of single-walled carbon nanotubes in amide solvents. J Am Chem Soc 2004;126(19):6095-6105.

Gaharwar AK, Sant S, Hancock MJ, Hacking SA. Nanomaterials in Tissue Engineering Fabrication and Applications. Woodhead Publishing. 2013 Jul 64-88

Gertz CC, Leach MK, Birrell LK, Martin DC, Feldman EL, Corey JM. Accelerated neuritogenesis and maturation of primary spinal motor neurons in response tonanofibers. Dev Neurobiol 2010; 70(8):589-603.

Gheith MK, Pappas TC, Liopo AV, Sinani V, Shim BS, Motamedi M, Wicksted JP, Kotov NA. Stimulation of neural cells by lateral layer-by-layer films of single-walled currents in conductive carbon nanotubes. Adv. Mater. 2006 Nov;18: 2975-78.

Gheith MK, Sinani VA, Wicksted JP, Matts RL and Kotov, NA. Single-walled carbon nanotube polyelectrolyte multilayers and freestanding films as a biocompatible platform for neuroprosthetic implants. Adv Mater 2005;17:2663-2667.

Gordon T, Udina E, Verge VM, de Chaves EI. Brief electrical stimulation accelerates axon regeneration in the peripheral nervous system and promotes sensory axon regeneration in the central nervous system. Motor Control. 2009 Oct;13(4):412-41.

Gouveia RM, Gomes CM, Sousa M, Alves PM, Costa J. Kinetic analysis of L1 homophilic interaction: role of the first four immunoglobulin domains and implications on binding mechanism. J Biol Chem. 2008 Oct 17;283(42):28038-47.

GrandPré T, Li S, Strittmatter SM. Nogo-66 receptor antagonist peptide promotes axonal regeneration. Nature. 2002 May 30;417(6888):547-51.

Guex N, Peitsch MC. SWISS-MODEL and the Swiss-PdbViewer: an environment for comparative protein modeling. Electrophoresis. 1997;18(15):2714-2723.

Haspel J, Friedlander DR, Ivgy-May N, Chickramane S, Roonprapunt C, Chen S, Schachner M, Grumet M. Critical and optimal Ig domains for promotion of neurite outgrowth by L1/Ng-CAM. J Neurobiol. 2000 Feb 15;42(3):287-302.

Haspel J, Grumet M. The L1CAM extracellular region: a multi-domain protein with modular and cooperative binding modes. Front Biosci. 2003 Sep 1;8:s1210-25.

Hirsch A. Functionalization of single-walled carbon nanotubes. Angewandte Chemie International Edition. 2002,41,1853-59.

Hsu YC, Chen SL, Wang DY, Chiu IM. Stem cell-based therapy in neural repair. Biomed J. 2013 May-Jun;36(3):98-105.

Hu H, Ni Y, Montana V, Haddon RC, Parpura V. Chemically Functionalized Carbon Nanotubes as Substrates for Neuronal Growth. Nano Lett 2004;4(3):507-511.

Hu H, Ni Y, Montana V, Haddon RC, Parpura V. Chemically Functionalized Carbon Nanotubes as Substrates for Neuronal Growth. Nano Lett 2004;4(3):507-511.

Huang YA, Kao JW, Tseng DT, Chen WS, Chiang MH, Hwang E. Microtubule-associated type II protein kinase A is important for neurite elongation. PLoS One. 2013 Aug 13;8(8):e73890.

Huang YJ, Wu HC, Tai NH, Wang TW. Carbon nanotube rope with electrical stimulation promotes the differentiation and maturity of neural stem cells. Small. 2012 Sep 24;8(18):2869-77.

Hurtado A, Cregg JM, Wang HB, Wendell DF, Oudega M, Gilbert RJ, McDonald JW. Robust CNS regeneration after complete spinal cord transection using aligned poly-L-lactic acid microfibers. Biomaterials. 2011 Sep;32(26):6068-79.

Inoue H, Lin L, Lee X, Shao Z, Mendes S, Snodgrass-Belt P, Sweigard H, Engber T, Pepinsky B, Yang L, Beal MF, Mi S, Isacson O. Inhibition of the leucine-rich repeat protein LINGO-1 enhances survival, structure, and function of dopaminergic neurons in Parkinson's disease models. Proc Natl Acad Sci U S A. 2007 Sep 4;104(36):14430-5.

Jan E, Kotov NA. Successful differentiation of mouse neural stem cells on layer-by-layer assembled single-walled carbon nanotube composite. Nano Lett. 2007 May;7(5):1123-8.

Jepson S, Vought B, Gross CH, Gan L, Austen D, Frantz JD, Zwahlen J, Lowe D, Markland W, Krauss R. LINGO-1, a transmembrane signaling protein, inhibits oligodendrocyte differentiation and myelination through intercellular self-interactions. J Biol Chem. 2012 Jun 22;287(26):22184-95.

Ji B, Li M, Wu WT, Yick LW, Lee X, Shao Z, Wang J, So KF, McCoy JM, Pepinsky RB, Mi S, Relton JK. LINGO-1 antagonist promotes functional recovery and axonal sprouting after spinal cord injury. Mol Cell Neurosci. 2006 Nov;33(3):311-20.

Jin GZ, Kim M, Shin US, Kim HW. Neurite outgrowth of dorsal root ganglia neurons is enhanced on aligned nanofibrous biopolymer scaffold with carbon nanotube coating. Neurosci Lett. 2011 Aug 21;501(1):10-4.

Joshi S, Guleria R, Pan J, DiPette D, Singh US. Retinoic acid receptors and tissue-transglutaminase mediate short-term effect of retinoic acid on migration and invasion of neuroblastoma SH-SY5Y cells. Oncogene. 2006 Jan 12;25(2):240-7.

Jouet M, Rosenthal A, Armstrong G, MacFarlane J, Stevenson R, Paterson J,Metzenberg A, Ionasescu V, Temple K, Kenwrick S. X-linked spastic paraplegia (SPG1), MASA syndrome and X-linked hydrocephalus result from mutations in the L1 gene. Nat Genet. 1994 Jul;7(3):402-7.

Kalus I, Schnegelsberg B, Seidah NG, Kleene R, Schachner M. The proprotein convertase PC5A and a metalloprotease are involved in the proteolytic processing of the neural adhesion molecule L1. J Biol Chem. 2003 Mar 21;278(12):10381-8.

Kamiguchi H, Lemmon V. Neural cell adhesion molecule L1: signaling pathwaysand growth cone motility. J Neurosci Res. 1997 Jul 1;49(1):1-8.

Kamiguchi H, Lemmon V. Recycling of the cell adhesion molecule L1 in axonal growth cones. J. Neurosci. 2000;20:3676–3686.

Keefer EW, Botterman BR, Romero MI, Rossi AF, Gross GW. Carbon nanotube coating improves neuronal recordings. Nat Nanotechnol. 2008 Jul;3(7):434-9.

Kelley LA, Sternberg MJ. Protein structure prediction on the Web: a case study using the Phyre server. Nat Protoc 2009;4(3):363-371.

Kenwrick S, Watkins A, De Angelis E. Neural cell recognition molecule L1: relating biological complexity to human disease mutations. Hum Mol Genet. 2000 Apr 12;9(6):879-86

Khang D, Kim SY, Liu-Snyder P, Palmore GT, Durbin SM, Webster TJ. Enhanced fibronectin adsorption on carbon nanotube/poly(carbonate) urethane: independent role

of surface nano-roughness and associated surface energy. Biomaterials. 2007 Nov;28(32):4756-68.

Kharaziha M, Shin SR, Nikkhah M, Topkaya SN, Masoumi N, Annabi N, Dokmeci MR, Khademhosseini A. Tough and flexible CNT-polymeric hybrid scaffolds for engineering cardiac constructs. Biomaterials. 2014 Aug;35(26):7346-54.

Kim JA, Jang EY, Kang TJ, Yoon S, Ovalle-Robles R, Rhee WJ, Kim T, Baughman RH, Kim YH, Park TH. Regulation of morphogenesis and neural differentiation of human mesenchymal stem cells using carbon nanotube sheets. Integr Biol (Camb). 2012 Jun;4(6):587-94.

Koh HS, Yong T, Chan CK, Ramakrishna S. Enhancement of neurite outgrowth using nano-structured scaffolds coupled with laminin. Biomaterials 2008;29(26):3574-3582.

Kolosnjaj-Tabi J, Hartman KB, Boudjemaa S, Ananta JS, Morgant G, Szwarc H, Wilson LJ, Moussa F. In vivo behavior of large doses of ultrashort and full-length single-walled carbon nanotubes after oral and intraperitoneal administration to Swiss mice. ACS Nano. 2010 Mar 23;4(3):1481-92.

Kotov AN, Winter JO, Clements IP, Jan E, Timko EP, Campidelli EP, Pathak S, Mazzatenta A, Lieber CM, Prato M, Bellamkonda RV,Silva GA, Shi Kam NW, Patolsky F, Ballerini L. Nanomaterials for Neural Interfaces. Adv. Mater. 2009, 21, 3970–04.

Lacerda L, Herrero MA, Venner K, Bianco A, Prato M, Kostarelos K. Carbon-nanotube shape and individualization critical for renal excretion. Small. 2008 Aug;4(8):1130-2.

Landers J, Turner JT, Heden G, Carlson AL, Bennett NK, Moghe PV, Neimark AV. Carbon nanotube composites as multifunctional substrates for in situ actuation of differentiation of human neural stem cells. Adv Health Mater. 2014Nov;3(11):1745-52.

Lee JH, Lee JY, Yang SH, Lee EJ, Kim HW. Carbon nanotube-collagen three-dimensional culture of mesenchymal stem cells promotes expression of neural phenotypes and secretion of neurotrophic factors. Acta Biomater. 2014 Oct;10(10):4425-36.

Lee JY, Bashur CA, Goldstein AS, Schmidt CE. Polypyrrole-coated electrospun PLGA nanofibers for neural tissue applications. Biomaterials. 2009 Sep;30(26):4325-35.

Li J, McNally H, Shi R. Enhanced neurite alignment on micro-patterned poly-L-lactic acid films. J Biomed Mater Res A. 2008 Nov;87(2):392-404.

Liopo AV, Stewart MP, Hudson J, Tour JM, Pappas TC. Biocompatibility of native and functionalized single-walled carbon nanotubes for neuronal interface. J Nanosci Nanotechnol. 2006 May;6(5):1365-74.

Liu JJ, Wang CY, Wang JG, Ruan HJ, Fan CY. Peripheral nerve regeneration using composite poly(lactic acid-caprolactone)/nerve growth factor conduits prepared by coaxial electrospinning. J Biomed Mater Res A. 2011 Jan;96(1):13-20.

Lizundia E, Sarasua JR, D'Angelo F, Orlacchio A, Martino S, Kenny JM, Armentano I. Biocompatible poly(L-lactide)/MWCNT nanocomposites: morphological characterization, electrical properties, and stem cell interaction. Macromol Biosci. 2012 Jul;12(7):870-81.

Llorens F, Gil V, Iraola S, Carim-Todd L, Martí E, Estivill X, Soriano E, del Rio JA, Sumoy L. Developmental analysis of Lingo-1/Lern1 protein expression in the mouse brain: interaction of its intracellular domain with Myt1l. Dev Neurobiol. 2008 Mar;68(4):521-41.

Loers G, Chen S, Grumet M, Schachner M. Signal transduction pathways implicated in neural recognition molecule L1 triggered neuroprotection and neuritogenesis. J Neurochem. 2005 Mar;92(6):1463-76.

Lopes FM, Schröder R, da Frota ML Jr, Zanotto-Filho A, Müller CB, Pires AS, Meurer RT, Colpo GD, Gelain DP, Kapczinski F, Moreira JC, Fernandes Mda C, Klamt F. Comparison between proliferative and neuron-like SH-SY5Y cells as an in vitro model for Parkinson disease studies. Brain Res. 2010 Jun 14;1337:85-94.

Lovat V, Pantarotto D, Lagostena L, Cacciari B, Grandolfo M, Righi M, Spalluto G, Prato M, Ballerini L. Carbon nanotube substrates boost neuronal electrical signaling. Nano Lett. 2005 Jun;5(6):1107-10.

Lowery LA, Van Vactor D. The trip of the tip: understanding the growth cone machinery. Nat Rev Mol Cell Biol. 2009 May;10(5):332-43.

Malarkey EB, Fisher KA, Bekyarova E, Liu W, Haddon RC, Parpura V. Conductive single-walled carbon nanotube substrates modulate neuronal growth. Nano Lett. 2009 Jan;9(1):264-8.

Maretzky T, Schulte M, Ludwig A, Rose-John S, Blobel C, Hartmann D, Altevogt P, Saftig P, Reiss K. L1 is sequentially processed by two differently activated metalloproteases and presenilin/gamma-secretase and regulates neural cell adhesion, cell migration, and neurite outgrowth. Mol Cell Biol. 2005 Oct;25(20):9040-53

Martinez-Arca S, Coco S, Mainguy G, Schenk U, Alberts P, Bouillé P, Mezzina M, Prochiantz A, Matteoli M, Louvard D, Galli T. A common exocytotic mechanism mediates axonal and dendritic outgrowth. J Neurosci. 2001 Jun 1;21(11):3830-8.

Matsumoto K, Sato C, Naka Y, Kitazawa A, Whitby RL, Shimizu N. Neurite outgrowths of neurons with neurotrophin-coated carbon nanotubes. J Biosci Bioeng 2007;103(3):216-220.

Mattson MP, Haddon RC, Rao AM. Molecular functionalization of carbon nanotubesand use as substrates for neuronal growth. J Mol Neurosci 2000;14(3):175-182.

Mazzatenta A, Giugliano M, Campidelli S, Gambazzi L, Businaro L, Markram H, Prato M, Ballerini L. Interfacing neurons with carbon nanotubes: electrical signal transfer and synaptic stimulation in cultured brain circuits. J Neurosci. 2007 Jun 27;27(26):6931-6.

McDonald JW, Liu XZ, Qu Y, Liu S, Mickey SK, Turetsky D, Gottlieb DI, Choi DW. Transplanted embryonic stem cells survive, differentiate and promote recovery in injured rat spinal cord. Nat Med. 1999 Dec;5(12):1410-2.

Mi S, Lee X, Shao Z, Thill G, Ji B, Relton J, Levesque M, Allaire N, Perrin S, Sands B, Crowell T, Cate RL, McCoy JM, Pepinsky RB. LINGO-1 is a component of the Nogo-66 receptor/p75 signaling complex. Nat Neurosci. 2004 Mar;7(3):221-8.

Mi S, Pepinsky RB, Cadavid D. Blocking LINGO-1 as a therapy to promote CNS repair: from concept to the clinic. CNS Drugs 2013;27(7):493-503.

Mikulak J, Negrini S, Klajn A, D'Alessandro R, Mavilio D, Meldolesi J. Dual REST-dependence of L1CAM: from gene expression to alternative splicing governed by Nova2 in neural cells. J Neurochem 2012;120(5):699-709.

Mosyak L, Wood A, Dwyer B, Buddha M, Johnson M, Aulabaugh A, Zhong X, Presman E, Benard S, Kelleher K, Wilhelm J, Stahl ML, Kriz R, Gao Y, Cao Z, Ling HP, Pangalos MN,

Walsh FS, Somers WS. The structure of the Lingo-1 ectodomain, a module implicated in central nervous system repair inhibition. J Biol Chem. 2006 Nov 24;281(47):36378-90.

Munnamalai V, Weaver CJ, Weisheit CE, Venkatraman P, Agim ZS, Quinn MT, Suter DM. Bidirectional interactions between NOX2-type NADPH oxidase and the F-actin cytoskeleton in neuronal growth cones. J Neurochem 2014;130(4):526-540.

Nikkhah M, Edalat F, Manoucheri S, Khademhosseini A. Engineering microscale topographies to control the cell-substrate interface. Biomaterials. 2012 Jul;33(21):5230-46.

Oudega M, Gautier SE, Chapon P, Fragoso M, Bates ML, Parel JM, Bunge MB. Axonal regeneration into Schwann cell grafts within resorbable poly(alpha-hydroxyacid) guidance channels in the adult rat spinal cord. Biomaterials. 2001 May;22(10):1125-36.

Park SY, Choi DS, Jin HJ, Park J, Byun KE, Lee KB, Hong S. Polarization-controlled differentiation of human neural stem cells using synergistic cues from the patterns of carbon nanotube monolayer coating. ACS Nano. 2011 Jun 28;5(6):4704-11.

Pêgo AP, Kubinova S, Cizkova D, Vanicky I, Mar FM, Sousa MM, Sykova E. Regenerative medicine for the treatment of spinal cord injury: more than just promises? J Cell Mol Med. 2012 Nov;16(11):2564-82.

Petrinovic MM, Duncan CS, Bourikas D, Weinman O, Montani L, Schroeter A, Maerki D, Sommer L, Stoeckli ET, Schwab ME. Neuronal Nogo-A regulates neurite fasciculation, branching and extension in the developing nervous system. Development. 2010 Aug 1;137(15):2539-50.

Pettersen EF, Goddard TD, Huang CC, Couch GS, Greenblatt DM, Meng EC, Ferrin TE. UCSF Chimera--a visualization system for exploratory research and analysis. J Comput Chem. 2004 Oct;25(13):1605-12.

Pettikiriarachchi JTS, Parish CL, Shoichet MS, Forsythe JS, Nisbet DR. Biomaterials for Brain Tissue Engineering. Aust. J. Chem. 201063:1143-1154

Porter AE, Gass M, Muller K, Skepper JN, Midgley PA, Welland M. Direct imaging of single-walled carbon nanotubes in cells. Nat Nanotechnol. 2007 Nov;2(11):713-7.

Pulskamp K, Diabaté S, Krug HF. Carbon nanotubes show no sign of acute toxicity but induce intracellular reactive oxygen species in dependence on contaminants. Toxicol Lett. 2007 Jan 10;168(1):58-74.

Puttagunta R, Schmandke A, Floriddia E, Gaub P, Fomin N, Ghyselinck NB, Di Giovanni S. RA-RAR-β counteracts myelin-dependent inhibition of neurite outgrowth via Lingo-1 repression. J Cell Biol. 2011 Jun 27;193(7):1147-56.

Reid AJ, Shawcross SG, Hamilton AE, Wiberg M, Terenghi G. N-acetylcysteine alters apoptotic gene expression in axotomised primary sensory afferent subpopulations. Neurosci Res. 2009 Oct;65(2):148-55.

Rietze RL, Reynolds BA. Neural stem cell isolation and characterization. Methods Enzymol. 2006;419:3-23.

Rodríguez Hernández JC, Salmerón Sánchez M, Soria JM, Gómez Ribelles JL,Monleón Pradas M. Substrate chemistry-dependent conformations of single lamininmolecules on polymer surfaces are revealed by the phase signal of atomic forcemicroscopy. Biophys J. 2007 Jul 1;93(1):202-7.

Ross RA, Spengler BA, Biedler JL. Coordinate morphological and biochemical interconversion of human neuroblastoma cells. J Natl Cancer Inst. 1983;71:741-747.

Saifuddin N, Raziah AZ, Junizah AR. Carbon nanotubes: a review on structure and their interaction with proteins. J Chem. 2013;2013:ID 676815.

Salice P, Fabris E, Sartorio C, Fenaroli D, Figà V, Casaletto, Cataldo S, Pignataro P, Menna E. An Insight into the Functionalisation of Carbon Nanotubes by Diazonium Chemistry: Towards a Controlled Decoration. Carbon. 2014;74,73-82.

Salice P, Fenaroli D, De Filippo CC, Menna E, Gasparini G, Maggini M. Efficient functionalization of carbon nanotubes: an opportunity enabled by flow chemistry. Chimica Oggi / Chemistry Today. 2012;30(6):37-39.

Scapin G, Salice P, Tescari S, Menna E, De Filippis V, Filippini F. Enhanced Neuronal cell differentiation combining biomimetic peptides and a carbon nanotube-polymer scaffold. Nanomedicine. 2014 Dec 26. pii: S1549-9634(14)00563-2. doi: 10.1016/j.nano.2014.11.001.

Scheib J, Höke A. Advances in peripheral nerve regeneration. Nat Rev Neurol. 2013 Dec;9(12):668-76.

Schmidt CE, Leach JB. Neural tissue engineering: strategies for repair andregeneration. Annu Rev Biomed Eng. 2003;5:293-347.

Schmidt CE, Shastri VR, Vacanti JP, Langer R. Stimulation of neurite outgrowth using an electrically conducting polymer. Proc Natl Acad Sci U S A. 1997 Aug 19;94(17):8948-53.

Shekaran A, Garcia AJ. Nanoscale engineering of extracellular matrix-mimetic bioadhesive surfaces and implants for tissue engineering. Biochim Biophys Acta. 2011 Mar;1810(3):350-60.

Silva GA, Czeisler C, Niece KL, Beniash E, Harrington DA, Kessler JA, Stupp SI. Selective differentiation of neural progenitor cells by high-epitope density nanofibers. Science. 2004 Feb 27;303(5662):1352-5.

Silva GA. Neuroscience nanotechnology: progress, opportunities and challenges. Nat Rev Neurosci. 2006 Jan;7(1):65-74.

Silva GA. Nanotechnology approaches for drug and small molecule delivery across the blood brain barrier. Surg Neurol. 2007 Feb;67(2):113-6.

Singh A, Rokes C, Gireud M, Fletcher S, Baumgartner J, Fuller G, Stewart J, Zage P, Gopalakrishnan V. Retinoic acid induces REST degradation and neuronal differentiation by modulating the expression of SCF(β-TRCP) in neuroblastoma cells. Cancer. 2011 Nov 15;117(22):5189-202.

Sorkin R, Greenbaum A, David-Pur M, Anava S, Ayali A, Ben-Jacob E, Hanein Y. Process entanglement as a neuronal anchorage mechanism to rough surfaces. Nanotechnology. 2009 Jan 7;20(1):015101.

Soroka V, Kiryushko D, Novitskaya V, Ronn LC, Poulsen FM, Holm A, Bock E, Berezin V. Induction of neuronal differentiation by a peptide corresponding to the homophilic binding site of the second Ig module of the neural cell adhesion molecule. J Biol Chem. 2002 Jul 5;277(27):24676-83.

Sridharan I, Kim T, Wang R. Adapting collagen/CNT matrix in directing hESC differentiation. Biochem Biophys Res Commun. 2009 Apr 17;381(4):508-12.

Staii C, Viesselmann C, Ballweg J, Williams JC, Dent EW, Coppersmith SN, Eriksson MA. Distance dependence of neuronal growth on nanopatterned gold surfaces. Langmuir. 2011 Jan 4;27(1):233-9.

Stein T, Walmsley AR. The leucine-rich repeats of LINGO-1 are not required for self-interaction or interaction with the amyloid precursor protein. Neurosci Lett. 2012;509(1):9-12.

Stout DA, Webster TJ. Carbon nanotubes for stem cell control. MaterialsToday. 2012 Jul;15(7-8):312-18.

Sucapane A, Cellot G, Prato M, Giugliano M, Parpura V, Ballerini L. Interactions Between Cultured Neurons and Carbon Nanotubes: A Nanoneuroscience Vignette. J Nanoneurosci. 2009 Jun 1;1(1):10-16.

Tay CY, Gu H, Leong WS, Yu H, Li HQ, Heng BC, Tantang H, Loo SCJ, Li LJ, Tan LP. Cellular behavior of human mesenchymal stem cells cultured on single-walled carbon nanotube film. Carbon. 2010 Apr;48(4):1095-04.

Tischfield MA, Baris HN, Wu C, Rudolph G, Van Maldergem L, He W, Chan WM, Andrews C, Demer JL, Robertson RL, Mackey DA, Ruddle JB, Bird TD, Gottlob I, Pieh C, Traboulsi EI, Pomeroy SL, Hunter DG, Soul JS, Newlin A, Sabol LJ, Doherty EJ, de Uzcátegui CE, de Uzcátegui N, Collins ML, Sener EC, Wabbels B, Hellebrand H, Meitinger T, de Berardinis T, Magli A, Schiavi C, Pastore-Trossello M, Koc F, Wong AM, Levin AV, Geraghty MT, Descartes M, Flaherty M, Jamieson RV, Møller HU, Meuthen I, Callen DF, Kerwin J, Lindsay S, Meindl A, Gupta ML Jr, Pellman D, Engle EC. Human TUBB3 mutations perturb microtubule dynamics, kinesin interactions, and axon guidance. Cell. 2010 Jan 8;140(1):74-87.

Tom VJ, Sandrow-Feinberg HR, Miller K, Santi L, Connors T, Lemay MA, Houlé JD. Combining peripheral nerve grafts and chondroitinase promotes functional axonalregeneration in the chronically injured spinal cord. J Neurosci. 2009 Nov 25;29(47):14881-90.

Vacca M, Albania L, Della Ragione F, Carpi A, Rossi V, Strazzullo M, De Franceschi N, Rossetto O, Filippini F, D'Esposito M. Alternative splicing of the human gene SYBL1 modulates protein domain architecture of Longin VAMP7/TI-VAMP, showing both non-SNARE and synaptobrevin-like isoforms. BMC Mol Biol. 2011;12:26.

Verreck G, Chun I, Li Y, Kataria R, Zhang Q, Rosenblatt J, Decorte A, Heymans K, Adriaensen J, Bruining M, Van Remoortere M, Borghys H, Meert T, Peeters J, Brewster ME. Preparation and physicochemical characterization of biodegradable nerve guides containing the nerve growth agent sabeluzole. Biomaterials. 2005 Apr;26(11):1307-15.

Von der Mark K, Park J, Bauer S, Schmuki P. Nanoscale engineering of biomimetic surfaces: cues from the extracellular matrix. Cell Tissue Res. 2010 Jan;339(1):131-53.

Wang F. Regenerative Medicine in Neurological Disorders: The Present Situation and Future Issues with Stem Cell Therapy. J Neurol Disord Stroke. 2013 Jul 1(1): 1005.

Wong BS, Yoong SL, Jagusiak A, Panczyk T, Ho HK, Ang WH, Pastorin G. Carbon nanotubes for delivery of small molecule drugs. Adv Drug Deliv Rev. 2013 Dec;65(15):1964-2015.

Wright KT, El Masri W, Osman A, Chowdhury J, Johnson WE. Concise review: Bone marrow for the treatment of spinal cord injury: mechanisms and clinical applications. Stem Cells. 2011 Feb;29(2):169-78.

Xie HR, Hu LS, Li GY. SH-SY5Y human neuroblastoma cell line: in vitro cell model of dopaminergic neurons in Parkinson's disease. Chin Med J (Engl). 2010 Apr 20;123(8):1086-92.

Xie J, Macewan MR, Willerth SM, Li X, Moran DW, Sakiyama-Elbert SE, Xia Y. Conductive Core-Sheath Nanofibers and Their Potential Application in Neural Tissue Engineering. Adv Funct Mater. 2009 Jul 24;19(14):2312-2318.

Xu H, Holzwarth JM, Yan Y, Xu P, Zheng H, Yin Y, Li S, Ma PX. Conductive PPY/PDLLA conduit for peripheral nerve regeneration. Biomaterials. 2014 Jan;35(1):225-35.

Yamada M, Tanemura K, Okada S, Iwanami A, Nakamura M, Mizuno H, Ozawa M, Ohyama-Goto R, Kitamura N, Kawano M, Tan-Takeuchi K, Ohtsuka C, Miyawaki A, Takashima A, Ogawa M, Toyama Y, Okano H, Kondo T. Electrical stimulation modulates fate determination of differentiating embryonic stem cells. Stem Cells. 2007 Mar;25(3):562-70.

Yang F, Murugan R, Ramakrishna S, Wang X, Ma YX, Wang S. Fabrication of nano-structured porous PLLA scaffold intended for nerve tissue engineering. Biomaterials. 2004;25(10):1891-1900.

Yang K, Jung K, Ko E, Kim J, Park KI, Kim J, Cho SW. Nanotopographical manipulation of focal adhesion formation for enhanced differentiation of human neural stem cells. ACS Appl Mater Interfaces. 2013 Nov 13;5(21):10529-40.

Yao L, McCaig CD, Zhao M. Electrical signals polarize neuronal organelles, direct neuron migration, and orient cell division. Hippocampus. 2009 Sep;19(9):855-68.

Yao L, Pandit A, Yao S, McCaig CD. Electric field-guided neuron migration: a novel approach in neurogenesis. Tissue Eng Part B Rev. 2011 Jun;17(3):143-53.

Yu W, Jiang X, Cai M, Zhao W, Ye D, Zhou Y, Zhu C, Zhang X, Lu X, Zhang Z. A novel electrospun nerve conduit enhanced by carbon nanotubes for peripheral nerve regeneration. Nanotechnology. 2014 Apr 25;25(16):165102.

Zahir T, Chen YF, MacDonald JF, Leipzig N, Tator CH, Shoichet MS. Neural stem/progenitor cells differentiate in vitro to neurons by the combined action of dibutyryl cAMP and interferon-gamma. Stem Cells Dev. 2009 Dec;18(10):1423-32.

Zhang X, Prasad S, Niyogi S, Morgan A, Ozkan M, Ozkan CS. Guided neurite growth on patterned carbon nanotubes. Sens Actuators B Chem. 2005;106:843-50.

Zhao X, Yip PM, Siu CH. Identification of a homophilic binding site in immunoglobulin-like domain 2 of the cell adhesion molecule L1. J Neurochem. 1998 Sep;71(3):960-71.

8. PUBLICATIONS

ARTICLE IN PRESS

NANO-01023; No of Pages 12

Nanomedicine: Nanotechnology, Biology, and Medicine
xx (2015) xxx–xxx

nanomedicine
Nanotechnology, Biology, and Medicine

nanomedjournal.com

Enhanced neuronal cell differentiation combining biomimetic peptides and a carbon nanotube-polymer scaffold☆

Giorgia Scapin[a], Patrizio Salice, PhD[b], Simone Tescari[c], Enzo Menna, PhD[b], Vincenzo De Filippis, PhD[c], Francesco Filippini, PhD[a,*]

[a]Department of Biology, University of Padua, Italy
[b]Department of Chemical Sciences, University of Padua, Italy
[c]Department of Pharmaceutical and Pharmacological Sciences, University of Padua, Italy

Received 1 July 2014; accepted 7 November 2014

Abstract

Carbon nanotubes are attractive candidates for the development of scaffolds able to support neuronal growth and differentiation thanks to their ability to conduct electrical stimuli, to interface with cells and to mimic the neural environment. We developed a biocompatible composite scaffold, consisting of multi-walled carbon nanotubes dispersed in a poly-L-lactic acid matrix able to support growth and differentiation of human neuronal cells. Moreover, to mimic guidance cues from the neural environment, we also designed synthetic peptides, derived from L1 and LINGO1 proteins. Such peptides could positively modulate neuronal differentiation, which is synergistically improved by the combination of the nanocomposite scaffold and the peptides, thus suggesting a prototype for the development of implants for long-term neuronal growth and differentiation.

Key words: Carbon nanotube scaffold; L1; LINGO1; Neuronal differentiation; Biomimetic peptides

Background

The development of scaffolds for neural regeneration could help in the repair of damaged central nervous system (CNS) tissue which has a limited regenerative potential as well as in peripheral nerve injuries when the nerve defect is too extended to be naturally regenerated.[1,2] Carbon nanotubes (CNTs) are attractive candidates for neurological applications thanks to their tunable electrical conductivity, excellent mechanical properties, morphological similarity to neurites and chemically modifiable surface.[3-6] CNTs are rolled layers of sp^2 carbon resembling in form and dimensions neural processes and proteins of the extracellular matrix (e.g. collagen); this ability to mimic neural environment topography is very important to boost neuronal cell adhesion, growth and differentiation.[5-12] CNTs are among the toughest and strongest nanomaterials; moreover, they are flexible and their tunable conductivity – stable in a biological environment[7] – can help to stimulate cultured neurons and to control cell migration, proliferation and differentiation.[13,14] CNT substrates can enhance neuronal network activity under culturing conditions, suggesting they might mediate charge redistribution along membrane surfaces, increasing neuronal excitability.[15,16] Furthermore, tunable CNT electro-conductive scaffolds promote the functional maturation of neurons[17] and can stimulate neurite outgrowth.[18] Nevertheless, CNTs suffer from biocompatibility issues depending on type and doses of CNTs employed and on cell population tested.[6,19] A convenient way to improve biocompatibility involves the functionalization of CNTs[20] by covalent or non-covalent chemistry to modify surface charge[6] or to attach biologically active molecules able to act as guidance cues to elongating neurites.[21] These characteristics make CNTs ideal candidates for designing new biomaterials, which can reestablish the connections between neurons after injury. In this

Funding from MIUR (grants PRIN-20085M27SS and FIRB-RBFR08-DUX6 to EM), from CaRiPaRo Foundation (Excellence Research Project 2011 to VDF) are gratefully acknowledged.

Statement: The authors declare that they have no competing interests.

*Corresponding author at: Dipartimento di Biologia, University of Padua, Padova (PD), Italy.

E-mail addresses: giorgia.scapin@bio.unipd.it (G. Scapin), patrizio.salice@unipd.it (P. Salice), simone.tescari@studenti.unipd.it (S. Tescari), enzo.menna@unipd.it (E. Menna), vincenzo.defilippis@unipd.it (V. De Filippis), francesco.filippini@unipd.it (F. Filippini).

http://dx.doi.org/10.1016/j.nano.2014.11.001
1549-9634/

Please cite this article as: Scapin G., et al., Enhanced neuronal cell differentiation combining biomimetic peptides and a carbon nanotube-polymer scaffold. *Nanomedicine: NBM* 2015;xx:1-12, http://dx.doi.org/10.1016/j.nano.2014.11.001

context, CNTs can find applicability as implants where long-term extracellular molecular cues for neurite outgrowth are necessary.[8]

Concerning the extracellular environment, biologically active molecules can be potentially used in regenerative medicine to act as guidance cues for neurite elongation and thus to activate intracellular pathways leading to cell differentiation. To this aim, peptides corresponding to motifs likely to mediate regulatory signals present significant advantages compared to using entire recombinant proteins: (i) low immunogenic activity, (ii) increased stability, (iii) low production costs and (iv) simplified preparation and immobilization onto substrates.[22]

L1 cell adhesion molecule (CAM) is important for a correct development of the nervous system in humans because it controls neurite outgrowth, adhesion, fasciculation, migration, myelination and axon guidance. L1 is a transmembrane protein with an ectodomain consisting of six immunoglobulin-like (Ig) domains and five fibronectin type-III (Fn) repeats.[23] L1 is exposed at the surface of both neurons and glial cells and binds to a diverse set of molecules sending intracellular signals through its cytoplasmic region.[24] In particular, neurite outgrowth is triggered by homophilic binding *in trans* occurring between two L1 molecules during axonal development. Even though it has been demonstrated that Ig1-Ig4 region is the minimal segment necessary to mediate homophilic binding,[25] Ig2 in particular possesses a homophilic interaction motif.[26] Leucine rich repeat (LRR) and Ig-like domain containing Nogo receptor interacting protein (LINGO1) is a transmembrane protein selectively expressed in CNS and playing an important role in neurite outgrowth. LINGO1 ectodomain is formed by twelve LRR motifs and one Ig-like domain.[27] LINGO1 forms at the neuron surface a complex with Nogo66-Receptor NgR1 and the neurotrophin receptor p75. NgR1/LINGO1/p75 complex interacts with Mag/NogoA/OMgp complex on oligodendrocyte surface and inhibits neurite elongation.[27] NgR1/LINGO1/p75 complex also interacts with neuronal NogoA, thus blocking neurite elongation and generating repulsion between neurites.[28] Furthermore, LINGO1 can homophilically interact *in trans*, suggesting that LINGO1 molecules from adjacent neuronal and oligodendrocytic membranes could interact inhibiting oligodendrocyte final differentiation.[29] Recent discoveries showed that the LINGO1 Ig domain alone mediates homophilic binding and heterotypic interactions.[30] LINGO1 expression is developmentally regulated, and it is upregulated after injury[27] and in a number of CNS diseases.[31-33] *In vitro* and *in vivo* studies demonstrated that when inhibiting LINGO1 function, its inhibitory effect is reversed and neurite elongation is promoted.[27,31,33,34] LINGO1 seems to be one of the molecules responsible for CNS neurons' inability to regenerate and thus it represents an ideal candidate for therapeutic targets in neural dysfunctions because of its restricted tissue distribution.

Here we present the design and preparation of a nanocomposite scaffold made of multi-walled CNTs (MWCNTs) in a poly-L-lactic acid (PLLA) matrix (CNT-PLLA scaffold) able to support neuronal cell growth and differentiation. In parallel, we developed biomimetic peptides, derived from L1 and LINGO1 proteins, to further modulate neuronal differentiation. Finally, we combined the CNT-PLLA scaffold and peptides to investigate a possible synergistic effect for developing scaffolds for neuronal regeneration.

Methods

(Please note: full methods are reported in the Supplementary file.)

CNT-PLLA scaffold preparation and characterization

Commercially available MWCNTs were purified by two-step treatment at high temperature, dispersion in aqueous HCl (37%), sonication and membrane filtration. Thermogravimetric analyses (TGA) indicated 0.18% as final metal impurities. MWCNTs were PhOMe-functionalized and dissolved with PLLA in chloroform under mild sonication. The resulting dispersion was drop-cast onto a glass dish to obtain the MWCNT-PhOMe@PLLA 1% scaffold. MWCNTs were characterized by micro-Raman spectroscopy, TGA and differential scanning calorimetry (DSC) analyses. Electrical resistance of the CNT-PLLA composite was measured by using a digital multimeter.

Peptide synthesis and characterization

LINGO1-A (^{467}SAKSNGRLTVFPDG^{480}), scrambled LINGO1-A_scr (TVFSRSKPLGNDGA), L1-A (^{178}HIKQDERVTMGQNG^{191}), scrambled L1-A_scr (IVDQGNREMGTKHQ) peptides, and N-terminally fluoresceinated derivatives of L1-A and LINGO1-A were synthesized by the solid-phase method, purified to homogeneity (>98%) by RP-HPLC and characterized by high-resolution mass spectrometry. The conformation of the peptides was analyzed by circular dichroism (CD) on a Jasco J-810 spectropolarimeter, equipped with a Peltier temperature control system.

SH-SY5Y culture and differentiation

24 h after cell seeding (day 0), human SH-SY5Y cells were differentiated by replacing the growth medium with differentiation medium containing all-*trans*-retinoic acid (RA) and lowered FBS. In experiments with peptides added to culture medium, cells were seeded in plates coated with a gelatine/poly-L-lysine solution; 24 h after RA induction (day 1) peptides were added (except for control samples) to the medium. In experiments with peptides adsorbed onto the substrate, peptides dissolved in gelatine solution were adsorbed onto the plate bottom prior to cell seeding. In experiments with cells growing onto CNT-PLLA scaffolds and treated with peptides, 24 h after RA induction (day 1) the peptides were added to culture medium. Control wells were coated with poly-L-lysine.

Analysis of cell viability/proliferation and neuronal differentiation

Resazurin reduction assay was performed to quantify metabolically active living cells and thus to monitor effects on cell proliferation and adhesion to the scaffolds. Cytotoxicity was determined (by a commercial assay) as release of lactate dehydrogenase from cells having lost membrane integrity. Staining with calcein acetoxymethyl ester (Calcein-AM) and fluorescence microscopy (GFP filter) were used to visualize full-length neural processes and cells growing onto the black CNT-PLLA scaffolds. Neurite length was measured using LAS AF lite software (Leica).

Cells were fixed using standard protocols (paraformaldehyde) and coated with gold particles prior to scanning electron microscopy (SEM) analysis.

Bioinformatic and statistic analyses

Structural models obtained by fold recognition/homology modeling were then compared by superposition. Statistical analyses were performed using paired Student's *t* test, and results were considered significant when $P < 0.05$. Values are expressed as mean ± standard error of the mean (M ± SEM).

Results

Set-up and validation of a polymer-CNT scaffold

Dispersion of CNTs into a biocompatible polymer matrix can help to generate a freestanding and implantable device.[35] Combination of a biocompatible polymer and a conductive nanostructure is expected to boost neuronal growth/differentiation by coupling polymer features (biocompatibility, processability, low cost, implantability) and CNT properties (mimicking of the topography of neural environment and conductivity). We chose PLLA as polymer matrix because of its biocompatibility and employment for neural tissue engineering applications.[36-38] Among the plethora of available CNTs, we chose MWCNTs because of high conductivity and shape mimicking nanoscale features of the extracellular matrix. We purified commercial MWCNTs to remove heavy metal impurities, which may result cytotoxic.[39] Moreover, to improve dispersibility, we functionalized the MWCNTs through addition of the diazonium salt of 4-methoxyaniline.[40,41] We determined, according to a previously reported approach,[42] a degree of functionalization (see Supplementary file) of 1/97. Characterization of MWCNTs by TGA analysis and micro-Raman spectroscopy is shown in Supplementary Figure S1A-B. The resulting CNT derivatives, soluble in chloroform, were used to prepare a polymer nanocomposite made of 1% w/w MWCNTs dispersed into a PLLA matrix by solvent evaporation (see Supplementary file for methods and Figure S1C). Raman spectroscopy, TGA and DSC confirmed CNTs to be well dispersed in the scaffold (Figure S1D-F). The electrical resistivity of the nanocomposite scaffold is around 130 kΩ with respect to >2000 kΩ of the pristine PLLA; in addition, it shows features compatible with a free-standing polymer film as required for implantable scaffolds. Indeed, we compared CNT-PLLA and PLLA scaffolds for both biocompatibility and neuritogenic properties. Calcein-AM staining revealed that cells can adhere and grow onto both CNT-PLLA and PLLA scaffolds and show homogeneous spreading (Figure 1, *A*). No difference in cell proliferation (Figure 1, *B*) and viability (Table 1) was observed when growing cells onto either poly-L-lysine or the scaffolds; however, as shown in Figure 1, *C*, cells better adhere to CNT-PLLA (~63%) than to PLLA alone (~39%). Furthermore, cells grown onto CNT-PLLA can be differentiated with RA as well as control samples and they present a total neurite length higher than samples grown onto PLLA (Figure 1, *D*). SEM images of cells cultured onto CNT-PLLA show a healthy morphology and the outgrowth of neurites attaching to the scaffold surface (Figure 2). At higher magnifications, the intimate contacts between the scaffold and neuronal membrane are evident (Figure 2, *D*). Furthermore, cells grown onto CNT-PLLA show a higher number of long filopodia extending from the growth cone and making contacts with the scaffold compared to cells grown onto poly-L-lysine substrate, suggesting an improved activity of growth cones in sensing topographical cues (Figure 2, *G*).

Identification of peptides derived from L1 and LINGO1

Cellular differentiation can be induced by peptides corresponding to interaction motifs likely to mediate differentiation signals. In order to provide signals driving correct neuronal growth and differentiation, we started from the evidence that neuritogenesis and process guidance/elongation are driven by CAM proteins such as L1.[43] In this work we tested biocompatibility and neuritogenicity of two peptides derived from L1 and LINGO1. The Ig2 repeat of the L1 ectodomain is involved in the homophilic binding and the interaction region corresponds to a 14-amino acid long peptide named L1-A.[26] Therefore, we reproduced L1-A as a synthetic peptide for our experiments. Then, we searched for structural homologues of the L1 Ig2 repeat, to find further regulators of neural differentiation by homo/heterophilic interactions. Fold recognition search intriguingly identified the Ig repeat of the LINGO1 ectodomain as the best template (99.7% confidence, 93% coverage). Given that identity between L1 Ig2 and LINGO1 Ig is 29%, we obtained a better refined model by homology modeling. Then, superposition (Figure 3, *A*) of the LINGO1 Ig template (Figure 3, *B*) and the L1 Ig2 model (Figure 3, *C*) revealed high structural similarity (RMSD = 0.65 Å). Intriguingly, the L1-A peptide segment, corresponding LINGO1 Ig sequence 467-480 (hereafter referred to as LINGO1-A), displayed high sequence similarity. In particular, four amino acids were identical in the two stretches and eight residues shared similar physico-chemical properties (Figure 3, *D*). It has to be stressed that: (i) both LINGO1 and L1 are neural proteins involved in neurite outgrowth control, (ii) LINGO1 Ig structure is quite similar to the L1 Ig2 domain, and (iii) the alignment between L1-A and LINGO1-A shows high conservation, including amino acid positions relevant to L1 function.[26] Therefore, we produced LINGO1-A as synthetic peptide for our experiments. In order to distinguish among specific and unspecific effects, we also synthesized the scrambled versions of the two peptides (L1-A_scr and LINGO1-A_scr). All peptides were produced by solid-phase synthesis and their chemical identities established by high-resolution mass spectrometry (Figure 3, *E* and *F*). As expected from both LINGO1-A and L1-A localization in flexible loop regions (see structural models in Figuer 3, *B* and *C*), the conformation of the synthetic peptides in solution is essentially disordered as documented by the far-UV CD spectra resembling those typical of an unfolded polypeptide chain[44] (Figure 3, *G* and *H*). Given that (i) L1-A was only investigated about its involvement in L1-L1 homophilic interactions (i.e. its role in cellular signaling was not determined[26]) and (ii) LINGO1 Ig domain alone both mediates homophilic bindings and heterotypic interactions,[30] but its interaction region has not been identified yet, we decided to test the two peptides using the SH-SY5Y cell system to asses if (i) L1-A can trigger neurite elongation and (ii) LINGO1-A can regulate neural differentiation as well.

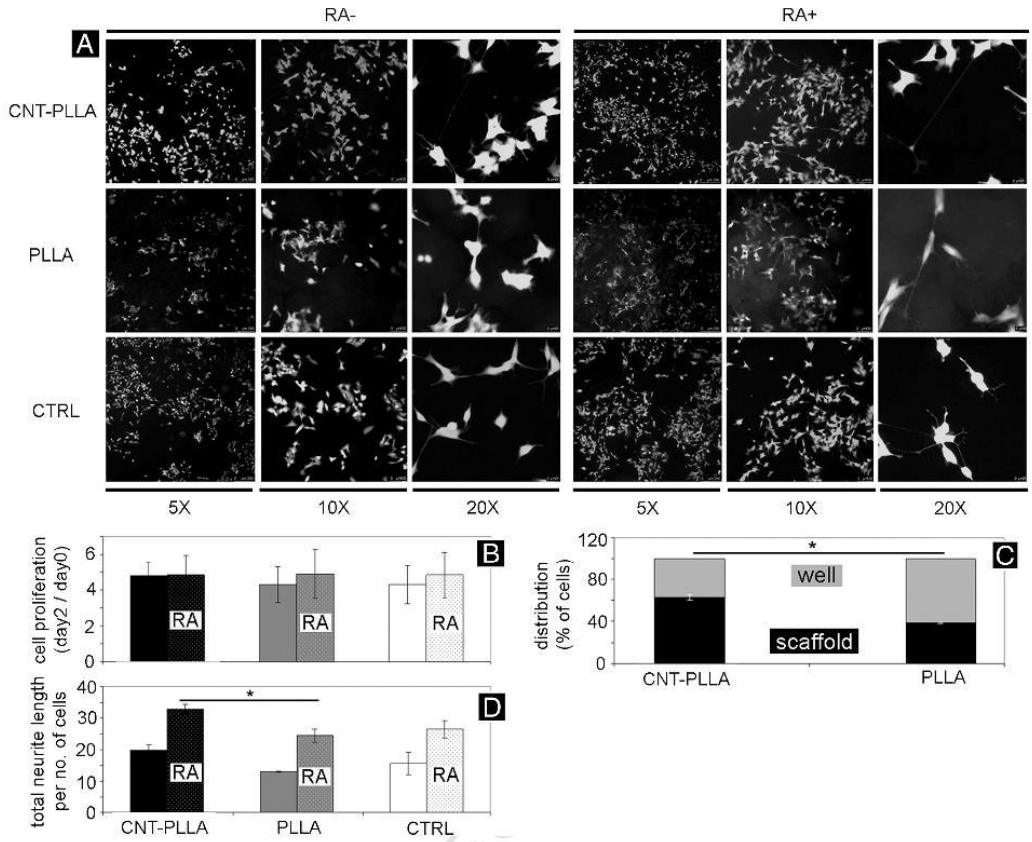

Figure 1. CNT-PLLA scaffold effect on SH-SY5Y cell adhesion, growth and differentiation. **(A)** SH-SY5Y cells stained with Calcein-AM. Image magnification is reported. Cell proliferation **(B)**, distribution **(C)** and differentiation **(D)**. Data represent the mean ± SEM of three independent experiments performed in duplicate. * shows significance at $P < 0.05$ between cells seeded onto CNT-PLLA and PLLA.

t1.1 Table 1
t1.2 Percentage of cell death relative to three independent experiments performed in duplicate.

t1.3 % cell death	DAY0	DAY2	DAY2 RA
t1.4 CNT-PLLA	14.71%	4.81%	3.82%
t1.5 PLLA	14.23%	8.50%*	7.04%
t1.6 CTRL	13.40%	2.84%	3.31%

Q1 t1.7 * Significance at $P < 0.05$ between samples grown onto scaffolds and control cells (grown onto poly-L-lysine).

L1-A and LINGO1-A effects on neuronal growth and differentiation

Peptides in solution

L1-A and LINGO1-A peptides were separately added to the medium at increasing peptide concentrations (0, 0.01, 0.1, 1, 10, 100 μM) to assess their effect on cell viability/proliferation and neuronal differentiation. As shown in Figure 4, *A*, both peptides do not alter cell proliferation with respect to control. Moreover, they are not cytotoxic as cell death in samples treated with the peptide is comparable to control (Table 2). Then, neuritogenic properties were analyzed and both peptides showed the highest effect on total neurite length at 1 μM concentration (Figure 4, *B*). In RA treated samples, L1-A addition increases total neurite length up to +~96%; in the absence of RA, the highest increase (+~115%) is mediated by LINGO1-A. In order to more precisely determine the optimal peptide concentration, a second series of experiments was performed narrowing dose response curves around 1 μM peak. Data in Figure 4, *C* indicate 1 μM as the optimal concentration for both peptides. Then, the number of neurites per cell and the percentage of neurites longer than 100 μm were calculated. In order to aggregate the two set of experiments, only 0, 0.1, 1, 10 μM peptide concentrations were considered. Again, dose response curves reveal a bell-shaped pattern with the highest neuritogenic effect at 1 μM concentration (Figure 4, *D* and *E*). The number of neurites per neuron (Figure 4, *E*) follows the same trend observed for the total neurite length: the highest effect is obtained with L1-A in RA induced samples (+~66%) and with LINGO1-A in the absence of RA (+~82%). The highest percentages of neurites longer than 100 μm (Figure 4, *D*) are found in samples treated with LINGO1-A (+~76%) and LINGO1-A RA (+~72%).

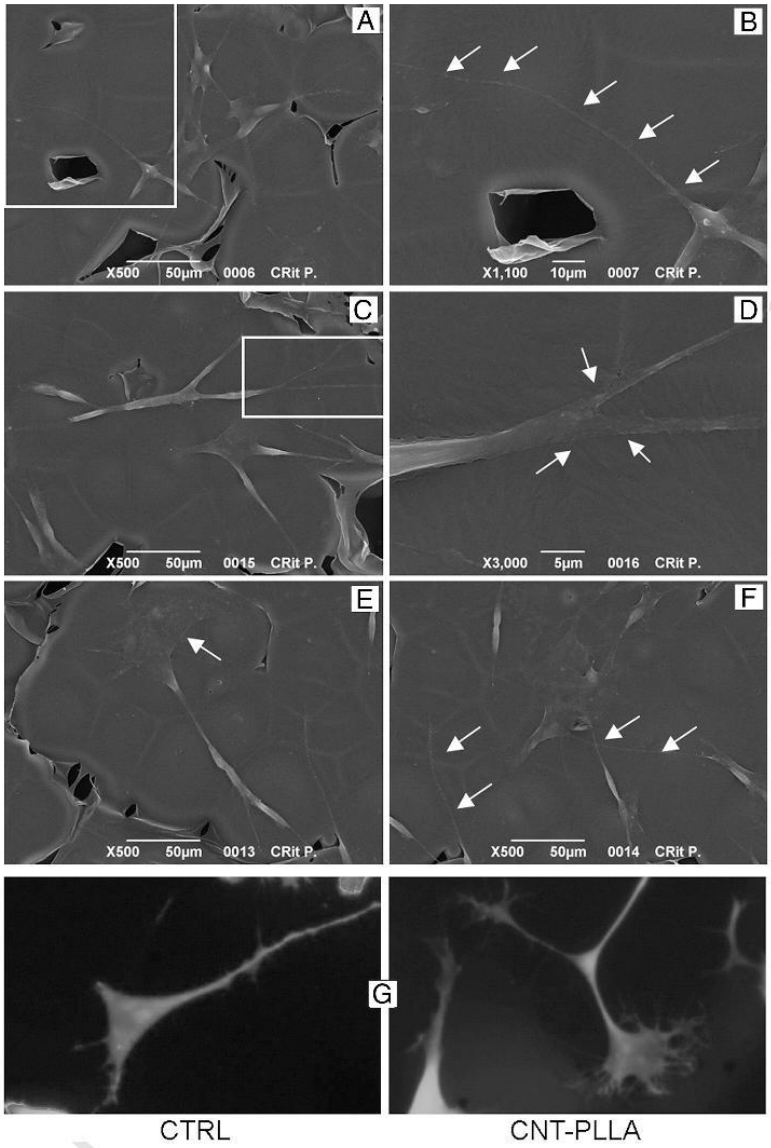

Figure 2. SH-SY5Y morphology when grown onto the CNT-PLLA scaffold.**(A-F)** Scanning electron microscopy images of SH-SY5Y cells grown onto CNT-PLLA scaffolds. Scale bar: A, C, E, F = 50 µm; B = 10 µm; D = 5 µm. Panels **(B)** and **(D)** show details of the framed area in A and C, respectively. **(B, F)** Outgrowth of neurites attaching to the scaffold surface. At higher magnification **(D)** the intimate contacts between CNT-PLLA scaffolds and neuronal membrane are evident. **(E)** Growth cone morphology of cells growing onto the scaffolds. **(G)** Typical growth cones observed when cell differentiation is induced with RA. Cells were stained with calcein-AM. Image magnification is 32×.

Given that both peptides mediated significant neuritogenic effects and according to established literature,[45] their scrambled versions (L1-A_scr and LINGO1-A_scr) were used to discriminate among sequence specific mechanisms and effects unspecifically depending on amino acid composition. Scrambled peptides, like native peptides, do not alter cell proliferation (Figure S2A). In samples treated by scrambled peptides, values for total neurite length, number of neurites per neuron and percentage of neurites longer than 100 µm are comparable or lower than control (Figure 4, *F-H*). Native peptides confirmed evidence from previous experiments, as the highest effect on total neurite length (Figure 4, *F*) and number of neurites per cell (Figure 4, *G*) is mediated by L1-A in RA-treated samples (+~88% total neurite length; +~71% neurites per cell) and by

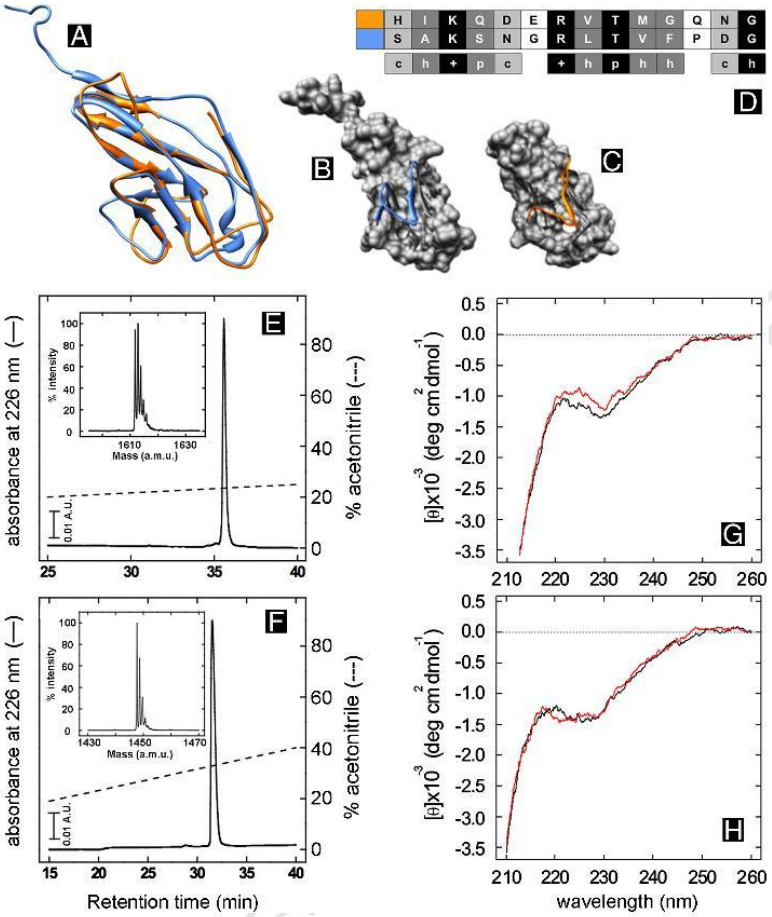

Figure 3. L1-A and LINGO1-A identification and characterization. **(A)** Superimposition between LINGO1 Ig domain (Blue) and L1 Ig2 domain (Orange). **(B)** LINGO1-A region (blue) and **(C)** L1-A region (orange) localization within the LINGO1 Ig and L1 Ig2 domains (gray) respectively. Models were obtained by UCSF Chimera software. **(D)** Alignment of L1-A and LINGO1-A peptide sequences. Black (identity), dark gray (same amino acid group), gray (compatible amino acid groups), white (different properties). Consensus code: c, compatible properties (polar and charged); h, hydrophobic; p, polar; +, positively charged. **(E, F)** RP-HPLC analysis of purified L1-A **(E)** and LINGO1-A **(F)** peptides by a C18 column eluted with an acetonitrile-0.078% TFA gradient (—). (Inset) Deconvoluted ESI-TOF mass spectrum of RP-HPLC purified peptides. The estimated molecular masses of L1-A (1611.79 ± 0.02 a.m.u.) and LINGO1-A (1447.72 ± 0.02 a.m.u.) peptides is in agreement with the theoretical values: 1611.78 and 1447.74 a.m.u., respectively. **(G, H)** Far-UV circular dichroism spectra of LINGO1-A **(G)** and L1-A **(H)** derivatives. All spectra were recorded at 25 °C in PBS. L1-A and LINGO1-A spectra are in black; spectra from the corresponding scrambled peptides are in red.

LINGO1-A in the absence of RA (+~82% total neurite length; +~44% neurites per cell). Furthermore, the percentage of neurites longer than 100 μm (Figure 4, *H*) is higher in LINGO1-A treated samples (+~60% LINGO1-A, +~63% LINGO1-A RA).

The neuritogenic effect of LINGO1-A and L1-A used in combination is lower than individual peptides.

Peptides adsorbed onto the substrate

The two peptides were designed to be used as guidance cues, mimicking ectodomains that could be biologically active either in solution or exposed at the surface of cells supporting neuronal growth. [23-34] Therefore, in order to assess variation of their effects when used in solution or adsorbed onto a substrate, L1-A or LINGO1-A (at 1 μM or 10 μM concentrations) was also used (individually or in combination) for coating well bottoms. The residual amount of peptides (prior to cell seeding) was found to be approximately 75% (see Supplementary file). As shown in Figure 5, *A* and *B*, both peptides are confirmed to have no meaningful effect on cell proliferation. Similarly, absence of cytotoxicity is confirmed (Table 3). Even when deposited onto the substrate, peptides exert a good neuritogenic effect. In fact, in all peptide-treated samples, the total neurite length is improved compared to control samples (Figure 5, *C* and *D*) and the highest neuritogenic effect is observed at 1 μM concentration.

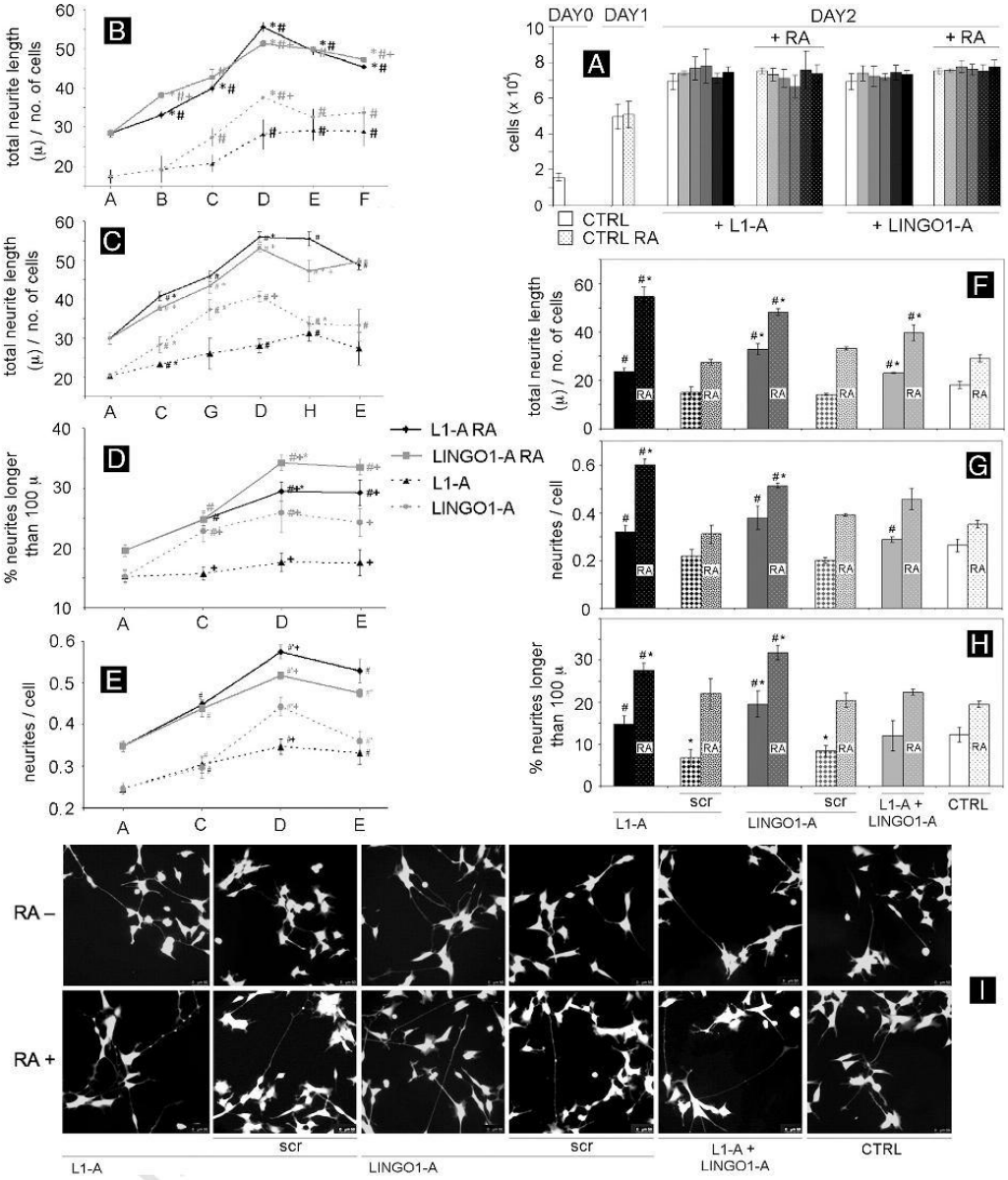

Figure 4. Effect of peptides added to the culture medium on SH-SY5Y cell proliferation and differentiation.Proliferation **(A)**, total neurite length **(B, C)**, neurites longer than 100 μm **(D)** and neurites per cell **(E)** from SH-SY5Y cells treated with increasing peptide concentrations in the absence or presence of RA. **(A)** White bars, control without peptides; other bars, the darker the color the higher the peptide concentration following this gradient (0.001, 0.1, 1, 10, 100 μM). **(B-E)** Peptide concentrations: A, no peptide; B, 10 nM; C, 100 nM; D, 1 μM; E, 10 μM; F, 100 μM; G, 316 nM; H, 3.16 μM. Data represent the mean ± SEM of three **(A-C)** and six **(D-E)** independent experiments performed in duplicate. # shows significance at $P < 0.05$ between cells treated with peptides and the control without peptides. * shows significance at $P < 0.05$ between sample 1X and sample 0.1X. + shows significance at $P < 0.05$ between samples treated with L1-A and LINGO1-A at the same concentration. Total neurite length **(F)**, neurites per cell **(G)**, neurites longer than 100 μm **(H)** and representative microscopy fields **(I)** from SH-SY5Y cells treated with 1 μM peptides or their scrambled versions in the absence or presence of RA. Data represent the mean ± SEM of three independent experiments performed in duplicate. * shows significance at $P < 0.05$ between samples treated with peptides and the control without peptides. # shows significance at $P < 0.05$ between samples treated with peptides and samples treated with their scrambled version. SH-SY5Y cells in **(I)** are stained with Calcein-AM. Image magnification is 20×.

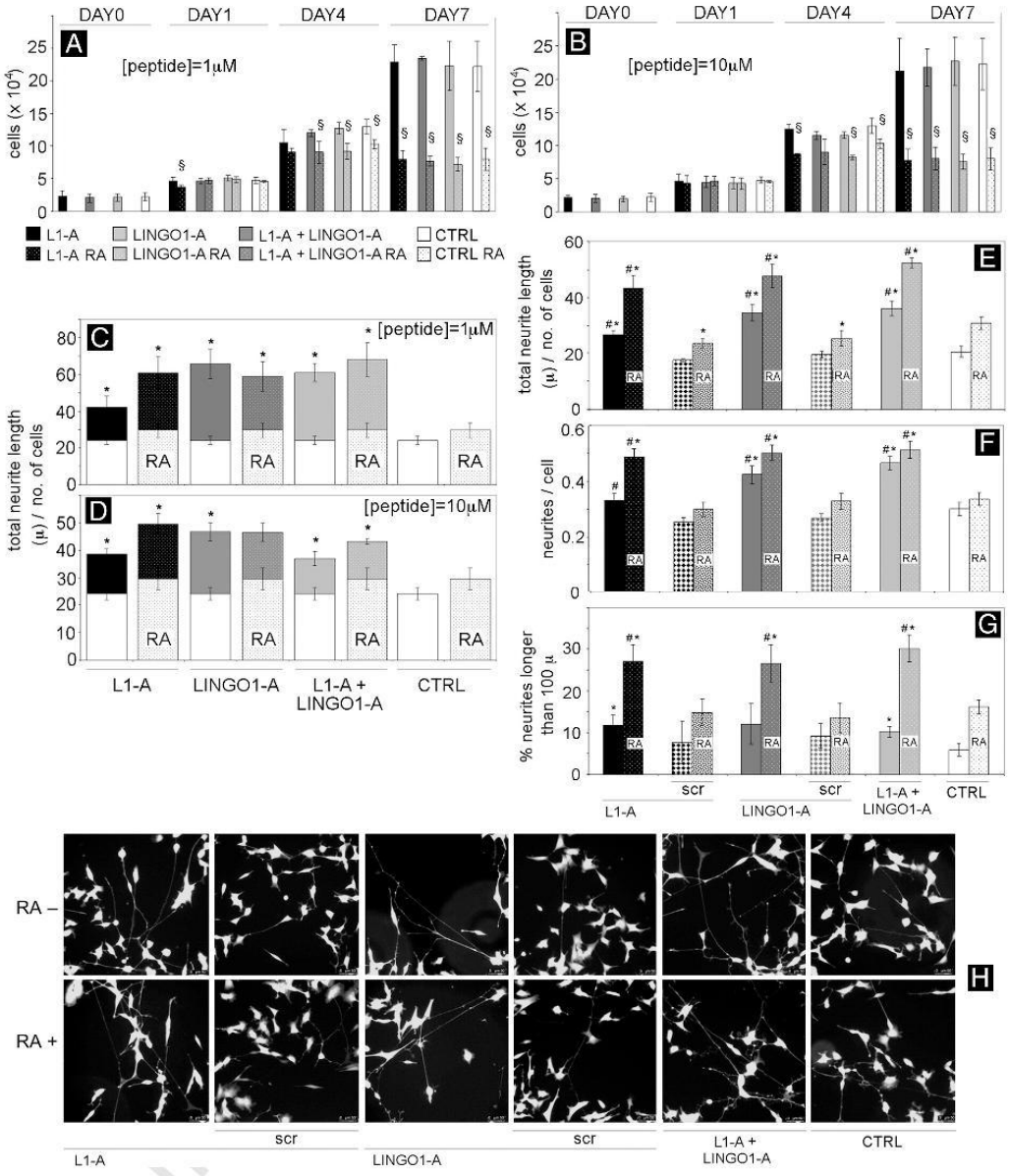

Figure 5. Effect of peptides deposited onto the substrate on SH-SY5Y cell proliferation and differentiation. Proliferation **(A, B)** and total neurite length **(C, D)** of SH-SY5Y cells seeded onto substrates coated with either 1 μM **(A, C)** or 10 μM **(B, D)** peptides. Data represent the mean ± SEM of three independent experiments performed in duplicate. § shows significance at $P < 0.05$ between samples treated with RA and their respective untreated controls. * shows significance at $P < 0.05$ between cells growing onto peptide substrate and the control (cells growing on poly-L-lysine). Incremental values compared to control are reported. Total neurite length **(E)**, neurites per cell **(F)**, neurites longer than 100 μm **(G)** and representative microscopy fields **(H)** from SH-SY5Y cells seeded onto substrates coated with 1 μM peptides or their scrambled versions in absence or presence of RA. Data represent the mean ± SEM of three independent experiments performed in duplicate. * shows significance at $P < 0.05$ between cells growing onto peptide surface and the control (cells grown onto poly-L-lysine). # shows significance at $P < 0.05$ between samples growing onto peptide surface and samples growing on their respective scrambled version. SH-SY5Y cells in **(H)** are stained with Calcein-AM. Image magnification is 20×.

t2.1 Table 2
t2.2 Percentage of cell death relative to three independent experiments performed in duplicate.

t2.3 % cell death	0 μM	0.01 μM	0.1 μM	1 μM	10 μM	100 μM
t2.4 L1-A	2.44%	2.19%	2.42%	2.05%	2.29%	2.34%
t2.5 LINGO1-A	2.44%	2.25%	1.99%	2.30%	2.31%	2.52%
t2.6 L1-A RA	2.12%	1.87%	2.03%	1.98%	1.99%	2.00%
t2.7 LINGO1-A RA	2.12%	2.04%	1.84%	1.89%	1.96%	1.96%

Experiments with scrambled peptides confirmed the sequence-dependent specificity observed with peptides in solution. In particular, no effect is observed on cell proliferation (Figure S2B) and cell death (not shown). Concerning total neurite length, number of neurites per neuron and percentage of neurites longer than 100 μm, values for scrambled peptides are always comparable or lower than control (Figure 5, *E-G*). Native peptides confirmed their neuritogenic potential as the total neurite length (Figure 5, *E*), the number of neurites per neuron (Figure 5, *F*) and the percentage of neurites longer than 100 μm (Figure 5, *G*) are improved by native peptides. Differently from experiments in solution, the effect of the two peptides in combination is comparable or higher than individual peptides, while difference among L1-A or LINGO1-A treated samples is less evident, possibly because of the prolonged culture time (i.e. four days after RA induction).

Combined effects of the CNT-PLLA scaffold and neuritogenic peptides on neuronal growth and differentiation

Separate characterization provided us with evidence that the CNT-PLLA scaffold is well suitable for neuronal culture and the peptides exert specific and important neuritogenic effects. Therefore, we performed experiments to determine if their combination could further promote neuronal differentiation. The scaffold + peptides combination neither altered cell proliferation nor cell death (Figure 6, *A* and Table 4), while showing instead evidence of synergy: total neurite length is significantly improved in RA induced samples treated by either L1-A or LINGO1-A when cells are grown onto the scaffold (Figure 6, *B*). Synergistic effect is also observed when cells are treated with L1-A in the absence of RA. Density of branch points per neurites and of neurites per cells was also determined and a synergistic effect is likely to occur as values for peptide and RA treated cells grown onto the scaffold are equal or higher than corresponding control samples (Figure 6, *C* and *D*). Synergistic effect can also be inferred when considering growth cone numbers. A growth cone was defined as a fan-shaped structure at the tip of a neurite, where the neurite began to increase in width. [46,47] When used separately, neither peptides nor the scaffolds show meaningful effect (Figure 6, *E*), but when RA induced cells are simultaneously grown onto the scaffold and treated with the peptides, growth cone number is considerably increased (+~97% L1-A RA; +~49% LINGO1-A RA).

Discussion

The positive role played by CNTs in supporting neuronal growth and differentiation is suggested by excellent works recently published (see Introduction). However, the limits of these systems also emerged (e.g., cytotoxicity of CNTs upon scaffold disaggregation). While immobilization of CNTs onto coverslips partially alleviate these problems,[5,6,15,18] such a strategy is not suitable for regenerative medicine purposes as coverslips are not implantable. Instead, nanocomposite CNT-PLLA scaffolds grant (i) full biocompatibility, (ii) good support of cell growth and differentiation and (iii) mechanical flexibility required for implant purposes. Moreover, the low percentage of purified CNTs within the scaffold reduces both costs and cytotoxicity by residual impurities, while preserving the ability of CNT-based scaffolds to support neuronal growth and differentiation. Indeed our data show that CNT-PLLA scaffolds support cell adhesion and differentiation better than PLLA alone. Synthetic peptides L1-A and LINGO1-A – designed to mimic the neural environment by reproducing interaction motifs involved in guidance of neuronal processes – were confirmed to improve neuronal differentiation and thus are good candidates for functionalizing neural regeneration implants. In all experimental conditions, L1-A and LINGO1-A showed full biocompatibility, neither exerting cytotoxic effects nor influencing cell proliferation, and their positive effect on neuronal differentiation (with 1 μM as optimal concentration) is sequence specific, as confirmed by control experiments with the scrambled peptides. Since the highest neuritogenic effect are mediated by L1-A and LINGO1-A (when added to the culture medium) in the presence or absence of RA induction, respectively, these peptides are likely to act through (at least partially) different pathways. RA induces the degradation of the Repressor Element-1 Silencing Transcription factor (REST).[48] REST mediates transcriptional repression of neuronal L1 and it is highly expressed in SH-SY5Y cells to maintain them poorly differentiated.[49] Therefore, RA induction promotes L1 expression and L1-A is likely to encounter an increased number of homophilic ligands on neuronal surfaces hence stimulating neurite outgrowth. Otherwise, RA downregulates LINGO1 expression[50] and therefore, in the absence of RA, the number of LINGO1 molecules at the neuronal surfaces is increased.

t3.1 Table 3
t3.2 Percentage of cell death relative to three independent experiments performed in duplicate.

t3.3 % cell death 1 μM	L1-A	LINGO1-A	L1-A + LINGO1-A	PLL
t3.4 A				
t3.5 DAY0	7.59%	7.41%	7.68%	7.68%
t3.6 DAY1	6.44%	5.56%	5.02%	5.64%
t3.7 DAY1 RA	6.91%	6.01%	5.67%	5.09%
t3.8 DAY4	2.60%	1.76%	2.02%	2.80%
t3.9 DAY4 RA	3.56%	3.27%	2.88%	3.29%
t3.10 DAY7	2.54%	2.18%	2.13%	2.00%
t3.11 DAY7 RA	3.75%	2.84%	2.66%	2.59%
t3.12				
t3.13 B				
t3.14 DAY0	8.79%	10.42%	9.38%	7.68%
t3.15 DAY1	5.66%	5.70%	5.67%	5.64%
t3.16 DAY1 RA	4.67%	4.10%	4.60%	5.09%
t3.17 DAY4	4.90%	4.40%	3.84%	2.80%
t3.18 DAY4 RA	6.21%	5.70%	5.35%	3.29%
t3.19 DAY7	2.49%	1.73%	1.99%	2.00%
t3.20 DAY7 RA	2.93%	2.27%	3.54%	2.59%

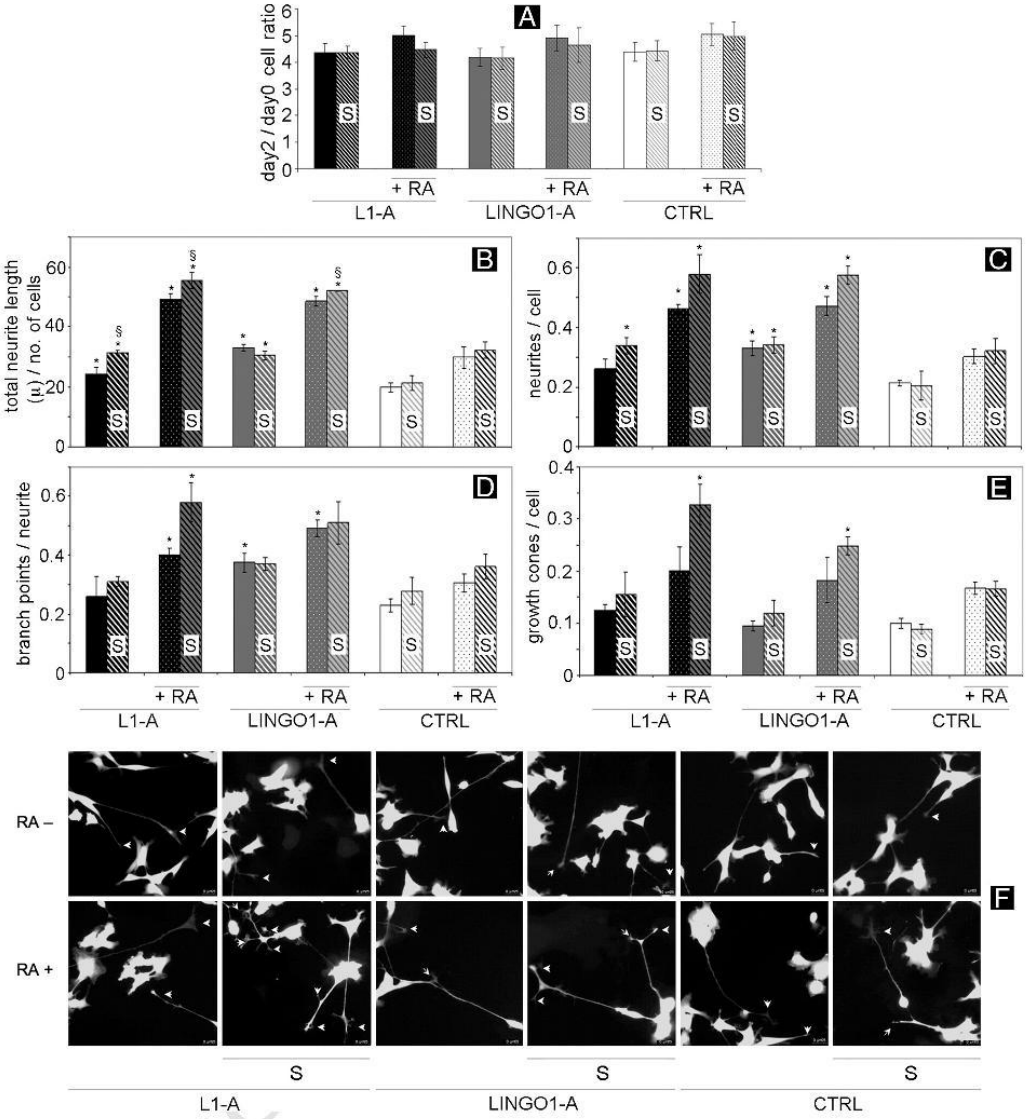

Figure 6. Comparison between SH-SY5Y cells seeded onto the CNT-PLLA scaffold (S) and control (poly-L-lysine coated wells) when treated with 1 μM peptides in the absence or presence of RA.Proliferation **(A)**, total neurite length **(B)**, neurites per cell **(C)**, branches per neurite **(D)**, growth cones per cell **(E)** and representative microscopy fields **(F)**. Data represent the mean ± SEM of three independent experiments performed in duplicate. * shows significance at $P < 0.05$ between samples treated with peptides and their respective control without peptides. § shows significance between samples growing onto CNT-PLLA scaffold and control (poly-L-lysine coated wells). SH-SY5Y cells in **(F)** are stained with Calcein-AM. Growth cones are indicated by white arrows. Image magnification is 32×.

When considering similarity between L1/L1-A and LINGO1/LINGO1-A systems, LINGO1 might interact with LINGO1-A peptide. In fact, homophilic binding between neuronal LINGO1 and oligodendrocyte precursor LINGO1 occurs and leads to oligodendrocyte differentiation inhibition.[29] Even though effects at neuronal level are still unclear, this interaction could stimulate neurite elongation. Alternatively, LINGO1-A peptide could act by masking LINGO1 interaction site with the other members of the NgR1/LINGO1/p75 complex or with neuronal NogoA. This in turn would lead to non-functional complex formation, blocking LINGO1 inhibitory effect on neurite elongation. These hypotheses are supported by evidence according to which LINGO1 mediates homo/heterotypic interactions through its Ig domain[30] and that when LINGO1 is inhibited neurite

t4.1 Table 4
t4.2 Percentage of cell death relative to four independent experiments performed in duplicate.

t4.3 % cell death	L1-A	LINGO1-A	Ctrl
t4.4 PLL	2.06%	2.15%	2.45%
t4.5 CNT-PLLA	2.14%	2.43%	2.43%
t4.6 PLL RA	1.61%	1.86%	2.18%
t4.7 CNT-PLLA RA	2.33%	1.83%	1.55%

elongation is promoted.[27,31,33,34] In this work, LINGO1-A treated samples presented the highest percentage of neurites longer than 100 μm; increased number of such long neurites could depend on "inhibition of the inhibitory effect" as inhibition of repulsive forces can prevent their sprouting from parental neurites, favoring elongation. Even when L1-A and LINGO1-A were used to coat wells prior to cell seeding, their positive effect on neuronal differentiation was confirmed. It is noteworthy that L1-A and LINGO1-A exert improved neuritogenic properties when cells are cultured onto CNT-PLLA scaffolds and in some conditions their effect is enhanced by the CNT-PLLA scaffold itself. This effect is particularly evident by analyzing the total neurite length, the branch points per neurite and the neurites per cell when cells are cultivated onto the CNT-PLLA scaffold and treated with L1-A or LINGO1-A after RA induction. The combination of CNT-PLLA scaffolds, L1-A or LINGO1-A treatment and RA induction also promotes the formation of growth cones, likely because of the larger amount of cue types available for the cells in their environment.

In conclusion, we developed a freestanding scaffold that combines the biocompatible properties of PLLA[36] with the conductive, mechanical and topographical features of CNTs. Furthermore, the L1-A and LINGO1-A peptides mediate positive effects on neuronal differentiation and, even though further studies are needed to investigate their mechanisms of action, they represent a promising regenerative medicine tool. Indeed, replacement of recombinant proteins by biomimetic peptides reproducing only active motifs dramatically cuts costs, simplifies preparation and functionalization of scaffolds. Moreover, short peptides display increased stability and lower immunogenic potential with respect to entire proteins and protein domains. Our CNT-PLLA scaffold, used in combination with the peptides, demonstrates synergistic effects in supporting neuronal cell growth and differentiation and thus it is a good starting point for setting up implantable scaffolds for autologous neuronal differentiation.

Appendix A. Supplementary data

Supplementary data to this article can be found online at http://dx.doi.org/10.1016/j.nano.2014.11.001.

References

1. Harrison BS, Atala A. Carbon nanotube applications for tissue engineering. *Biomaterials* 2007;**28**(2):344-53.
2. Saracino GA, Cigognini D, Silva D, Caprini A, Gelain F. Nanomaterials design and tests for neural tissue engineering. *Chem Soc Rev* 2013;**42**(1):225-62.
3. Dai HJ, Wong EW, Lieber CM. Probing electrical transport in nanomaterials, conductivity of individual carbon nano-tubes. *Science* 1996;**272**:523-6.
4. Wong EW, Sheehan PE, Lieber CM. Nanobeam mechanics: elasticity, strength, and toughness of nanorods and nanotubes. *Science* 1997;**277**:1971-5.
5. Mattson MP, Haddon RC, Rao AM. Molecular functionalization of carbon nanotubes and use as substrates for neuronal growth. *J Mol Neurosci* 2000;**14**(3):175-82.
6. Hu H, Ni Y, Montana V, Haddon RC, Parpura V. Chemically functionalized carbon nanotubes as substrates for neuronal growth. *Nano Lett* 2004;**4**(3):507-11.
7. Chao TI, Xiang S, Chen CS, Chin WC, Nelson AJ, Wang C, et al. Carbon nanotubes promote neuron differentiation from human embryonic stem cells. *Biochem Biophys Res Commun* 2009;**384**(4):426-30.
8. Fabbro A, Prato M, Ballerini L. Carbon nanotubes in neuroregeneration and repair. *Adv Drug Deliv Rev* 2013;**65**(15):2034-44.
9. Chua JS, Chng CP, Moe AA, Tann JY, Goh EL, Chiam KH, et al. Extending neurites sense the depth of the underlying topography during neuronal differentiation and contact guidance. *Biomaterials* 2014;**35**(27):7750-61, http://dx.doi.org/10.1016/j.biomaterials.2014.06.008.
10. Resende RR, Fonseca EA, Tonelli FM, Sousa BR, Santos AK, Gomes KN, et al. Scale/topography of substrates surface resembling extracellular matrix for tissue engineering. *J Biomed Nanotechnol* 2014;**10**(7):1157-93.
11. Boccafoschi F, Rasponi M, Ramella M, Ferreira AM, Vesentini S, Cannas M. Short-term effects of microstructured surfaces: role in cell differentiation toward a contractile phenotype. *J Appl Biomater Funct Mater* 2014;**18**, http://dx.doi.org/10.5301/JABFM.5000186 [Epub ahead of print].
12. Bokara KK, Kim JY, Lee YI, Yun K, Webster TJ, Lee JE. Biocompatibility of carbon nanotubes with stem cells to treat CNS injuries. *Anat Cell Biol* 2013;**46**(2):85-92.
13. Mazzatenta A, Giugliano M, Campidelli S, Gambazzi L, Businaro L, Markram H, et al. Interfacing neurons with carbon nanotubes: electrical signal transfer and synaptic stimulation in cultured brain circuits. *J Neurosci* 2007;**27**(26):6931-6.
14. Liopo AV, Stewart MP, Hudson J, Tour JM, Pappas TC. Biocompatibility of native and functionalized single-walled carbon nanotubes for neuronal interface. *J Nanosci Nanotechnol* 2006;**6**(5):1365-74.
15. Lovat V, Pantarotto D, Lagostena L, Cacciari B, Grandolfo M, Righi M, et al. Carbon nanotube substrates boost neuronal electrical signaling. *Nano Lett* 2005;**5**(6):1107-10.
16. Cellot G, Toma FM, Varley ZK, Laishram J, Villari A, Quintana M, et al. Carbon nanotube scaffolds tune synaptic strength in cultured neural circuits: novel frontiers in nanomaterial-tissue interactions. *J Neurosci* 2011;**31**(36):12945-53.
17. Fabbro A, Sucapane A, Toma FM, Calura E, Rizzetto L, Carrieri C, et al. Adhesion to carbon nanotube conductive scaffolds forces action-potential appearance in immature rat spinal neurons. *PLoS One* 2013;**8**(8):e73621. Q5
18. Malarkey EB, Fisher KA, Bekyarova E, Liu W, Haddon RC, Parpura V. Conductive single-walled carbon nanotube substrates modulate neuronal growth. *Nano Lett* 2009;**9**(1):264-8.
19. Cui HF, Vashist SK, Al-Rubeaan K, Luong JH, Sheu FS. Interfacing carbon nanotubes with living mammalian cells and cytotoxicity issues. *Chem Res Toxicol* 2010;**23**(7):1131-47.
20. Prato M, Kostarelos K, Bianco A. Functionalized carbon nanotubes in drug design and discovery. *Acc Chem Res* 2008;**41**(1):60-8.
21. Matsumoto K, Sato C, Naka Y, Kitazawa A, Whitby RL, Shimizu N. Neurite outgrowths of neurons with neurotrophin-coated carbon nanotubes. *J Biosci Bioeng* 2007;**103**(3):216-20.
22. Chen H, Yuan L, Song W, Wu Z, Li D. Biocompatible polymer materials: role of protein–surface interactions. *Prog Polym Sci* 2008;**33**:1059-87.
23. Haspel J, Grumet M. The L1CAM extracellular region: a multi-domain protein with modular and cooperative binding modes. *Front Biosci* 2003;**8**:s1210-25.

24. Kenwrick S, Watkins A, De Angelis E. Neural cell recognition molecule L1: relating biological complexity to human disease mutations. *Hum Mol Genet* 2000;**9**(6):879-86.
25. Gouveia RM, Gomes CM, Sousa M, Alves PM, Costa J. Kinetic analysis of L1 homophilic interaction: role of the first four immunoglobulin domains and implications on binding mechanism. *J Biol Chem* 2008;**283**(42):28038-47.
26. Zhao X, Yip PM, Siu CH. Identification of a homophilic binding site in immunoglobulin-like domain 2 of the cell adhesion molecule L1. *J Neurochem* 1998;**71**(3):960-71.
27. Mi S, Lee X, Shao Z, Thill G, Ji B, Relton J, et al. LINGO-1 is a component of the Nogo-66 receptor/p75 signaling complex. *Nat Neurosci* 2004;**7**(3):221-8.
28. Petrinovic MM, Duncan CS, Bourikas D, Weinman O, Montani L, Schroeter A, et al. Neuronal Nogo-A regulates neurite fasciculation, branching and extension in the developing nervous system. *Development* 2010;**137**(15):2539-50.
29. Jepson S, Vought B, Gross CH, Gan L, Austen D, Frantz JD, et al. LINGO-1, a transmembrane signaling protein, inhibits oligodendrocyte differentiation and myelination through intercellular self-interactions. *J Biol Chem* 2012;**287**(26):22184-95.
30. Stein T, Walmsley AR. The leucine-rich repeats of LINGO-1 are not required for self-interaction or interaction with the amyloid precursor protein. *Neurosci Lett* 2012;**509**(1):9-12.
31. Inoue H, Lin L, Lee X, Shao Z, Mendes S, Snodgrass-Belt P, et al. Inhibition of the leucine-rich repeat protein LINGO-1 enhances survival, structure, and function of dopaminergici neurons in Parkinson's disease models. *Proc Natl Acad Sci U S A* 2007;**104**(36):14430-5.
32. Mi S, Pepinsky RB, Cadavid D. Blocking LINGO-1 as a therapy to promote CNS repair: from concept to the clinic. *CNS Drugs* 2013;**27**(7):493-503.
33. Fernandez-Enright F, Andrews JL, Newell KA, Pantelis C, Huang XF. Novel implications of Lingo-1 and its signaling partners in schizophrenia. *Transl Psychiatry* 2014;**4**:e348, http://dx.doi.org/10.1038/tp.2013.121.
34. Ji B, Li M, Wu WT, Yick LW, Lee X, Shao Z, et al. LINGO-1 antagonist promotes functional recovery and axonal sprouting after spinal cord injury. *Mol Cell Neurosci* 2006;**33**(3):311-20.
35. Gheith MK, Sinani VA, Wicksted JP, Matts RL, Kotov NA. Single-walled carbon nanotube polyelectrolyte multilayers and freestanding films as a biocompatible platform for neuroprosthetic implants. *Adv Mater* 2005;**17**:2663-7.
36. Yang F, Murugan R, Ramakrishna S, Wang X, Ma YX, Wang S. Fabrication of nano-structured porous PLLA scaffold intended for nerve tissue engineering. *Biomaterials* 2004;**25**(10):1891-900.
37. Koh HS, Yong T, Chan CK, Ramakrishna S. Enhancement of neurite outgrowth using nano-structured scaffolds coupled with laminin. *Biomaterials* 2008;**29**(26):3574-82.
38. Gertz CC, Leach MK, Birrell LK, Martin DC, Feldman EL, Corey JM. Accelerated neuritogenesis and maturation of primary spinal motor neurons in response to nanofibers. *Dev Neurobiol* 2010;**70**(8):589-603.
39. Furtado CA, Kim UJ, Gutierrez HR, Pan L, Dickey EC, Eklund PC. Debundling and dissolution of single-walled carbon nanotubes in amide solvents. *J Am Chem Soc* 2004;**126**(19):6095-105.
40. Salice P, Fenaroli D, De Filippo CC, Menna E, Gasparini G, Maggini M. Efficient functionalization of carbon nanotubes: an opportunity enabled by flow chemistry. *Chim Oggi* 2012;**30**(6):37-9.
41. Salice P, Fabris E, Sartorio C, Fenaroli D, Figà V, Casaletto MP, et al. An insight into the functionalisation of carbon nanotubes by diazonium chemistry: towards a controlled decoration. *Carbon* 2014;**74**:73-82.
42. D'Este M, De Nardi M, Menna E. A co-functionalization approach to soluble and functional single-walled carbon nanotubes. *Eur J Org Chem* 2006;**11**:2517-22.
43. Alberts P, Rudge R, Hinners I, Muzerelle A, Martinez-Arca S, Irinopoulou T, et al. Cross talk between tetanus neurotoxin-insensitive vesicle-associated membrane protein-mediated transport and L1-mediated adhesion. *Mol Biol Cell* 2003;**14**(10):4207-20.
44. Brahms S, Brahms J. Determination of protein secondary structure in solution by vacuum ultraviolet circular dichroism. *J Mol Biol* 1980;**138**(2):149-78.
45. Soroka V, Kiryushko D, Novitskaya V, Ronn LC, Poulsen FM, Holm A, et al. Induction of neuronal differentiation by a peptide corresponding to the homophilic binding site of the second Ig module of the neural cell adhesion molecule. *J Biol Chem* 2002;**277**(27):24676-83.
46. Abney JR, Meliza CD, Cutler B, Kingma M, Lochner JE, Scalettar BA. Real-time imaging of the dynamics of secretory granules in growth cones. *Biophys J* 1999;**77**(5):2887-95.
47. Dent EW, Gupton SL, Gertler FB. The growth cone cytoskeleton in axon outgrowth and guidance. *Cold Spring Harb Perspect Biol* 2011;**3**(3). Q6
48. Singh A, Rokes C, Gireud M, Fletcher S, Baumgartner J, Fuller G, et al. Retinoic acid induces REST degradation and neuronal differentiation by modulating the expression of SCF(β-TRCP) in neuroblastoma cells. *Cancer* 2011;**117**(22):5189-202.
49. Mikulak J, Negrini S, Klajn A, D'Alessandro R, Mavilio D, Meldolesi J. Dual REST-dependence of L1CAM: from gene expression to alternative splicing governed by Nova2 in neural cells. *J Neurochem* 2012;**120**(5):699-709.
50. Puttagunta R, Schmandke A, Floriddia E, Gaub P, Fomin N, Ghyselinck NB, et al. RA-RAR-β counteracts myelin-dependent inhibition of neurite outgrowth via Lingo-1 repression. *J Cell Biol* 2011;**193**(7):1147-56.

Enhancement of neuronal cell differentiation combining biomimetic peptides and a carbon nanotube-polymer scaffold

Giorgia Scapin[1], Patrizio Salice[2], Simone Tescari[3], Thomas Bertalot[3], Nicola Vicentini[2], Rosa Di Liddo[3], Maria Teresa Conconi[3], Enzo Menna[2], Vincenzo De Filippis[3], and Francesco Filippini[1]

1 Department of Biology, 2 Department of Chemical Sciences, 3 Department of Pharmaceutical Sciences, University of Padua, Padua, Italy

Carbon nanotubes (CNTs) are attractive candidates for the development of scaffolds for neural regeneration thanks to their ability to conduct electrical stimuli, to interface with cells and to mimic the neural environment (Mattson et al, J Mol Neurosci. 2000). We developed a freestanding nanocomposite scaffold of multi-walled CNTs in a PLLA matrix that combines the conductive, mechanical and topographical features of CNTs with the biocompatible properties of the PLLA. Such CNT-PLLA scaffold resulted to support growth and differentiation of human neuronal cells better than CNTs or PLLA alone. Moreover, to mimic guidance cues from the neural environment, we also designed biomimetic peptides, derived from L1 and LINGO1 proteins that are involved in neurite outgrowth control (Zhao et al, J Neurochem. 1998; Mi et al, Nat. Neurosci. 2004). Both peptides - which neither alter cell proliferation nor induce cell death - could specifically and positively modulate neuronal differentiation (with highest effect at 1 µM concentration). Furthermore, cell differentiation resulted to be synergistically improved by the combination of the nanocomposite scaffold and the peptides, thus suggesting a prototype for the development of implants for long-term neuronal growth and differentiation. The ongoing work is about the use of new scaffolds consisting of multi-walled CNTs in a PLLA matrix and electrospinned into fibers. These scaffolds were shown to be biocompatible and to promote the formation of new neurites that extend along the scaffold fibers. Since cells are influenced by the scaffold topography, the orientation of the scaffold fibers opens up the perspective to promote a polarized neurite outgrowth. Moreover, the neuritogenic properties of the scaffolds are further enhanced when adding peptides to culture medium; thus they represent a good starting point for developing next generation scaffolds upon peptide functionalization. Currently, we are growing human circulating multipotent cells (hCMCs) onto the CNT-PLLA scaffolds to asses if this autologous and accessible source of stem cells is capable of neuronal differentiation thanks to the scaffold characteristics. Our preliminary results show that cells can adhere and grow onto the scaffold showing features (such as neurites and growth cones) typical of cells of the neuronal lineage.

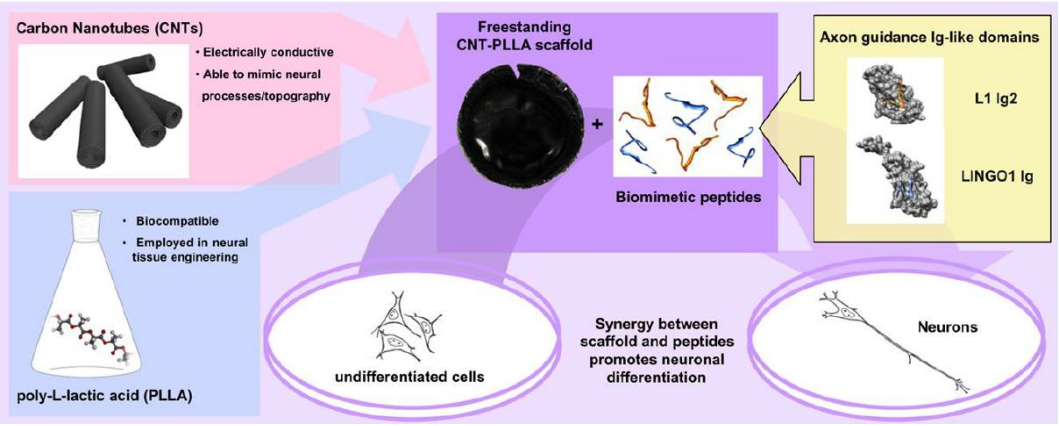

Carbon Nanotubes-Polymer Electrospun Nanofibers as Biocompatible Scaffold for Neuronal Cells Differentiation

Teresa Gatti [a], Nicola Vicentini [a], Patrizio Salice [a], Giorgia Scapin [b], Carla Marega [a], Francesco Filippini [b], and Enzo Menna [a]

[a] *Dipartimento di Scienze Chimiche, Università di Padova, via Marzolo 1, 35131 Padova*

[b] *Dipartimento di Biologia, Università di Padova, via Ugo Bassi 58/B, 35131-Padova*

E-mail: teresa.gatti@unipd.it

Carbon nanotubes (CNTs) are attractive candidates for the development of scaffolds able to support neuronal growth and development thanks to their ability to conduct electrical stimuli, to interface with cells and to mimic the neural environment. We recently proposed a freestanding nanocomposite scaffold that combines the conductive and topographical features of functionalized multi wall carbon nanotubes (MWCNTs) with the biocompatible and mechanical properties of a polylactide matrix (PLLA) [1]. We will present here a novel morphology for the neuritogenetic nanocomposite substrate, based on electrospun nanofibers deposited onto a glass support. Details on the preparation and characterization of such nanofibers will be reported, together with preliminary evidences of polarized neurite outgrowth along the scaffold nanofibrous topography.

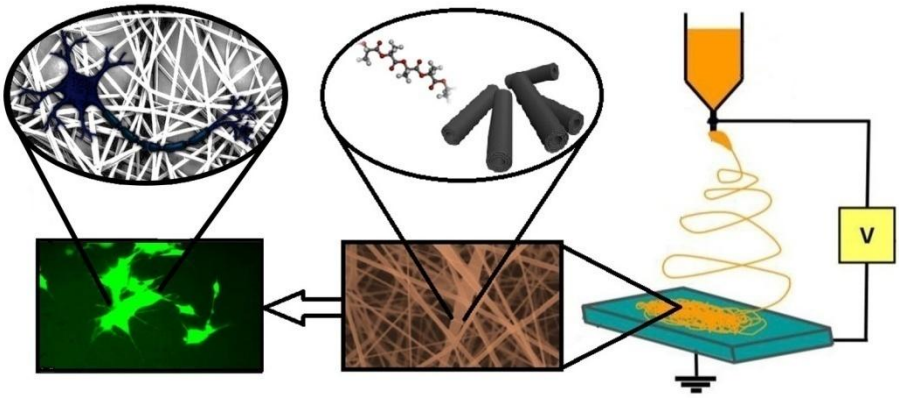

Figure 1: Neuronal growth onto MWCNTs-PLLA electrospun nanofibers

References:

[1] G. Scapin, P. Salice, S. Tescari, E. Menna, V. De Filippis, and F. Filippini, Enhanced Neuronal Cell Differentiation Combining Biomimetic Peptides and a Carbon Nanotubes-Polymer Scaffold, *Submitted*.

AKNOWLEDGMENTS

My first thanks go to my supervisor prof. Filippini, he has been a precious scientific guiding light during my PhD and has directed me toward many collaborations giving me the possibility to face an interdisciplinary environment.

I would like to thank all the people involved in this project: prof. Menna, prof. De Filippis, Prof. Di Liddo, Thomas, Nicola, Patrizio and Simone for all their enthusiasm, time and efforts put in the project.

Thank to all past and present members of the MOLBINFO team: Valeria, Adelaide, Irene, Pizzo, Daniela, Marianna, Ventu and Gloria for the beautiful experience of working and having good time together.

A special thank goes to my "Svampies" Minky, Balles, Pinny, Ross and Vale for their constant presence despite the distance and for the priceless time passed together .

I want to thank Eli and Cri, for their lasting friendship during all these years and for having been at my side every time I needed.

I wish to thank from the heart my parents, my sister and grandmother for their everlasting love and understanding, for encouraging me to strive towards my goal and for always having believed in me.

And most of all thank to my beloved Mirco for his golden patience and his priceless support, he has always been at my side during my good and bad times, knowing every time how to calm me down when I started to become irritable and insicure, thank for lovingly taking care of me.